

Aus der Klinik für  
Visceral-, Thorax- und Gefäßchirurgie  
Direktor: Prof. Dr. med. Detlef K. Bartsch

in Zusammenarbeit mit der

Klinik für Neurochirurgie  
Direktor: Prof. Dr. med. Christopher Nimsky

des Fachbereichs Medizin der Philipps-Universität Marburg

**Roles of ADAM8 and PRMTs in  
tumor-stroma-interactions in  
Pancreatic Ductal Adenocarcinoma**

**Inaugural-Dissertation**  
zur Erlangung des Doktorgrades  
der gesamten Naturwissenschaften  
(Dr. rer. nat.)

dem Fachbereich Medizin der Philipps-Universität Marburg vorgelegt

von

**Yeşim Yılmaz (geb. Verel)**  
aus Burtenbach  
Marburg, 2023

Angenommen vom Fachbereich Medizin der Philipps-Universität Marburg am:

Gedruckt mit Genehmigung des Fachbereichs Medizin:

Referenten: Prof. Dr. med. Detlef K. Bartsch, Prof. Dr. rer. nat. Jörg-Walter

Bartsch Korreferent: Prof. Dr. Malte Buchholz

Dekanin: Frau Prof. Dr. Denise Hilfiker-Kleiner

*“The only source of knowledge is experience”*

- Albert Einstein

# Inhaltsverzeichnis

LIST OF ABBREVIATIONS .....	IV
LIST OF FIGURES.....	VI
1 INTRODUCTION .....	1
1.1.1 Pancreatic Ductal Adenocarcinoma Precursor Lesions.....	2
1.2 TUMOR MICROENVIRONMENT IN PDAC .....	3
1.2.1 T cells in PDAC .....	5
1.2.2 Macrophages in PDAC .....	6
1.3 EXTRACELLULAR VESICLES.....	7
1.3.1 Exosomes in Cancer.....	8
1.3.2 Exosome encapsulated miRNAs as based prognostic biomarkers for PDAC.....	10
1.4 ADAM8.....	12
1.5 PROTEIN ARGININE METHYLTRANSFERASES .....	14
1.6 AIM OF THE STUDY.....	16
2 SUMMARY OF THE PUBLICATIONS .....	17
2.1 COHORT ANALYSIS OF ADAM8 EXPRESSION IN THE PDAC TUMOR STROMA.....	17
2.1.1 Scientific summary of the publication .....	17
2.1.2 Description of the personal contribution .....	18
2.2 PRMT1 PROMOTES THE TUMOR SUPPRESSOR FUNCTION OF P14 <sup>ARF</sup> AND IS INDICATIVE FOR PANCREATIC CANCER PROGNOSIS .....	19
2.2.1 Scientific summary of the publication .....	19
2.2.2 Description of the personal contribution .....	26
2.3 EXTRACELLULAR VESICLE-BASED DETECTION OF PANCREATIC CANCER .....	26
2.3.1 Scientific summary of the publication .....	26
2.3.2 Description of the personal contribution .....	28
3 DISCUSSION .....	29
3.2 ADAM8-POSITIVE SERUM EVS AS A PROMISING BIOMARKER IN PDAC .....	32
3.2.1 Domains of ADAM8 .....	36
3.3 PRMTs AS A DIAGNOSTIC IN PDAC.....	37
3.3.1 PRMT1 as a novel therapeutic target in PDAC .....	38
3.3.2 PRMT4 as a novel therapeutic target in PDAC - paper in review .....	39
3.3.3 Determination of serum ADMA levels in PDAC - paper in review.....	40
4 SUMMARY.....	41
5 ZUSAMMENFASSUNG.....	43
6 REFERENCES.....	45
7 PUBLICATIONS.....	57
8 APPENDIX .....	96
8.1 CURRICULUM VITAE.....	96
8.2 VERZEICHNIS AKADEMISCHER LEHRER .....	98
8.3 DANKSAGUNG.....	99
8.4 EHRENWÖRTLICHE ERKLÄRUNG.....	100

## List of abbreviations

AD2	Activator domain 2
ADAM	A disintegrin and metalloproteinase
ADM	Acinar-to-ductal metaplasia
ADMA	Asymmetric dimethylarginine
Akt2	RAC-beta serine/ threonine-protein kinase
ATM	Ataxia telangiectasia mutated
BRCA	Breast cancer gene
CA 19-9	Carbohydrate antigen 19-9
CAF	Cancer-associated fibroblasts
CARM1	Coactivator-associated arginine methyltransferase 1
CD	Cluster of differentiation
CDKN2A	Cyclin dependent kinase inhibitor 2A
cDNA	Complementary deoxyribonucleic acid
CP	Chronic pancreatitis
DNA	Deoxyribonucleic acid
ECM	Extracellular matrix
EGF	Epidermal growth factor
ERK1/2	Extracellular signal-regulated 1/2 kinases
EV	Extracellular vesicles
FACS	Fluorescence activated cell sorting
FOXO1	Forkhead box O1
H	Histone
HLA-DR	Human Leukocyte Antigen – DR isotype
HPLC	High-performance liquid chromatography
IHC	Immunohistochemistry
KPC	Kras <sup>LSL-G12D</sup> , Trp53 <sup>R172H/+</sup> , PdxCre <sup>+/+</sup>
KRAS	Kirsten rat sarcoma virus
LCN2	Lipocalin 2
M	Macrophage
MHC	Major histocompatibility complex
miRNA	MicroRNA
MLH	MutL homolog
MMA	Monomethyl arginine
MMP	Matrix metalloprotease

mRNA	Messenger ribonucleic acid
MVB	Multivesicular bodies
NK	Natural killer
NLR	Neutrophil-to-leukocyte ratio
nm	Nanometer
nSMase2	Neutral sphingomyelinase 2
PanIN	Pancreatic intraepithelial neoplasia
PDAC	Pancreatic Ductal Adenocarcinoma
p16INK4A	Cyclin-dependent kinase inhibitor 2A
PI3K	Phosphoinositide 3-kinase
p14ARF	Alternate reading frame protein product
PM	Plasma membrane
RNA	Ribonucleic acid
pre-miRNA	precursor miRNA
pri-miRNA	primary miRNA
PRMT	Protein arginine methyltransferase
qPCR	Quantitative polymerase chain reaction
RISC	RNA-induced silencing complex
RNAse	Ribonuclease
SAM	S-adenosylmethionine
SDMA	Symmetric dimethylarginine
SMA	Smooth-muscle actin
SMAD4	Small mothers against decapentaplegic family member 4
TAM	Tumor-associated macrophage
T cell	Thymus- derived lymphocytes
TME	Tumor microenvironment
TNBC	Triple-negative breast cancer
TNF	Tumor necrosis factor
TP53	Transformation related protein 53
UTR	Untranslated region
VTG	Viszeral-, Thorax- und Gefäßchirurgie

## List of figures

<b>Figure 1. Illustration of the biogenesis of several types of EVs, including microvesicles, apoptotic bodies and exosomes .....</b>	<b>8</b>
<b>Figure 2. Pathway of the microRNA maturation and the mechanism of post-transcriptional repression of protein biosynthesis .....</b>	<b>11</b>
<b>Figure 3. Basic modular structure of ADAM8 with possible three entities .....</b>	<b>13</b>
<b>Figure 4. PRMT catalysis and classification .....</b>	<b>15</b>





# 1 Introduction

## 1.1 Pancreatic Ductal Adenocarcinoma

Pancreatic cancer, also known as pancreatic carcinoma or adenocarcinoma of the pancreas, is a relatively rare but very aggressive cancer, which accounts for about 3 % of all cancers in Germany. This kind of cancer is indeed responsible for about 6 % of all cancer deaths and is respectively classified as the ninth and tenth most common cause of cancer death (Christmann, 2015). Pancreatic cancers can be classified into different subgroups: cystic adenocarcinomas, acinar tumor as well as ductal adenocarcinomas. Pancreatic ductal adenocarcinoma (PDAC) accounts for over 95 % of pancreatic cancers making it the most common pancreatic cancer type (Herrmann, 2018). PDAC holds the highest mortality rate of all solid organ cancers and is classified as the fourth leading cause of cancer related deaths with an approximate 5 year survival rate of around 9 % (Siegel *et al.*, 2020). PDAC results from the malignant transformation of exocrine pancreas cells which coat the small excretory ducts of the glandular portion responsible for digestive secretions (Christmann, 2015). The aggressive nature of cancer, which is responsible for metastasis, late detection due to nonspecific symptoms, and resistance to therapy speak to the poor prognosis of PDAC, which is also reflected in the low survival rate of affected individuals (Siegel *et al.*, 2020; Bartsch *et al.*, 2018). For instance, PDAC is known to be one of the most chemoresistant carcinomas. The effect of therapies targeting cancer-associated molecular pathways in this disease has therefore been unsuccessful. At the time of diagnosis, metastasis has already occurred in 90 % of patients (Song *et al.*, 2020). However, no screening methods are currently available. To date, the best curative treatment is complete surgical tumor resection (Springer Medizin, 2019). Since symptoms of this disease appear very late and metastasis has already occurred in 90 % of patients at the time of diagnosis, only a remaining 10 % of PDAC patients have resectable PDAC stages (Song *et al.*, 2020; Orth *et al.*, 2019). Consequently, to detect PDAC at early stages, there is an enormous need for research in this area to develop new therapies and discover better diagnostic markers. Indeed, very few biomarkers only are routinely used to detect its presence and lesions before its development (Bartsch *et al.*, 2018). The prognosis of increasing incidence is based on causes of PDAC such as demographic risk factors due to aging in society, but also environmental and lifestyle factors such as obesity, type 2 diabetes, chronic

pancreatitis, and increased alcohol and tobacco use. In a small proportion of PDAC patients, genetic predispositions due to germline mutations in Breast cancer genes 1 and 2 (BRCA1/2), Ataxia telangiectasia mutated (ATM), MutL homolog 1 (MLH1), tumor suppressor protein p53 (TP53) and cyclin-dependent kinase inhibitor 2A (CDKN2A), were found to be additional risk factors (Petersen *et al.*, 2010; Pihlak *et al.*, 2017; Hu *et al.*, 2018).

### **1.1.1 Pancreatic Ductal Adenocarcinoma Precursor Lesions**

The development of PDAC is based on a process called "acinar-to-ductal metaplasia" (ADM). This involves transdifferentiation of exocrine gland cells (acinar) to epithelial-like (ductal) cells in response to various stimuli from the tumor microenvironment (TME), such as tissue damage and inflammatory or stress-related influences. Since the pancreas, unlike other organs of the gastrointestinal tract, does not have a defined stem cell compartment, the maintenance of pancreatic homeostasis and tissue regeneration is provided by the exocrine (acinar) glandular cells. For this purpose, acinar cells are characterized by high plasticity. These acinar cells acquire "progenitor" properties during the before mentioned transdifferentiation process, which makes them more susceptible to pro-oncogenic changes. This includes e. g., a gain-of-function mutation of the proto-oncogene Kirsten Rat Sarcoma virus (KRAS). It is known that 95 % of PDACs originate in mutations of the KRAS gene. The onset of the ADM process is characterized as the initial step in the development of PDAC (Orth *et al.*, 2019). However, in most cases, there is an initial formation of precursor lesions called pancreatic intra-epithelial neoplasias (PanINs) in various stages of severity, PanIN1-3 with intermediate forms (Klimstra *et al.*, 1994; Hruban *et al.*, 2008). Next-generation sequencing showed that mutations in the KRAS gene as well as in tumor suppressor genes, such as TP53, CDKN2A, and SMAD4, are very common in PDAC.

The development of pancreatic adenocarcinoma starting from an initial PanIN (PanIN1) is accompanied by the acquisition of early mutations of the KRAS oncogene, which is the most common mutation in PDACs (Hingorani *et al.*, 2003). In the vast majority of cases, inactivation of the p16INK4A protein and the ARF-P53 tumor suppressor pathway follow in PanIN3, which corresponds to the form of carcinoma in situ (Weinberg, 2014). Additional mutations of cancer-related genes, such as overexpression of RAC-beta serine/threonine-protein kinase

(Akt2) and increased activity of its upstream regulator phosphoinositide 3-kinase (PI3K) lead to invasive pancreatic cancer in stepwise progression, resulting in an overall increase of tumor cell survival (Orth *et al.*, 2019; Weinberg, 2014).

## **1.2 Tumor Microenvironment in PDAC**

In the theory of immune surveillance of tumors, Paul Ehrlich (Ehrlich, 1909) as well as Lewis Thomas (Thomas and Lawrence, 1959), and Macfarlane Burnet (Burnet, 1970) already postulated that changes in a cell during the development of a tumor can be recognized by the immune system as foreign and attacked. Cancer cells can efficiently present their own antigens and activate immune responses leading to their elimination. To escape immune surveillance and attack by the immune system, tumor cells develop various strategies (Ribatti, 2017). These include antigen loss, downregulation of major histocompatibility complex (MHC) molecules, deregulation or loss of components of the endogenous antigen priming signaling pathway, tumor-induced immunosuppression driven by cytokine release, or direct interactions between tumor ligands and immune cell receptors (Garcia-Lora *et al.*, 2003). Immunoediting also contributes to this process by causing the selection of tumor cell subpopulations that are recognized and eliminated by the immune system, leaving behind resistant tumor cells that can continue to proliferate and thus contribute to tumor formation (Bui and Schreiber, 2007). Tumor stroma and the TME continue to play a critical role in PDAC progression and metastasis. A desmoplastic stromal reaction (desmoplasia) is considered as one of the characteristic features for PDACs, leading to massive activation of stroma and stromal cells in the TME (Huber *et al.*, 2020). Tumor stroma is the term used to describe the connective tissue around carcinoma foci, which is very rich in collagen (Chu *et al.*, 2007). The cellular components of the PDAC stroma include the extracellular matrix (ECM), endothelial cells, cancer-associated fibroblasts (CAFs), mesenchymal stem cells, and various innate immune cells such as macrophages, T cells, natural killer cells (NK cells), and neutrophils (Ungefroren *et al.*, 2011). Among themselves, these components communicate and interact by means of either autocrine or paracrine signal transduction (Grivennikov *et al.*, 2010). An extensive stroma is not only present in PDAC, but also chronic pancreatitis (Helm *et al.*, 2014). This indicates that the beginning of

stromal development can be observed in the environment of the earliest PanIN lesions before the maturing of PDAC (Detlefsen *et al.*, 2005; Clark *et al.*, 2007).

Stromal cells strongly influence TME as well as immune system interaction with tumors (Coussens and Werb, 2002; Vasievich and Huang, 2011). Immune cells residing in the TME, especially tumor-associated macrophages (TAMs), were initially viewed as the body's response to eliminate the tumor. There is now some evidence that tumor-associated immune cells contribute significantly to tumor development.

As early as 1863, the German pathologist Rudolf Virchow provided due to his observations of the presence of immune cells within tumors the first indication of a possible link between inflammation and cancer (Balkwill and Mantovani, 2001). Yet, in the last decade, clear evidence has been obtained that the TME with its inflammatory nature is an essential component of all tumors (Mantovani *et al.*, 2008) and inflammation has a tumor-promoting effect (Karin, 2006).

Also, in PDAC, immune cells and their involvement in tissue inflammation play a significant role. This is reflected by the fact that chronic pancreatitis is a recognized risk factor for the formation of pancreatic cancer (Grover and Syngal, 2010). In 2012, the Rhim *et al.* group was able to demonstrate a link between tumor cell dissemination and inflammation in their PDAC mouse model, whereby induction of pancreatitis allowed an increase in circulating pancreatic ductal epithelial cells to be detected in the blood. In contrast, anti-inflammatory treatment of pancreatitis with dexamethasone blocked cell dissemination. Histological examination of the inflammatory areas showed numerous pancreatic ductal epithelial cells with a mesenchymal and invasive phenotype already detected in the PanIN stages. It can be concluded that inflammation enhances cancer progression by entry into the circulation (Rhim *et al.*, 2012).

Normal pancreatic tissue exhibits low infiltration of immune cells, in contrast, the pancreatic stromal compartment undergoes fundamental changes during progression to invasive PDAC (Protti and De Monte, 2013). With the formation of an immunosuppressive milieu, there is an accumulation of diverse immune cells (Helm *et al.*, 2014). The main part of the immune infiltrate in the tumor stroma of PDAC is formed by high numbers of TAMs and T cells (Komura *et al.*, 2015). The TAMs represent the largest fraction and are present in chronic pancreatitis, PanIN as well as in PDAC (Clark *et al.*, 2007; Kurahara *et al.*, 2011).

### 1.2.1 T cells in PDAC

T lymphocytes are the central effectors of specific cellular immunity. The totality of T cells is detected with the surface protein CD3. This is expressed on thymocytes and T cells. After their differentiation in the thymus, they are divided into the main subgroups of CD8<sup>+</sup> and CD4<sup>+</sup> T cells, according to their surface marker. Depending on their function (killing, activation, regulation) and immunophenotypic surface molecules, these immune cells can be distinguished (Janeway and Murphy, 2009). Under healthy conditions, the number of CD3<sup>+</sup> T cells in the blood is higher than that of their subpopulations and the number of CD4<sup>+</sup> T cells is higher than the number of CD8<sup>+</sup> T cells (Bosire *et al.*, 2013). During PDAC progression, there is an enrichment of CD4<sup>+</sup> T cells. In contrast, the number of cytotoxic CD8<sup>+</sup> T cells declines (Clark *et al.*, 2007). This statement was also confirmed by the Hiraoka *et al.* group. Their studies showed that there is an accumulation of CD4<sup>+</sup> T cells during progression from PanIN to invasive PDAC compared with the non-neoplastic inflammatory pancreatic stroma (Hiraoka *et al.*, 2006). Conversely, there was a decrease in intraepithelial cytotoxic CD8<sup>+</sup> T cells during progression from PanIN to invasive PDAC. Moreover, PDAC escapes immune surveillance by attracting and accumulating CD4<sup>+</sup> T cells. Although the proportions of CD4<sup>+</sup> and CD8<sup>+</sup> T cells were significantly lower in PDAC, the number of CD4<sup>+</sup> regulatory T cells was higher than in chronic pancreatitis (Helm *et al.*, 2014). The CD4<sup>+</sup> accumulation is observed in blood and tumor tissue of PDAC patients, which correlates with poor prognosis (Grivennikov *et al.*, 2010; Hiraoka *et al.*, 2006; Liyanage *et al.*, 2002). In contrast, high CD8<sup>+</sup> T cell density is associated with longer survival (Fukunage *et al.*, 2004). However, the study by Ino *et al.* reported that higher expression levels of CD3<sup>+</sup> T, CD4<sup>+</sup> T, and CD8<sup>+</sup> T cells significantly correlate with longer and disease-free survival in PDAC patients, whereas the opposite was observed with lower expression levels of CD8<sup>+</sup> T (Ino *et al.*, 2019). It is also known that increased activation of CD4<sup>+</sup> T cells leads to increased inflammation in PDAC and as well as accelerated tumor progression (Ochi *et al.*, 2012; Grage-Griegenov *et al.*, 2014). All in all, T lymphocytes, as one of the predominant subsets of immune cells, exert both tumor-promoting and tumor-suppressing effects on PDAC (Liu *et al.*, 2019).

### 1.2.2 Macrophages in PDAC

Macrophage infiltration can be observed in the early precursor lesions of PDAC (Clark *et al.*, 2007). Many studies demonstrate that for many human tumors, a correlation can be identified between the number of infiltrating macrophages and the prognosis for the patient. This observation indicates that macrophages are important for tumor biology, for instance in invasive breast carcinoma, prostate cancer, oral squamous cell carcinoma, gastric cancer, uveal melanoma, lung adenocarcinoma, and in PDAC (Clark *et al.*, 2007; Leek *et al.*, 1996; Lissbrant *et al.*, 2000; Fujii *et al.*, 2012; Zhang *et al.*, 2011; Kawahara *et al.*, 2010; Mäkitje *et al.*, 2001; Steidl *et al.*, 2010). For example, it has been demonstrated that compared to normal pancreatic tissue, there is an increase in CD68<sup>+</sup> macrophage number in PDAC tissue (Esposito *et al.*, 2004).

It is well known that this increased amount of macrophages in some human tumors such as invasive breast carcinoma, prostate cancer, oral squamous cell carcinoma, gastric cancer, uveal melanoma, lung adenocarcinoma, and in PDAC correlates with a worse prognosis and a decreased average survival time (Leek *et al.*, 1996; Lissbrant *et al.*, 2000; Fujii *et al.*, 2012; Zhang *et al.*, 2011; Kawahara *et al.*, 2010; Mäkitje *et al.*, 2001; Steidl *et al.*, 2010; Ino *et al.*, 2013). In contrast, the study by the Esposito *et al.* group provided that a correlation with cumulative survival could not be observed in PDAC tissue (Esposito *et al.*, 2004). Several scientific studies demonstrate that M2- polarized macrophages from PDAC patients exhibit a progression-promoting effect on tumors (Kurahara *et al.*, 2011; Ino *et al.*, 2013). It has been shown that the number of M1- (HLA-DR<sup>+</sup>) polarized macrophages decrease with progression from chronic pancreatitis to PDAC, whereas heavy infiltration of M2 polarized macrophages (CD163<sup>+</sup>, CD204<sup>+</sup>), on the other hand, significantly correlates with poorer prognosis and survival (Ino *et al.*, 2013). In addition, the research group of Kurahara *et al.* demonstrated that a high incidence of M2 polarized TMAs (CD163<sup>+</sup>, CD204<sup>+</sup>) correlates with increased lymphangiogenesis as well as lymph node metastasis and poor prognosis (Kurahara *et al.*, 2013). However, in the scientific studies, the group of Helm *et al.* showed that the CD68<sup>+</sup> macrophages were more abundant in chronic pancreatitis compared with PDACs but localized more closely to carcinoma cells in PDAC. A similar observation was made for both M1- and M2- polarized TMAs. Thereby, M1- (HLA-DR<sup>+</sup>) macrophages also show up in areas with high

numbers of M2- (CD163<sup>+</sup>) macrophages. This leads to the assumption that macrophages of the PDAC infiltrate show M1 and M2 characteristics equally and that it is primarily a mixed phenotype (Helm *et al.*, 2014). These results suggest that TAMs have both anti-inflammatory and pro-inflammatory properties, through which they equally influence the induction of epithelial-mesenchymal transition and the development of PDAC (Helm *et al.*, 2014). Although it is known that high numbers of TAMs are associated with poor prognosis, the role of this cell type in pancreatic cancer remains partially still elusive.

### **1.3 Extracellular Vesicles**

Extracellular vesicles (EVs) are membrane vesicles that are released by various types of mammalian cells into the extracellular space. Based on their biogenesis, EVs can be classified in microvesicles, exosomes (Van Niel *et al.*, 2018), and apoptotic bodies (Yáñez-Mó *et al.*, 2015). Microvesicles arise by outward budding from the plasma membrane and range from 50-500 nm (Van Niel *et al.*, 2018). Apoptotic bodies are membrane blebs released by cells undergoing apoptosis and are 50-5000 nm in diameter (Raposo and Stoorvogel, 2013). The exosomes ranging in size from 30 to 100 nm originate from the multivesicular endosome and are released by the fusion of multivesicular bodies (MVB) with the plasma membrane (Sumrin *et al.*, 18) (Figure 1).

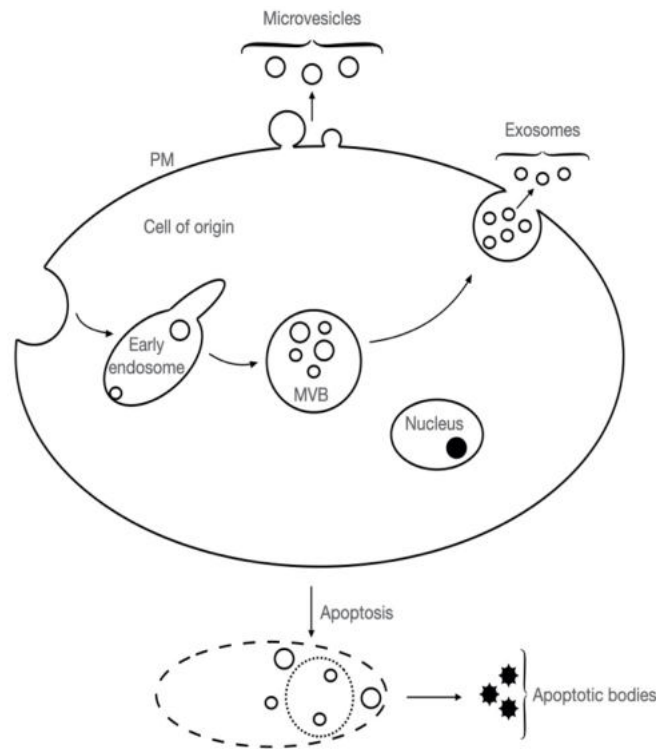


**Figure 1. Illustration of the biogenesis of several types of EVs, including microvesicles, apoptotic bodies and exosomes.** Exosomes are released upon fusion with the plasma membrane (PM) of multivesicular bodies (MVBs). Microvesicles are formed by outward budding from the plasma membrane and apoptotic bodies are released from cells undergoing apoptosis.

### 1.3.1 Exosomes in Cancer

In addition to immune cells, tumor cells are also capable of secreting EVs that are related to cancer immunity used as a means of intercellular communication (Sumrin *et al.*, 2018). Several cancer cells produce elevated levels of exosomes, for instance, in the breast (King *et al.*, 2012), glioblastoma (Skog *et al.*, 2008), colorectal (Silva *et al.*, 2012), brain (Graner *et al.*, 2009), ovarian (Escrevente *et al.*, 2011), prostate (Mitchell *et al.*, 2009; Nilsson *et al.*, 2009), bladder (Welton *et al.*, 2010) and lung cancer patients compared to that of healthy individuals (Rabinowits *et al.*, 2009). In 2016, it has been demonstrated by Chiarugi and Cirri that tumor cells even release at least 10 - fold higher number of exosomes into the microenvironment than normal cells do. This leads to a manipulation of their microenvironment from a normal state to a tumor state making it more favorable for tumor growth, invasion, and drug resistance (Chiarugi and Cirri, 2016). For instance, exosomes released from glioblastoma were found to be enriched in angiogenic proteins that allowed them to stimulate angiogenesis in endothelial cells (Skog *et al.*, 2008). Besides the fact that tumor cells release a larger number



of exosomes compared to healthy individuals, it was shown by Akers et al. in 2013 that tumor-derived exosomes are capable of facilitating communication between tumor and normal cells through the transport of growth factors, chemokines, miRNAs, and other tumor molecular signatures that may contribute to facilitating the discrimination between cancer afflicted patients and healthy individuals (Akers *et al.*, 2013). Moreover, tumor-derived exosomes seem to be capable of playing different roles. In 2001, the research group Wolfers published that tumor-derived exosomes serve as promoters of an anti-tumor immune response by transferring tumor antigens to dendritic cells, resulting in CD8<sup>+</sup> T cell-dependent anti-tumor effects (Wolfers *et al.*, 2001). In contrast to the last-mentioned case, exosomes released by tumor cells have also been implicated in promoting tumor immune resistance as Andreola et al. showed that melanoma cell derived exosomes induce apoptosis of T cells (Andreola *et al.*, 2002). Thus, exosomes from tumor cell seem to be involved in both, immunosurveillance and immunotolerance. As it is previously reported exosomes play an important role in pancreatic cancer progression. Pancreatic cancer exosomes induce the formation of pre-metastatic niches in the liver by allowing the fibrotic environment associated with exosomes to lead to the recruitment of macrophages from the bone marrow, thus creating a pro-metastatic inflammatory environment (Costa-Silva *et al.*, 2015). It is known from various research groups that there are good diagnostic markers for early detection of pancreatic cancer such as lipocalin 2 (Chakraborty *et al.*, 2012) or miRNA-196a/ -b and even combinations of biomarkers (Bartsch *et al.*, 2018; Slater *et al.*, 2013; Slater *et al.*, 2014). Glypican-1 was suggested as a biomarker in PDAC exosomes (Melo *et al.*, 2015), however, not found to be a good diagnostic marker for detection of PDAC in early stages (Bartsch *et al.*, 2018). For this reason, the search for more specific biomarkers released by PDAC exosomes, in particular, will continue.

### **1.3.2 Exosome encapsulated miRNAs as based prognostic biomarkers for PDAC**

It is known that exosomes carry a characteristic and cell type-specific composition of molecular cargo including proteins, lipids, miRNA, and mRNA inherited from the parental cell (Raposo and Stoorvogel, 2013). In addition, EV mediated miRNA transfer between immune cells, recent reports have suggested a pathological significance for EV-mediated transport of tumor cell-associated miRNAs.

MiRNAs, which were first described in 1993, are small noncoding RNAs and consist of only 18-24 nucleotides in length (Lee *et al.*, 1993). They are involved in the negative regulation of gene expression at the post-transcriptional level by binding to the highly conserved 3' untranslated region (3'-UTR) of target mRNAs. These target mRNAs are either inhibited from translation or degraded by cutting, depending on the complementarity of the binding sequence and the proteins involved. Thus, they participate in cellular protein synthesis, however, perform a function virtually opposite to that of mRNA (He and Hannon, 2004).

MiRNAs undergo a processing procedure for maturation. Like all RNAs, miRNAs are transcribed from DNA. The primary transcripts originate either from introns of mRNA precursors, specific genes, or clusters from which multiple miRNAs can be produced (Treiber *et al.*, 2017). Initially, multiple primary miRNAs (pri-miRNAs) are present in a large transcript. These pri-mRNAs are several hundred to a thousand nucleotides long and contain the sequences of at least one miRNA. At some sites, "stem-loop" structures of about 70 nucleotides in length are formed (Lodish *et al.*, 2013). These are recognized by the nuclear double-strand-specific RNase III DROSHA in the nucleus and excised from this transcript, giving rise to individual precursor miRNAs (pre-miRNAs) (Treiber *et al.*, 2017). Then the pre-miRNAs can be transported from the nucleus into the cytoplasm with the help of the transport protein "Exportin 5". There, they are trimmed by another RNase III (Dicer), thus forming a mature double-stranded miRNA called miRNA duplex. One of these two miRNA strands is now incorporated into the RNA-induced silencing complex, which is an enzyme complex abbreviated as "RISC". The bound miRNA now associates with complementary regions of the 3'UTR of the corresponding target mRNA. Here, more than one RISC loaded with miRNA bind

to the mRNA for translational inhibition to occur (Lodish *et al.*, 2013). Finally, either inhibition of translation or degradation by cutting is initiated. Which of the two effects occurs depends on the extent of complementarity between miRNA and mRNA: in the case of full complementarity, cleavage of the mRNA occurs; in the case of partial complementarity, only translational inhibition occurs (He and Hannon, 2004) (Figure 2).

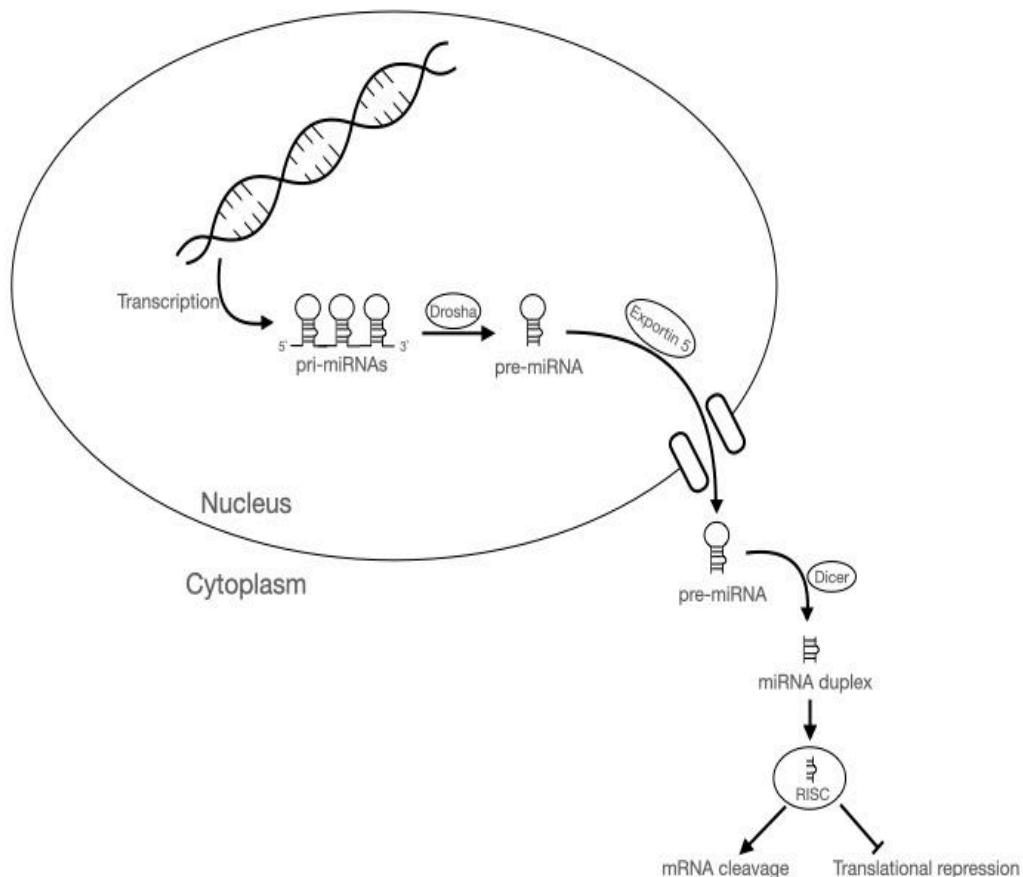


**Figure 2. Pathway of the microRNA maturation and the mechanism of post-transcriptional repression of protein biosynthesis.** In the nucleus the pri-miRNA is processed to pre-miRNA by the RNase DROSHA. Pre-miRNAs are transported into the cytoplasm with the help of exportin 5, where it is converted into the mature double-stranded miRNA by the RNase Dicer. One strand of the miRNA duplex is loaded onto the RNA induced silencing complex (RISC). This fusion associates with the target mRNA and induces inhibition of translation or mRNA degradation by cutting.

There is plenty of evidence that miRNAs are dysregulated in different types of cancer. Depending on which mRNA they affect, microRNAs can function either as tumor suppressors, such as let-7b, miRNA-15a, and miRNA-16-1, or oncogenes like miRNA-21 and -155 (Croce, 2009).

Many miRNAs show aberrantly high levels in cancer, contributing to tumorigenesis and metastasis. In 2007, Szafranska *et al.* performed the first analysis to study miRNA expression in PDAC in PDAC tissue cells (Szafranska *et*

*al.*, 2007). Many research groups have discovered that, for instance, miRNA-21, -155, and -196 were consistently dysregulated in PDAC, indicating that these miRNAs may serve as potential biomarkers for lesions and early-stage cancer (Szafranska *et al.*, 2007; Lee *et al.*, 2007; Hernandez and Lucas, 2016). In this regard, Lee *et al.* developed a survey of the expression pattern of microRNAs associated with pancreatic cancer. They found that increased expression levels of miRNA-221, -100, -125b, and -21 are observed in both exocrine and endocrine pancreatic tumors (Lee *et al.*, 2007). Based on these findings, Schultz *et al.* attempted to compare the miRNA profile in the blood of pancreatic cancer patients with healthy controls (Schultz *et al.*, 2014). This new approach aims to use EV encapsulated miRNAs as prognostic biomarkers for PDAC to enable early diagnosis. In addition, ADAM8 will be investigated as a potential biomarker in the context of miRNAs encapsulated in EVs and as a surface protein of EVs for the early diagnosis of PDAC.

#### **1.4 ADAM8**

ADAM8 is a member of a disintegrin and metalloproteinase family which consists of 21 human ADAM proteins (Murphy, 2008). It is a membrane-bound metalloproteinase located on the surface of EVs with proteolytic activity (Shimoda and Khokha, 2017; Das *et al.*, 2016). This metalloproteinase is composed of a basic modular structure of three entities with several segments as seen in figure 3. ADAM8 is initially synthesized as a proteolytically inactive proform protein with multiple domains of 120 kDa. Autocatalytic cleavage of the prodomain results in an active membrane-bound metalloprotease with a molecular weight of 90 kDa, which can be further processed to a residual form of 60 kDa by the release of the metalloproteinase domain into the extracellular matrix (Das *et al.*, 2016; Schlomann *et al.*, 2015) (Figure 3).

As a cell surface protein, it fulfills important roles in many biological processes (Roemer *et al.*, 2004). With the help of its multidomain structure, ADAM8 can perform diverse cellular functions ranging from cell adhesion, cell fusion, cell signaling to proteolysis. The metalloprotease-disintegrin ADAM8 is also involved in promoting PDAC tumor progression, invasion, and metastasis (Schlomann *et al.*, 2015). However, the expression profile of ADAM8 in the TME remains still elusive.

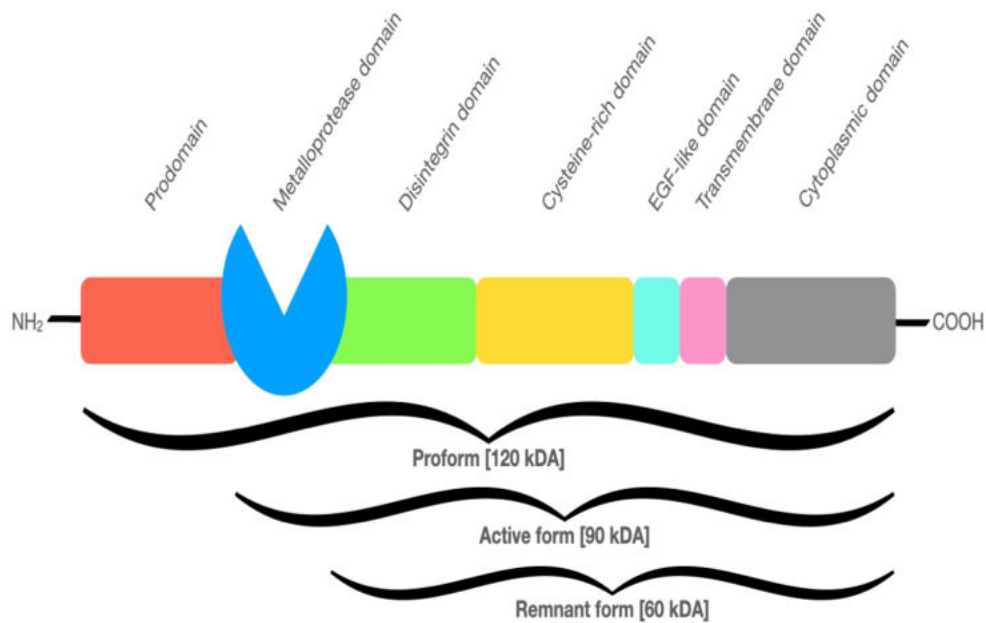


**Figure 3. Basic modular structure of ADAM8 with possible three entities.** ADAM8 consists of an N-terminal prodomain, a metalloprotease domain, a disintegrin domain, a cysteine-rich region, an EGF-like (epidermal growth factor) domain followed by a single-span transmembrane domain and a cytoplasmic tail at the C-terminal. Totally, three entities of ADAM8 are possible (Das *et al.*, 2016; Schlomann *et al.*, 2015).

Since ADAM8 is secreted by pancreatic cancer exosomes and these exosomes have been shown to modulate TME through mechanisms that ADAM8 can provide, ADAM8 serves as a mediator of signal transduction (Costa-Silva *et al.*, 2015). High levels of ADAM8 expression negatively correlate with patient prognosis, resulting in shortened survival and an increased metastatic spread in PDAC (Valkovskaya *et al.*, 2007). Further, ADAM8 was reported to be highly expressed in the vast majority of lung cancers (Ishikawa *et al.*, 2004), in renal cancer (Roemer *et al.*, 2004) and in PDAC (Schlomann *et al.*, 2015). An increased ADAM8 expression was also observed in TAMs as shown in glioblastoma (Gjorgjevski *et al.*, 2019). It is known that in triple-negative breast cancer (TNBC) patient serum ADAM8 specifically is involved in inducing miR-720 which results in increased tumor migration and invasion (Das *et al.*, 2016).

This novel approach aims to use ADAM8 as a potential biomarker in the context of EVs as well as of miRNAs for the early diagnosis of PDAC.

## 1.5 Protein Arginine Methyltransferases

To relate to the research question, protein arginine methyltransferases (PRMTs) are presented in this section, as well as previous findings related to PDAC.

PRMTs are enzymes that are involved in several cellular functions. The main task of PRMTs is to transfer a methyl group from the methyl donor S-adenosylmethionine (SAM) to the N-terminal of arginine residues of either cytoplasmic or nuclear proteins, including histones (Jahan and Davie, 2015). This transfer highlights the importance of PRMTs as key regulators in post-translational modifications (Kim *et al.*, 2016). Based on this, histone methylation can alter chromatin architecture. Thus, the recruitment of protein complexes such as transcription factors is facilitated and gene expression is influenced (Kim *et al.*, 2020). Besides the remodeling of the chromatin, arginine methylation plays a role in various cellular processes, such as DNA repair, signal transduction, regulation of gene expression like mRNA splicing, cell proliferation, translocations, protein-protein interactions, and also immunological processes, for instance (Kim *et al.*, 2016). There are currently nine identified members of the PRMT family in mammals. As seen in figure 4, PRMTs are classified into three types and catalyze the formation of monomethyl arginine (MMA), which later develop to dimethylarginines in Type II symmetric- (SDMA) or Type I asymmetric (ADMA) conformation of the methyl groups by placing the second methyl group on the substrate (Bedford and Richard, 2005) (Figure 4).

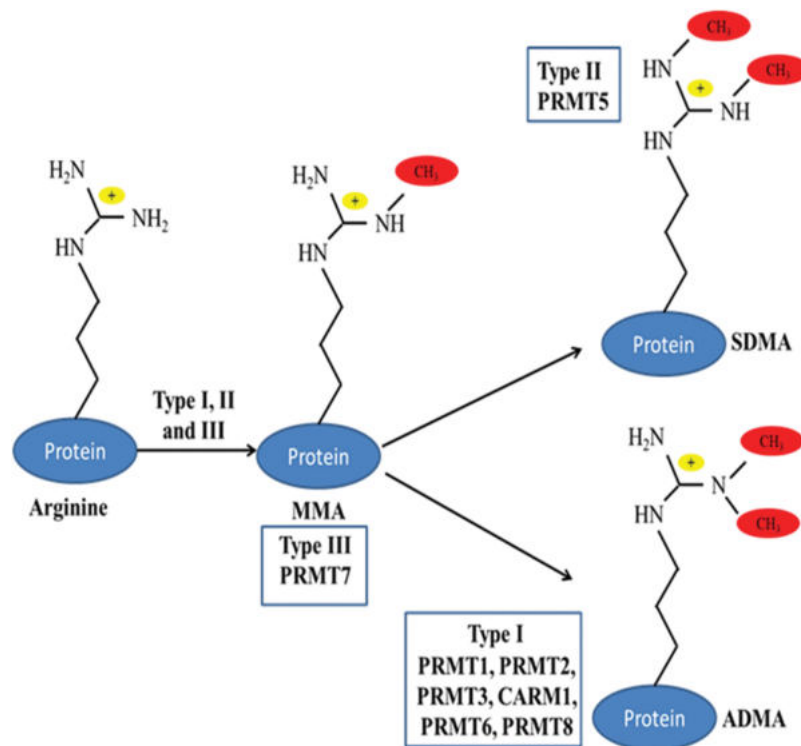


**Figure 4. PRMT catalysis and classification.** Nine members of the PRMT family are identified in mammals. The formation of monomethylarginine (MMA) is catalyzed by type I, II and III PRMTs. By placing the second methyl group on the substrate Type I PRMTs catalyse asymmetric dimethylarginine (ADMA), while type II PRMTs form symmetric dimethylarginine (SDMA). The PRMTs 1, 2, 3, 4, 6 and 8 belong to Type I PRMTs while type II PRMT includes PRMT5 and 7 is a type III PRMT. The enzymatic activity of PRMT9 remains still elusive (Morettin *et al.*, 2015).

According to the substrate, PRMTs can function as a transcriptional activator but also as a suppressor in pancreatic cancer (Kim *et al.*, 2016; Wang *et al.*, 2016) and are deregulated (Wang *et al.*, 2016) or hyperactive (Song *et al.*, 2020) in tumor cells. Many PRMT-related publications focused on cancer show that PRMTs promote oncogenesis in PDAC tumor cells (Song *et al.*, 2020; Jarrold and Davies, 2019). In particular, the members of the type I PRMTs, namely PRMT1 and PRMT4, were those proteins we were interested in, as their biological functions of expression in PDAC remain still elusive.

## 1.6 Aim of the study

The main goal of this study is to identify good diagnostic markers to diagnose PDAC at early stages, as the search for new potential biomarkers is a major challenge for oncology and early detection is key to reducing disease and mortality. In this context, exosomes are promising candidates for early PDAC diagnosis. They are released by all cell types but play a poorly understood role in cell communication. For this reason, I performed my experimental analyses on serum exosomes based on both the protein and miRNA levels to detect promising candidates as diagnostic markers to discriminate precursor lesions or PDAC from healthy controls.

ADAM8, a disintegrin and metalloprotease 8, was detected on the surface of serum exosomes and leads to increased metastatic capacity in PDAC. To achieve the main objective of this work, my task was to determine the localization, distribution, and amount of ADAM8 in PDAC and tumor microenvironment by IHC. Evaluations were performed to elucidate ADAM8-dependent signaling and its effects on the TME of the PDAC.

In addition, dysregulations in the expression pattern of serum exosome miRNAs reported to be differentially expressed in different cancer types were to be identified. In this context, I investigated miRNAs in ADAM8-positive serum exosomes, which could also serve as potential biomarkers for the prognosis and diagnosis of PDAC.

A total cohort of 72 PDAC patients was studied, and 20 healthy individuals were used as a comparison. All experiments were performed with the same patient cohort to build an information network about PDAC and its potential biomarkers.

To establish a correlation between the regulation of serum exosome miRNAs and protein arginine methyltransferases and to investigate their role in PDAC and its microenvironment, PRMT1 and PRMT4 were investigated as potential biomarker proteins in PDAC by IHC. Based on the knowledge already gained, the expression of PRMT1 and PRMT4 should be investigated in the same patient cohort as before, which is currently being continued in another ongoing project.

Asymmetric arginine dimethylation is catalyzed by type I PRMTs such as PRMT1 and PRMT4. Further functional characterization of the serum proteins PRMT1 and PRMT4 in PDAC will be one of the tasks in the further course of the project already started.



## 2 Summary of the publications

### 2.1 Cohort Analysis of ADAM8 Expression in the PDAC Tumor Stroma

Christian Jaworek<sup>1#</sup>, Yesim Verel Yilmaz<sup>2#</sup>, Sarah Driesch<sup>2</sup>, Sarah Ostgathe<sup>1</sup>, Lena Cook<sup>1</sup>, Steffen Wagner<sup>3</sup>, Detlef K. Bartsch<sup>2</sup>, Emily P. Slater<sup>2</sup>, Jörg W. Bartsch<sup>1</sup>

<sup>#</sup>These authors have contributed equally to this work

(2021). Cohort analysis of ADAM8 expression in the PDAC tumor stroma. *Journal of Personalized Medicine*, 11(2), 113.

#### 2.1.1 Scientific summary of the publication

Tumor stroma and the TME continue to play a critical role in PDAC progression and metastasis. A desmoplastic stromal reaction, desmoplasia, is considered as one of the characteristic features for PDACs, leading to massive activation of stroma and stromal cells in the TME. There is now some evidence that tumor-associated immune cells can be observed in the environment of the earliest PanIN lesions secreted by tumor cells and that these immune cells contribute significantly to tumor development. ADAM8 is highly expressed in pancreatic cancer cells, modulates cell migration and invasion and promotes tumor progression and metastasis of PDAC. Based on a scientific study of glioblastoma in which ADAM8 was strongly expressed in tumor-associated immune cells, we examined ADAM8 expression in the stroma of PDAC tumor tissue sections derived of a cohort of 72 patients. These sections were recruited by the Department of Visceral Surgery at the University Hospital Marburg, histologically evaluated, and classified according to the Union for International Cancer Control; Tumor, Node, Metastasis (UICC-TNM) classification for preparing this study.

50 PDAC patients of the cohort were split into two groups depending on their median survival time with less than 22 months or longer than 22 months (Figure 1). Immunohistochemical (IHC) single staining was performed of PDAC tissue sections with 3,3'-diaminobenzidine (DAB)-stained for ADAM8. Signal intensities and IHC scores were determined on each section ranging from 0 to 3 with no (Figure 1A), low (Figure 1B), moderate (Figure 1C) and strong (Figure 1D) ADAM8 expression levels in PDAC tumor cells. With the exception of two PDAC sections, which hardly showed any ADAM8 expression, all tumor tissues stained positive for ADAM8. However, no significant difference in

ADAM8 expression was observed between the two survival groups (Figure 1E). To investigate the expression cluster of ADAM8 in specific tumor-associated cells and for a deeper understanding of their association in the tumor microenvironment, immunohistochemical double staining of 10 PDAC tissue sections was performed with ADAM8 and several stromal cell markers (Figure 2). Co-localization of ADAM8 was observed with macrophage marker (CD68; Figure 2B) for 0-17 %, NK-cell marker (CD56; Figure 2F) for 18-75 %, and neutrophil marker myeloperoxidase (MPO; Figure 2H) for 30-90 %. No significant expression revealed for T-cell markers CD3 (Figure 2C), CD4 (Figure 2D), CD8 (Figure 2E), and stellate cell marker smooth-muscle actin (SMA; Figure 2G).

A quantification of the co-localization of ADAM8 with several stromal cells in PDAC sections as performed in figure 2 revealed or reflected the same results of expression levels of ADAM8 positive cells (Figure 3).

Furthermore, a common observation of ADAM8 expression in neutrophils was mainly in the post-capillary veins (Figure 4C-D) from where neutrophils normally enter the tissue beside its expression in ducti (Figure 4A) and in tumor stroma of PDAC (Figure 4B).

For further analysis, ADAM8-positive neutrophil density ( $n/\mu\text{m}^2$ ) was quantified by scoring neutrophils in at least three independent postcapillary veins with an area of  $>2000 \mu\text{m}^2$  in PDAC tumor tissue (Figure 5). It was confirmed that an increased number of ADAM8 positive neutrophils in post-capillary veins negatively correlates with PDAC patient survival (Figure 5A). Moreover, density of neutrophils was significantly higher in PDAC patients with a median survival of fewer than 18 months compared to PDAC patients with a median survival of more than 18 months (Figure 5B). However, there was no correlation between neutrophils present in peripheral blood (Figure 5C) and the neutrophil-to-leukocyte ratio (Figure 5D) with PDAC patient survival.

### **2.1.2 Description of the personal contribution**

Personal contribution to the preparation of this scientific research article includes involvement in the experimental design, conduct and data analysis of tables 1 and 2, figures 1A-E, 2A-H, 3 and 4, as well as all staining procedures in PDAC patients in a cohort of 72 patients.

## 2.2 PRMT1 promotes the tumor suppressor function of p14<sup>ARF</sup> and is indicative for pancreatic cancer prognosis

Antje Repenning<sup>1†</sup>, Daniela Happel<sup>1†</sup>, Caroline Bouchard<sup>1</sup>, Marion Meixner<sup>1</sup>, Yesim Verel-Yilmaz<sup>2</sup>, Hartmann Raifer<sup>3,4</sup>, Lena Holembowski<sup>1</sup>, Eberhard Krause<sup>5</sup>, Elisabeth Kremmer<sup>6</sup>, Regina Feederle<sup>7</sup>, Corinna U Keber<sup>8</sup>, Michael Lohoff<sup>4</sup>, Emily P Slater<sup>2</sup>, Detlef K Bartsch<sup>2</sup>, Uta-Maria Bauer<sup>1\*</sup>

† These authors have contributed equally to this work

(2021). PRMT1 promotes the tumor suppressor function of p14<sup>ARF</sup> and is indicative for pancreatic cancer prognosis. The EMBO Journal, 40(13), e106777.

### 2.2.1 Scientific summary of the publication

p14<sup>ARF</sup> is a nucleolar protein with tumor suppressor function and bound to its nucleolar interaction partner nucleophosmin (NPM) in unstressed situation. The protein arginine methyltransferase 1 (PRMT1), is mainly located in the nucleus and covers vital functions. Therefore, a complete deletion of PRMT1 expression leads to loss of cell viability and embryonic mortality in mice, indicating an essential role of arginine methylation in embryonic development. Moreover, in the absence of cellular stress, PRMT1 ensures that p14<sup>ARF</sup> is more stable in the nucleolus. If the cell is under genotoxic stress, p14<sup>ARF</sup> has been activated by PRMT1-mediated arginine methylation of the C-terminal residues of p14<sup>ARF</sup>. In this case, the methylated p14<sup>ARF</sup> leaves the nucleolus and migrates to nucleo- and cytoplasm, where it functions as a tumor suppressor and promotes cell apoptosis as an emergency case, associated with reduced protein stability.

The hypothesis is that this PRMT1-p14<sup>ARF</sup> cooperation is tumor-relevant and predictive of PDAC prognosis, as a cell with stress-induced over-expression of PRMT1 and thus apoptosis triggered by p14<sup>ARF</sup> is well-equipped to respond to stress signals such as chemotherapy, possibly resulting in longer survival of PDAC patients. PRMT1-mediated arginine methylation is an important trigger for the stress-induced tumor suppressive function of p14<sup>ARF</sup>. Therefore, this study focused on verifying the role of PRMT1-mediated methylation of p14<sup>ARF</sup>.

To verify that p14<sup>ARF</sup> is arginine methylated a metabolic labelling of methylated p14<sup>ARF</sup> was performed. Methylation of p14<sup>ARF</sup> was detected by fluorography (Figure 1A). To determine, which of the PRMT members is involved in the

methylation of p14<sup>ARF</sup>, a methyl transferase (MT) assay was performed using labelled p14<sup>ARF</sup> and PRMTs. As a result, PRMT1 and PRMT5 were found to methylate arginine residues in p14<sup>ARF</sup>, whereas PRMT4 showed no signal for p14<sup>ARF</sup>-modification (Figure 1B-C). Using GST-tagged p14<sup>ARF</sup> deletion constructs, it was verified that the methylation site of PRMT1 is located within the C-terminus of p14<sup>ARF</sup> (aa 65-132) (Figure 1D). In particular, by mass spectrometric analysis two specific arginine residues (R96/R99) in the C-terminal nuclear/nucleolar localization sequence (NLS/NoLS) of p14<sup>ARF</sup> modified by PRMT1 as the major mono- and dimethylation sites were identified (Figure 1E). Furthermore, PRMT1 was confirmed to modify the arginine residues in p14<sup>ARF</sup> (Figure 1F). Moreover, westernblot analysis of co-immunoprecipitation experiments verified that there is an interaction between Myc-tagged PRMT1 and Flag-tagged p14<sup>ARF</sup> interact (Figure 1G). All these data indicate that PRMT1 is an interaction partner of p14<sup>ARF</sup>, since p14<sup>ARF</sup> is arginine methylated within its C terminus by PRMT1 (Figure 1A-G).

Examination of the subcellular localization of endogenous p14<sup>ARF</sup> in HeLa cells by immunofluorescent staining revealed that endogenous p14<sup>ARF</sup> in control-transfected HeLa cells was mainly localized in the nucleolus (\*) and only rarely (<) in the nucleus and cytoplasm, whereas p14<sup>ARF</sup> after overexpression of PRMT1 showed an altered cellular distribution with predominant localization in the nucleus and cytoplasm (Figure 2A). This finding was also confirmed by cell counting, where the number of cells with nucleolar localization of exogenous p14<sup>ARF</sup> was greatly reduced with PRMT1 overexpression (Figure 2B) and the exogenous p14<sup>ARF</sup> mainly found in the nucleoli of U2OS cells (Figure 2C-D). By PRMT1 overexpression, an increased translocation of endogenous p14<sup>ARF</sup> to the nucleolus and cytoplasm was observed, relative to the translocation that was reduced when the mutated PRMT1 was overexpressed (Figure 2C-E). Furthermore, it was observed in several experiments that siRNA-mediated PRMT1 depletion resulted mainly in nucleolar p14<sup>ARF</sup> localization compared to the controls (Figure 2F-I). All in all, these findings suggest that PRMT1 regulates the cellular localization of p14<sup>ARF</sup>.

To examine whether the arginine residues within the NLS/NoLS of p14<sup>ARF</sup> methylated by PRMT1 crucial for the mainly nucleolar localization of p14<sup>ARF</sup>, four mutant arginines (R87/88/96/99) of p14<sup>ARF</sup> (glycines (RG), phenylalanines (RF) or lysines (RK)) were constellated. Overexpression of EGFP-tagged-p14<sup>ARF</sup>

wild type and these four mutant arginines (R87/88/96/99) of p14<sup>ARF</sup> in U2OS cells showed under three localization conditions that the mutant RK of p14<sup>ARF</sup> was localized as the highest in the nucleolus, like p14<sup>ARF</sup> wild type (Figure 3A-B). In contrast, the RG and RF arginine mutants of p14<sup>ARF</sup> showed significant nucleolus-to-cytoplasm localization, whereas the RF-mutant is most abundant in the cytoplasm (Figure 3A-B). These results suggest that the charge of the arginine residues determines the localization of p14<sup>ARF</sup>. Furthermore, overexpression of PRMT1 was found to result in a higher number of cells with nucleolar/cytoplasmic localization of wild-type p14<sup>ARF</sup> compared to the RK mutant (Figure 3C). To investigate whether PRMT1 is involved in the association of p14<sup>ARF</sup> with NPM, a co-immunoprecipitation analysis was performed. This revealed that when PRMT1 is overexpressed, endogenous p14<sup>ARF</sup> interacts at a lower level with endogenous NPM in HeLa cell extracts (Figure 3D). Stable p14<sup>ARF</sup> is known to interact with NPM in the nucleolus, while NPM associates with several protein regions of p14<sup>ARF</sup>, such as the C-terminal NLS/NoLS containing the arginine methylation sites R96 and R99 of PRMT1. To investigate whether methylation of these arginines affects the interaction between p14<sup>ARF</sup> and NPM, a pull-down assay was performed using two NLS/NoLS peptides of p14<sup>ARF</sup> (aa 91-99, aa 92-103) and their methylated versions. The NPM protein showed a stronger binding interaction with unmodified NLS/NoLS peptides than with modified peptides. These data suggest that PRMT1 regulates the nucleolar localization of p14<sup>ARF</sup> as the arginine methylation of the NLS/NoLS of p14<sup>ARF</sup> by PRMT1 results in the release of its nucleolar binding partner NPM (Figure 3E).

By Western blot analysis an overexpression of Flag-p14<sup>ARF</sup> wild type and its mutant arginines (RG/ RF/ RK) in several human cell lines showed that the mutant RK of p14<sup>ARF</sup> was overexpressed similarly to p14<sup>ARF</sup> wild type in U2OS and HeLa cells and even higher in HEK293 cells. In contrast, the RG and RF arginine mutants of p14<sup>ARF</sup> showed reduced protein levels (Figure 4A). Considering their transcript levels, it can be observed that transcript levels of RK and RG are higher than p14<sup>ARF</sup> wild type, whereas RK is the most abundant and RF is similar to p14<sup>ARF</sup> wild type (Figure 4B). In addition, a depletion of PRMT1 caused by siRNA resulted in an increased expression of endogenous p14<sup>ARF</sup> protein levels, while overexpression of PRMT1 caused a decrease in p14<sup>ARF</sup> protein levels (Figure 4C-D). To investigate whether PRMT1 affects the stability of p14<sup>ARF</sup> protein, a doxycycline (Dox)-inducible shRNA was used to deactivate

the endogenous PRMT1 in HeLa cells, which conversely leads to an enrichment of p14<sup>ARF</sup> protein levels and its stability (Figure 4E-G), similar to the addition of the translation inhibitor cycloheximide (CHX) (Figure 4F-G). Taken together, these results suggest that a redistribution of nucleolar p14<sup>ARF</sup> into the nucleo- and cytoplasm caused by PRMT1-mediated methylation is associated with reduced protein stability.

To investigate if stress-induced p14<sup>ARF</sup> activation is affected by PRMT1, in wild-type and PRMT1-depleted HeLa cells were exposed to UVC and then location of p14<sup>ARF</sup> was examined by immunofluorescence staining. After treatment with UVC radiation, the nucleolar localization of p14<sup>ARF</sup> was strongly reduced in wild-type cells compared to the untreated conditions (Figure 5A-B). Observing the PRMT1-depleted HeLa cells, there was a clear trend of increase of p14<sup>ARF</sup> located in the nucleolus from untreated to treated UVC radiation conditions (Figure 5A-B). Additionally, in the case of PRMT1 knockdown, there was an accumulation of p14<sup>ARF</sup> protein levels in both treated and untreated UVC cells (Figure 5C). To detect methylated p14<sup>ARF</sup>, an amonoclonal methyl-arginine-specific antibody (a-me-p14<sup>ARF</sup>) was developed that recognizes PRMT1-induced methylation of arginine residues of p14<sup>ARF</sup> (R96 and R99) as confirmed by Western blot analyses, overexpressed wild-type p14<sup>ARF</sup> compared to the RK mutant and PRMT1-depleted cell extracts (Figure 5D-E). After couple of hours of UVC treatment of HeLa cells a trend of increase of methylated p14<sup>ARF</sup> protein levels could be observed whereas the endogenous p14<sup>ARF</sup> got reduced, indicating that p14<sup>ARF</sup> methylation and p14<sup>ARF</sup> protein stability counter-correlate (Figure 5F). Moreover, PRMT1 knockout and PRMT1 control HeLa cell lines were established by CRISPR/Cas9 technology, to check whether PRMT1-mediated arginine methylation of p14<sup>ARF</sup> is triggered by UVC radiation. As a result, control cells revealed UVC-dependent methylation and reduced protein levels of endogenous p14<sup>ARF</sup>, while PRMT1 knockout cells demonstrated increased levels of p14<sup>ARF</sup> protein and no detectable methylation of p14<sup>ARF</sup> (Figure 5G). Observing a stress-dependent role of PRMT1 in p14<sup>ARF</sup> regulation in co-immunoprecipitation experiments with wild-type HeLa cells, the interaction between endogenous p14<sup>ARF</sup> and endogenous PRMT1 was increased upon UVC radiation and coexisted with endogenous p14<sup>ARF</sup> methylation (Figure 5H). Altogether, these data suggest that genotoxic stress triggers the interaction between p14<sup>ARF</sup> and PRMT1, together with methylation and nuclear release of p14<sup>ARF</sup>, resulting in a less stable but

probably functionally active tumor suppressor protein.

To investigate whether PRMT1 affects the tumor suppressor activities of p14<sup>ARF</sup>, such as induction of apoptosis, the cell cycle distribution in PRMT1-depleted HeLa cells was analyzed by FACS upon stressed or unstressed conditions. Under unstressed conditions, siRNA-mediated depletion of PRMT1 did not result in any significant changes in the cell cycle distribution compared to the control cells, whereas after stress supply by UVC radiation, PRMT1-depleted HeLa cells had a significantly lower number of cells in subG1 phase than the control cells (Figure 6A-B). In Addition, there was no significant difference between endogenous p14<sup>ARF</sup> methylation levels before and after stress treatment in PRMT1-depleted cells (Figure 6C). In respect to the hypothesis that PRMT1 expression induced by genotoxic stress causes apoptosis in the cell, apoptosis indication by PARP cleavage and AnnexinV staining, were used in the PRMT1 knockout HeLa cell lines. It was found that the PRMT1 knockout HeLa cell lines had less PARP cleavage and AnnexinV-positive cells after UVC treatment compared to the control clones (Figure 6D-E). To investigate whether apoptosis is promoted by PRMT1 through its arginine methylation sites in p14<sup>ARF</sup>, the p14<sup>ARF</sup> mutants RK and RF, were overexpressed in PRMT1 knockout HeLa cells. It was observed that the RF mutant had more AnnexinV-positive cells after UVC treatment compared to the RK (Figure 6F), suggesting that PRMT1 and arginine methylation of p14<sup>ARF</sup> contribute to the activation of apoptosis upon genotoxic stress. It was investigated whether the PRMT1 methylation sites in p14<sup>ARF</sup> affect its binding ability towards the pro-apoptotic protein p32. The p32 were identified as direct interaction partners of p14<sup>ARF</sup>. This p14<sup>ARF</sup>-p32 association induces apoptosis in cellular stress situations. The corresponding pull-down experiments showed that the p14<sup>ARF</sup> mutant has a stronger interaction with p32 than the wild type p14<sup>ARF</sup> (Figure 6G). By endogenous co-immunoprecipitation analyses, it is obvious that p14<sup>ARF</sup> interacts less efficiently with p32 in HeLa cell lines with PRMT1 knockout than in control cell lines (Figure 6H). Taken together, these data suggest that methylation of p14<sup>ARF</sup> by PRMT1 promotes p14<sup>ARF</sup>-p32 association. In order to further investigate not only the tumor suppressive activity of PRMT1, but also the clinical relevance of PRMT1 in association with p14<sup>ARF</sup> in PDAC, known as one of the most aggressive and lethal solid human tumors, the expression analyses of PRMT1 were performed on transcript and protein level with respect to survival of 75 PDAC patients. In this context, high transcript

levels of PRMT1 were found to correlate significantly with longer survival of PDAC patients (>500 days), while there was no significant difference for the short survival group (<500 days) (Figure 7A). To perform protein-level expression analysis of PRMT1 and p14<sup>ARF</sup> in PDAC, IHC was carried out on surgically resected tissue samples from 75 PDAC patients receiving postoperative adjuvant chemotherapy with gemcitabine. Here, the expression levels of PRMT1 in PDAC tumor cells were categorized into three categories, namely highly elevated, moderately elevated, and not elevated PRMT1 protein levels compared to the expression levels in normal pancreatic tissue, in which PRMT1 is expressed in islet and acinar cells but not in ductal cells (Figure 7B). Based on this analysis it revealed that 45 % of 75 PDAC patients presented highly elevated, 32 % moderately elevated and 23 % not elevated PRMT1 expression levels (Figure 7C), indicating that the majority of PDAC patients (77 %, n=58) had elevated PRMT1 expression levels in their tumor cells. Significantly, out of the 31 PDAC patients with survival of at least 24 months after surgery, 55 % had highly elevated, 26 % moderately elevated and only 19 % no elevated PRMT1 expression levels (Figure 7D), indicating that highly elevated PRMT1 expression levels correlate with a favorable prognosis of PDAC patients after curative resection. IF staining was performed to determine the expression levels of p14<sup>ARF</sup> in the PDAC tumor cell cohort. It was found that 29 % of PDAC patients had strong nucleolar and cytoplasmic/nuclear p14<sup>ARF</sup> expression levels in their PDAC cells, indicating high p14<sup>ARF</sup> expression levels like normal pancreatic tissue (Figure 7E). Considering the short- and long-term survival of p14<sup>ARF</sup>-positive patients in terms of PRMT1 expression, it was found that the percentage of p14<sup>ARF</sup>-positive PDAC patients who had highly elevated PRMT1 levels was significantly greater in the group with survival of at least 24 months (35 %) than in the group with short-term survival of 12 months or less (12.5 %) (Figure 7F). These data highlight that long-term survival of PDAC patients may profit from co-expression of p14<sup>ARF</sup> with only high PRMT1 expression levels.

It is usual for PDAC patients to be treated with postoperative adjuvant chemotherapy with nucleoside analogues (gemcitabine or 5-fluorouracil as being part of folfirinox) to destroy remaining tumor cells. Based on this knowledge, the question arose whether DNA damage caused by gemcitabine would also trigger p14<sup>ARF</sup> activation. Therefore, several human pancreatic tumour cell lines were examined for their p14<sup>ARF</sup> expression. All PDAC cell lines that were tested



showed high PRMT1 expression. However, only PaTu8988t cells showed high levels of p14<sup>ARF</sup> expression located in the nucleolus (Figure 8A). The treatment of PaTu8988t cells with gemcitabine resulted in a decrease in p14<sup>ARF</sup>-protein content and increased p14<sup>ARF</sup>-methylation (Figure 8B-C), suggesting that p14<sup>ARF</sup> also functions as a stress indicator. To test whether PRMT1 affects the effectiveness of anticancer drugs such as gemcitabine, PDAC cell lines PaTu8988t (p14<sup>ARF</sup>-proficient) and MiaPaCa-2 (p14<sup>ARF</sup>-deficient) were treated with gemcitabine in the presence or absence of PRMT1 using the PRMT-type I inhibitor MS023. It can be observed that after gemcitabine treatment, cell death is induced in all PDAC cell lines both in the presence or absence of p14<sup>ARF</sup>, with apoptosis indicated by AnnexinV staining. However, an inhibition of PRMT1 by MS023 resulted in a reduced gemcitabine-induced apoptosis of PaTu8988t but not in the case of MiaPaCa-2 cells and also not compared to the untreated PaTu8988t cells (Figure 8D). Western blot analysis also confirmed that apoptotic cell expression was reduced when PaTu8988 cells were treated simultaneously with gemcitabine and MS023, compared to treating these cells with gemcitabine alone. In this case, apoptosis was indicated by PARP cleavage. Additionally, the treatment with MS023 led to an increased p14<sup>ARF</sup> protein level expression (Figure 8E). To further investigate the specific influence of the PDAC cell lines PaTu8988t and MiaPaCa-2 on apoptosis due to their mutations, these cell lines were generated as p14<sup>ARF</sup> depleted (PaTu8988t) and p14<sup>ARF</sup> expressing (MiaPaCa-2) which were then assessed for their ability to undergo gemcitabine-induced apoptosis and for their reaction to MS023 treatment. As confirmed in Figure 8D with wild-type PaTu8988t cells, it was shown that in control siRNA transfected PaTu8988t cells, gemcitabine-induced apoptosis was reduced by treatment with MS023, whereas siRNA-mediated depletion of p14<sup>ARF</sup> resulted in predominantly increased gemcitabine-induced apoptosis of PaTu8988t cells by treatment with MS023 (Figure 8G). These data may indicate that p14<sup>ARF</sup> and PRMT1 functionally cooperate in apoptosis-induction of PaTu8988t cells. Overexpression of p14<sup>ARF</sup> in MiaPaCa-2 cells did not alter apoptosis numbers under gemcitabine-induced apoptosis without MS023 treatment. In contrast, there is a decrease in apoptosis number with MS023 and MS023/gemcitabine treatment compared to transfected control cells (Figure 8I). Altogether, these results strongly support that p14<sup>ARF</sup> and PRMT1 functionally cooperate in their tumor suppressive behavior in vivo.

## 2.2.2 Description of the personal contribution

Personal contribution to the preparation of this scientific research article includes involvement in the experimental design, conduct and data analysis of figures 7A-D, 7F as well as all staining procedures in PDAC patients in a cohort of 75 patients, not all of which are published.

## 2.3 Extracellular Vesicle-Based Detection of Pancreatic Cancer

Yesim Verel-Yilmaz<sup>1†</sup>, Juan Pablo Fernández<sup>1†</sup>, Agnes Schäfer<sup>2</sup>, Sheila Nevermann<sup>1</sup>, Lena Cook<sup>2</sup>, Norman Gercke<sup>1</sup>, Frederik Helmprobst<sup>3</sup>, Christian Jaworek<sup>2</sup>, Elke Pogge von Strandmann<sup>4</sup>, Axel Pagenstecher<sup>3</sup>, Detlef K. Bartsch<sup>1</sup>, Jörg W. Bartsch<sup>2†</sup>, Emily P. Slater<sup>1†\*</sup>

† These authors have contributed equally to this work

(2021). Extracellular Vesicle Based Detection of Pancreatic Cancer. *Frontiers in Cell and Developmental Biology*, 9.

### 2.3.1 Scientific summary of the publication

PDAC is a cancer with a very poor survival rate. However, little is known about its diagnosis at early stages. For this reason, there is an urgent need to find potential biomarkers to detect PDAC at early stages. In this context, exosomes obtained from bodily fluids such as blood of PDAC patients are promising candidates for early tumor detection because their composition is specific to their donor cell. Therefore, exosomes were investigated at their protein and mRNA level.

The protein ADAM8 (disintegrin and metalloprotease 8), which is highly expressed in PDAC and negatively correlated with patient survival, is associated with exosomes as a protein cargo. In addition, ADAM8 induces miR720 in triple-negative breast cancer, which serves as a diagnostic marker. These microRNAs (miRNAs) are small non-coding RNAs which are 18-22 nucleotides in size. It is known that typical tumor cell processes such as proliferation, migration and invasion are influenced by miRNA-mediated dysregulation of certain genes. Therefore, investigating the role of exosomal miRNAs in tumor cross-talk, which could potentially provide new diagnostic markers for the early detection of PDAC became popular in the scientific field.

Based on these facts, the aim of this study was to analyze the ability of ADAM8-

positive extracellular vesicles (EVs) isolated from the serum of PDAC patients and miRNAs as cargo of serum EVs to find good potential biomarkers in order to distinguish precursor lesions or PDAC from healthy controls.

Firstly, exosomal vesicles were isolated by appropriate methods like ultracentrifugation and filtration from blood-sera of 20 healthy individuals, 7 patients with precursor lesions and 72 PDAC patients in total in order to examine their characteristic properties. As a pre-taste an electron microscopy of a representative serum-exosome allowed the typical bilayer structure like an erythrocyte shaped and its size of 100 nm (Figure 1A). By ZetaView measurement the size of a serum EV of 100 nm was measured in healthy individuals (Figure 1B) and PDAC patients (Figure 1C). Among the serum EV preparations from the different sources, ranging from healthy individuals to PDAC patients, the mean particle size (Figure 1D) and mean vesicle concentration remained relatively constant (Figure 1E). The EV-associated protein CD9, used as an EV biomarker, was successfully detected in all serum EV samples. The only difference was that the control samples had a relatively stable amount of CD9 levels (Figure 1F), whereas the PDAC samples did vary in the abundance of CD9 levels (Figure 1G). A bead-coupled fluorescence activated cell sorting (FACS) analysis was performed to detect A8 located on the surface of exosomes (Figure 2A). As a result, A8 was detected in all kinds of samples (Figure 2B-H) and a clear trend of increase of ADAM8 levels ranging from healthy individuals to PDAC patients was observed isolated from serum EVs (Figure 2B-H). Flotillin-1 was used as a normalization control (Figure 2E-G).

To check if ADAM8 in serum EVs is active, a proteolytic activity assay was performed by using exosomes derived from PDAC patients on a Förster resonance energy transfer (FRET)-based CD23 substrate. As a result, the proteolytic activity of serum EVs derived from PDAC patients was higher (Figure 3B) compared to the healthy controls (Figure 3A) means that ADAM8 which is located on the surface of EVs is given in an activated form in PDAC. By microarray analysis a set of miRNAs derived from serum EVs appeared to be differentially expressed in PDAC as compared to the control samples. Among all 7 potential candidates, miR-451 showed the significantly strongest upregulation and miR-720 the significantly strongest downregulation in PDAC patients compared to healthy individuals (Figure 3C). A quantitative polymerase chain reaction (qPCR) analysis of the entire patient cohort also confirmed these results by observing an

upregulation of exo-miRNA451 levels (Figure 3D-E) and a downregulation of exo-miRNA720 levels in PDAC patients compared to controls (Figure 3F-G). Based on this experimental design, exosomes derived from Panc89 wild-type cells expressing ADAM8 and Panc89 ADAM8 knockout cells served to validate the remaining miRNA-ADAM8 association in PDAC. As a result, it arised that in Panc89 ADAM8 knockout cells the exo-miR-451 expression levels were 11-fold down, and exo-miR-720 3.2-fold upregulated in compared to exosomes derived from Panc89 wild-type cells expressing ADAM8 (Figure 3H).

### **2.3.2 Description of the personal contribution**

Personal contribution to the preparation of this scientific research article includes participation in the experimental design, the execution, and data analysis of table 1, figures 1A-G and 3D-H, and the isolation of serum-exosomes from healthy individuals, precursor lesions and PDAC patients by appropriate methods for experimental preparation of a cohort of 72 patients.

## 3 Discussion

### 3.1 The impact of EVs on PDAC

The search for specific and sensitive biomarkers remains a major oncological challenge and its early detection is the key to disease and mortality reduction. As mentioned before, there already exist diagnostic markers for the early detection of PDAC such as lipocalin 2 (LCN2) (Chakraborty *et al.*, 2012), miRNA-196a /-196b, and even combinations of biomarkers (Bartsch *et al.*, 2018; Slater *et al.*, 2013; Slater *et al.*, 2014) which are presently used in the screening program. But the search for more specific biomarkers released by PDAC exosomes is still ongoing. It is to mention that we have already tested Glypican 1 in EVs, however, it did not prove to be a reliable biomarker for PDAC. For this reason, there is an urgent need to discover and test new potential biomarkers in order to trace PDAC and its precursor lesions at an early stage. We had the idea to investigate many better biomarkers focusing on both the protein as well as at the miRNA level in exosomes.

In view of the scientific papers published recently, much attention has been paid to EVs, which can serve as very promising and mostly undiscovered biomarkers for early tumor diagnostics in the field of PDAC research. A blood-based test as part of the concept of liquid biopsy allows diagnosis and monitoring of various types of cancer. To date, only 1 % of the literature addresses PDAC (Otandault *et al.*, 2019). Liquid biopsy, especially of serum-based EVs in PDAC, with analysis of their molecular content, has provided a very promising diagnostic tool for the early detection of PDAC. However, the workflow for the isolation and analysis of EVs from serum still needs to be optimized (Yee *et al.*, 2020).

These EVs are extracellular membrane-derived nanovesicles that arise by exocytosis of multivesicular endosomes. They are secreted by all cell types, including cancer cells (Sumrin *et al.*, 2018), and can be isolated from body fluids such as blood, saliva, urine, and breast milk (H Rashed *et al.*, 2017). Because of their small size of about 30 - 100 nm exosomes can reach distant parts of the body with the help of the bloodstream and other body fluids mentioned above (Raposo and Stoorvogel, 2013). In 1983, the research groups of Harding and Stahl (Harding and Stahl, 1983) as well as Pan and Johnstone (Pan and Johnstone, 1983) independently reported in the same week that reticulocytes secreted these

vesicles during the maturation to erythrocytes. A few years later, Johnstone coined the term “exosome” as it is used today: vesicles originating from the endosome that is externalized (Johnstone *et al.*, 1987).

Originally, these vesicles were first considered as cellular garbage bins which eliminate excessive proteins and other undesirable molecular components from the releasing cells (Johnston, 1992). Until 1996 it was not thought that exosomes have an immunological function when Raposo’s group found that Epstein-Barr-Virus transformed B cell lines released exosomes containing Major histocompatibility class II molecules that were capable of stimulating CD4<sup>+</sup> T cells *in vitro*. This was the first evidence that these vesicles derived from immune cells function as activators of the immune system (Raposo *et al.*, 1996). In 1998, Zitvogel *et al.* revealed that human dendritic cells secreted antigen-presenting exosomes that were capable of suppressing tumor growth *in vivo* (Zitvogel *et al.*, 1998). Importantly, the dendritic cell-derived exosomes served as a novel cell-free vaccine. Since then, a number of studies have confirmed that exosomes play an important role in intercellular communication and they are involved in several physiological functions and cellular processes, both normal and pathological. These findings established the concept that exosomes are not only regulators of the immune system, they might also be a potential immunotherapeutic candidate (Colombo *et al.*, 2014). Accordingly, there are many reports showing that various types of cells release exosomes with functions that mirror those of their originating cells despite the differences between the contents of exosomes and those of the cells from which they originate (Sheldon *et al.*, 2010). It is known that exosomes carry a characteristic and cell type-specific composition of molecular cargo including proteins, lipids, miRNA and mRNA inherited from the parental cell (Raposo and Stoorvogel, 2013). The function of exosomes, their mechanisms, biogenesis, secretion and their molecular composition including proteins, lipids and nucleic acids, have been comprehensively studied (Théry *et al.*, 2002). For instance, release of exosomes is regulated in a calcium-dependent manner (Savina *et al.*, 2003). Kosaka’s group revealed that reduced activity of neutral nSMase2 (sphingomyelinase 2), a rate-limiting enzyme in ceramide biosynthesis, leads to in the decreased secretion of miRNAs (Kosaka *et al.*, 2010). However, the mechanisms regarding the exosome packaging process remains still elusive. According to the statement of Katsuda *et al.*, a selective enrichment of certain molecules in exosomes could be observed (Katsuda *et al.*, 2013). The

detection of functional mRNA and miRNA in exosomes crystallized as an additional major breakthrough in the field of scientific research. This phenomenon has sparked enormous interest in the study of human diseases and their development (Sumrin *et al.*, 2018). As reported by Ratajczak *et al.* in 2006, mRNA can be transferred by exosomes to the target cells and translated into the corresponding proteins (Ratajczak *et al.*, 2006). Moreover, in 2010, the groups of Pegtel, Zhang and Kosaka independently from each other found that miRNA delivery via exosomes suppresses the expression of target genes in recipient cell showing the first evidence of intercellular transfer of miRNAs (Kosaka *et al.*, 2010; Pegtel *et al.*, 2010; Zhang *et al.*, 2010). The research group of Mittelbrunn also reported exosome mediated unidirectional transfer of miRNAs from T cells to antigen-presenting cells and that an immune synapse between these two cell types significantly enhanced the efficiency of exosome mediated delivery of the miRNAs (Mittelbrunn *et al.*, 2011).

Observing all the aspects above, it is very likely that exosomes serve as a medium of intercellular cargo exchange and cell-cell communication between different cell types in the body and thus affecting normal and pathological conditions including neurodegenerative diseases and tumors (Sumrin *et al.*, 2018). It is to mention that molecules retrieved from exosomes can still help the parent cells play their roles (Colombo *et al.*, 2014; Sheldon *et al.*, 2010).

In general, there are biomarkers that are similarly present in all EVs because they are related to the pathway of exosome biogenesis. These proteins are, for example, tetraspanins (CD9, CD63, CD81, CD82) or flotillins (flotillin-1/ 2), that are parent cell-characteristic in exosomes. It is to mention, that, although the content of the exosomes does not completely resemble the profile of the parental cell, the partial similarity inspired the idea of using exosomes as biomarkers for tumors. Beside these general used EV biomarkers, the search for specific biomarkers released by exosomes in tumors, particularly PDAC exosomes, does still exist, in order to facilitate the detection of PDAC in early stages.

Based on these aspects, EVs were isolated from sera of PDAC patients by ultracentrifugation and proteins such as ADAM8, flotillin-1 and CD9 were successfully detected by western blotting and FACS analysis method as a preliminary work as a pre-taste. These biomarkers could be used in the future to determine any differences between PDAC EVs and healthy single EVs. However, CD81 was only detected in serum EVs by Western blotting and not in FACS

analysis of serum EVs whereas it is published to be a marker for all EVs (Kowal *et al.*, 2016). Therefore, it is important to investigate whether and how the PDAC or the TME regulates the CD81 content in serum EVs. Furthermore, Bartsch *et al.* have found some evidence of a correlation between a high CD81 content and a significantly longer median survival time of the patients (unpublished data). Therefore, in the future, it may be important to compare the mean survival time of PDAC patients with high CD81 levels to the mean survival time of patients with low or no CD81 levels.

### **3.2 ADAM8-positive serum EVs as a promising biomarker in PDAC**

Moreover, this work aimed to investigate the hypothesis whether ADAM8 mediates pancreatic cancer progression through secretion in serum EVs from PDAC patients and precursor lesions, as it has been previously shown that pancreatic cancer EVs modulate not only the TME but also distant organs, through mechanisms that ADAM8 can provide (Costa-Silva *et al.*, 2015).

In the search for diagnostic markers in early diagnosis of PDAC, ADAM8 has previously been observed as a potential candidate for PDAC with high expression levels and correlating with poor patient survival (Schlomann *et al.*, 2015; Valkovskaya *et al.*, 2007), as it has already been proposed as a biomarker for lung cancer (Ishikawa *et al.*, 2004) and renal cancer (Roemer *et al.*, 2004). It is also well known that the ADAM8 is involved in promoting PDAC progression, invasion and metastasis (Schlomann *et al.*, 2015) and its expression is associated with poor patient survival in PDAC (Valkovskaya *et al.*, 2007). However, the expression profile of ADAM8 in the TME of PDAC is still elusive.

To address these aspects and to continue the research on ADAM8 not only in PDAC, but also in the TME of PDAC, we first introduced a bead-based FACS analysis method to detect ADAM8 on the surface of EVs. Indeed, it could be proved that ADAM8 is located on the surface of EVs. By FACS analysis it was observed a clear trend of increase of ADAM8-positive EVs from healthy controls to PDAC patients. This is a very new result in the history of scientific research which means on the diagnostic aspect that ADAM8 protein levels in EVs from patients' serum could be a promising biomarker for PDAC. However, the normalization remains still elusive, because we did the amount of proteins and the number of vesicles which were performed by Zeta-View in collaboration with AG Pogge von Strandmann but the levels of flotillin-1 and CD9 vary. Therefore, in this case one does not know what to use as normalization. This has to be further examined in the future.



After demonstrating that ADAM8 is present in serum EVs, the next hypothesis was to check if ADAM8 in serum EVs is active with the help of PrAMA assay (Miller *et al.*, 2011). The result was an activity enrichment of ADAM8-related EVs in PDAC compared to the control samples, which means that ADAM8, which is located on the surface of EVs, is present in an activated form in PDAC.

Additionally, in collaboration with AG Pagenstecher as a pre-taste in deed we have taken an electron micrograph of one EV in native form, clearly showing its double membrane in the form of an erythrocyte and its size of 100 nm. As a possible model for the extension of this study in order to check the amount of ADAM8 on the surface of only one EV, we have started immunogold labelling of PDAC serum EVs as preliminary work, which is presently being optimized. Since we do not know exactly how many ADAM8 proteins are on just one EV, we also do not know how strongly each ADAM8 protein influences the progression of PDAC. This aspect needs further analysis.

Among others, the association between ADAM8 and immune cells like macrophages and neutrophils was already demonstrated when ADAM8 was found to play a critical role in the development of allergic asthma in mice (Naus *et al.*, 2010). In this respect, to describe the role of ADAM8 in the TME of PDAC, in particular to investigate the effect of ADAM8 in stromal cells on tumor growth, what has not yet been investigated, IHC was performed with stromal cell types expressing ADAM8 on PDAC tissue. Hence, in PDAC, ADAM8 is significantly expressed in tumor-associated stromal cells, most notably in macrophages (6 %), natural killer cells (40 %) and neutrophils (63 %) as seen in publication 2.2. Moreover, the determination of neutrophil density in the venules of tumor areas crystallized as a promising indicator associated with progression and patient survival of PDAC that could be used to trace PDAC in early stages. Further analysis need to be done to understand ADAM8-dependent signaling and its impact on TME in PDAC. Based on these results of this study, it is an important aspect to investigate the effect of ADAM8 in macrophages and neutrophils on PDAC growth *in vivo* with the help of for example KPC cells.

Beside all these aspects, it is well known as already mentioned that increased ADAM8 levels in TNBC patient serum correlate with increased miR-720 levels. There, elevated miR-720 levels serve as a diagnostic marker (Das *et al.*, 2016).

Based on this fact and the actual detection of ADAM8 on the surface of EVs, we investigated a number of potential exosomal miRNAs showing the highest

expression profile such as miR-451, miR-21, miR-16, miR-320, miR-155 and let-7b in addition to miR-720 as EV cargos that could serve as potential diagnostic markers in PDAC and that could be regulated by ADAM8. For this study, we used the same patient cohort that we had used for the FACS analysis, too. One more reason of this objective was to understand the ADAM8 dependent communication between miRNAs and PDAC cells. Therefore, miRNA was isolated from ADAM8-positive serum EVs of patients with precursor lesions, with PDAC and healthy control individuals. Among all miRNAs examined, exosomal miRNA-720 and exosomal miRNA-451 were the most significantly dysregulated.

Based on literature it is already known that mRNA, as a cargo component of EVs, can be transferred to target cells through exosomes (Ratajczak *et al.*, 2006) and can regulate the expression of target genes in the recipient cell (Kosaka *et al.*, 2010; Pegtel *et al.*, 2010; Zhang *et al.*, 2010). It is even reported that miRNA-720 is up-regulated in TNBC and its regulation is dependent on ADAM8 expression levels (Das *et al.*, 2016). However, there is also evidence that miRNA-720 is down regulated in primary breast cancer which occurs frequently and miRNA-720 inhibits tumor invasion and migration (Li *et al.*, 2014). In addition, miRNA-720 is decreased in pancreatic cancer where it functions as a suppressor of pancreatic cancer cell proliferation and invasion (Zhang *et al.*, 2017). In contrast, miRNA-451 is over-expressed in PDAC where its elevated expression contributes to promotion of cell proliferation and metastasis (Guo *et al.*, 2017). But one does not know whether the expression profile of both of these miRNAs, miRNA-720 and miRNA-451, isolated from ADAM8-positive serum EVs suppresses or positively influences the progression of PDAC. This issue needs to be investigated further in the future.

Observing our results, we found that exosomal miRNA-720 was significantly down-regulated in serum samples of PDAC patients, whereas exosomal miRNA-451 showed the highest expression in PDAC as well as in its precursor lesions correlating with a higher ADAM8 expression for both of these miRNAs. These results indicated a perfect discrimination between patients with precursor lesions or PDAC and healthy individuals with high accuracy in the diagnosis of PDAC. It might be that miRNA-720 expression at low levels in PDAC patients as observed in Zhang *et al.*, in 2017 could have a potential tumor-suppressing effect, too (Zhang *et al.*, 2017). Thus, as observed in Guo *et al.*, in 2017 elevated miRNA-

451 levels in PDAC might promote cell proliferation and metastasis (Guo *et al.*, 2017).

By the way, it is possible that ADAM8 induces the expression of certain miRNAs via the ERK1/2 pathway, as it has been described in TNBC with miR720 as already mentioned (Das *et al.*, 2016), leading to increased metastasis or induction of a pre-metastatic niche in surrounding tissues, possibly through release with serum EVs (Costa-Silva *et al.*, 2015).

Thus, placing ADAM8 in serum EVs could be a way for cells to modulate the content of EVs or remodel the TME. The secretion of ADAM8 into EVs may even transfer these capabilities to target cells (Shimoda and Khokha, 2017). Furthermore, to understand the influence of ADAM8 on PDAC development, many more analysis could be done with Adam8-knockout KPC mice. Since the function of ADAM8 in PDAC cells is already known (Schlomann *et al.*, 2015), an ADAM8 inhibitor therapy could be started to stop PDAC progression as a more forward-looking future perspective to extend this experiment.

All in all, downregulated levels of exosomal miRNA-720 and elevated levels of exosomal miRNA-451 could be used as biomarkers in blood screening in PDAC. Furthermore, in this study, a clear trend of increasing ADAM8-positive EVs from healthy controls to PDAC patients could be observed and since we already know that high expression levels of ADAM8 correlate with poor survival of PDAC patients (Schlomann *et al.*, 2015; Valkovskaya *et al.*, 2007), the increase of ADAM8 in serum EVs could be used for the early diagnosis of PDAC patients. Extracellular vesicles from a cohort of 72 PDAC patients and 20 control individuals were isolated via ultra-centrifugation. The same samples were used for all experiments in IHC in order to make a better comparison and to form a network of communication among the PDAC patients and the TME in order to trace PDAC in early stages. Of course, this experiment could be expanded with many more individuals to achieve the highest possible reliability in the early diagnosis of PDAC. As the amount of ADAM8 proteins located on only one EV is still unknown, we do not really know how strongly a single ADAM8 protein influences the progression of PDAC. This aspect has to be further analyzed. This study also shows that ADAM8 is significantly expressed in PDAC in tumour-associated stromal cells such as macrophages (6 %), natural killer cells (40 %) and neutrophils (63 %). A further experiment to explain the communication between PDAC and TME could be started, for example, with a Boyden chamber assay.

Since the expression profile of ADAM8 in the TME of PDAC was poorly known, this study could make a positive contribution to science.

### 3.2.1 Domains of ADAM8

The prodomain of ADAM proteins facilitates correct protein folding during biosynthesis (Van Goor *et al.*, 2009). It also maintains the metalloprotease domain in an inactive form (Schlomann *et al.*, 2015). Most of the ADAM family members possess a consensus sequence localized between the pro- and metalloprotease domains for activation by furin-like proteases (Yoshida *et al.*, 1990). As ADAM8 does not contain this consensus sequence, ADAM8 is activated in the trans-Golgi by autocatalytic cleavage of the prodomain (Schlomann *et al.*, 2002).

The main function of the metalloprotease domain is thought to be in proteolytically cleaving and releasing (or shedding) signaling molecules as well as their receptors from cell surfaces (Das *et al.*, 2016). Prominent examples of such factors are TNF- $\alpha$  (Black *et al.*, 1997) or the degradation of ECM components such as collagen (Mochizuki and Okada, 2007).

In this way, ADAM8 is involved in extracellular matrix remodeling, which is important for the massive infiltration of PDACs (Schlomann *et al.*, 2015). Considering these mechanisms, it is clear that ADAMs play an important role in cell-cell signaling as well as cell-ECM interactions, which explains their ability to promote tumor growth and proliferation, as previously observed in pancreatic cancer (Valkovskaya *et al.*, 2007).

Cell adhesion is enabled by the disintegrin- and cysteine-rich domains, as they are able to bind integrins and other receptors. This interaction is probably facilitated by the three-dimensional structure of the disintegrin loop (Das *et al.*, 2016). As a disintegrin, it binds to  $\beta$ 1-integrin on the cell surface and activates the ERK1/2 signaling pathway, leading to increased migration and proliferation ability (Schlomann *et al.*, 2015). Moreover, the disintegrin, cysteine-rich and EGF-like domains of ADAM8 specifically are involved in inducing miR-720 through an ERK1/2 signaling pathway in TNBC cells. At the same time, increased ADAM8 levels in TNBC patient serum correlated with increased miR-720 levels which results in increased tumor migration and invasion (Das *et al.*, 2016). Therefore, ADAM8 might be capable of promoting tumor progression directly and indirectly. The transmembrane domain is responsible for anchoring the protein to the cell

membrane, while the cytoplasmic domain is involved in intracellular signaling (Edwards *et al.*, 2008).

### **3.3 PRMTs as a diagnostic in PDAC**

PRMTs are deregulated (Wang *et al.*, 2016) or hyperactive (Song *et al.*, 2002) in tumor cells and in TME (Tang *et al.*, 2000). Many PRMT-related publications focusing on cancer show that PRMTs promote oncogenesis in PDAC tumor cells (Song *et al.*, 2002; Jarrold and Davies, 2019). However, their biological functions in PDAC are not completely understood. According to the substrate, PRMTs can function as a transcriptional activator but also as a suppressor in pancreatic cancer (Kim *et al.*, 2016; Wang *et al.*, 2016) as shown in the publication 2.3.

Of all nine members of the PRMT family, PRMT1, PRMT4 and PRMT5 are the most expressed in cancer (Kim and Ze'ev, 2020). Since this work focuses on the study of the members of the type I PRMTs in PDAC, PRMT1 and PRMT4 were investigated, as their biological functions of expression in PDAC remain still elusive. In this purpose, many more members of PRMT could be investigated on protein and mRNA levels in the future as in the case of experiments dealing with ADAM8 in this study.

It is well known that inflammation is an important defense response of the body that can cause various types of diseases, including some cancers. There is evidence of a link between PRMTs and inflammatory responses, as PRMTs appear to have an important function in regulating the inflammatory system (Kim *et al.*, 2016). However, studies linking PRMTs to inflammation are still at a very early stage, and current evidence is circumstantial. Recent data indicate that PRMTs are highly expressed in immune cells of the PDAC especially in T-cells (Mowen *et al.*, 2004). Therefore, in this study, immunohistochemical stainings of PRMT1<sup>+</sup> tumor and stromal cell types including macrophages and T cells was performed on PanIN and PDAC tissue sections and healthy controls to further understand its biological role in TME and to show its localization and the expression profile. Tissue sections from PDAC patients and healthy controls were used for comparison. The same procedure was also performed with PRMT4 by me. However, our work is presently being optimized will and be carried out in another project that has already started at the current time.

### 3.3.1 PRMT1 as a novel therapeutic target in PDAC

PRMT1 represents the most abundant form among PRMTs, is ubiquitously expressed in most tissues and is responsible for approximately 85 % of the total arginine methylation activity in mammalian cells (Tang *et al.*, 2000). As PRMT1 covers vital functions like transcription activation, signal transduction, RNA splicing and DNA repair. A complete deletion of PRMT1 expression leads to loss of cell viability and embryonic mortality in mice, indicating an essential role of arginine methylation in embryonic development (Nicholson *et al.*, 2009; Moretinet *et al.*, 2015). PRMT1 is the major enzyme responsible for histone H4 methylation and is primarily localized in the nucleus (Wang *et al.*, 2001). PRMT1 methylates the transcription factor forkhead box O1 (FOXO1) and increases its transcriptional activity as it is retained in the nucleus by methylation (Yamagata *et al.*, 2008). Numerous reports demonstrate that PRMT1 is upregulated in various types of tumors, including in PDAC. The research group of Song demonstrated that increased PRMT1 expression in PDAC is associated with an increasing tumor size and a worse survival in postoperative patients (Song *et al.*, 2002). It was also found that PRMT1 contributes to pancreatic cancer growth and an inhibition of PRMT1 in pancreatic progenitor cells in mice leads to hyperglycemia and a hypoplastic pancreas (Lee *et al.*, 2019).

Treiber et al. 2017, defined PRMT1, among others, as an RNA-binding protein, as it binds miRNA precursors and thus influences their maturation. Since miRNAs are considered as regulatory RNAs for mRNAs, it indirectly affects the biosynthesis of the corresponding proteins. Treiber et al, showed an interaction of PRMT1 and miRNA-451, indicating that PRMTs regulate the synthesis of certain proteins. It would be possible to perform further experimental analyses in the future to more clearly establish the relationship between EV encapsulated miRNAs and PRMTs. Moreover, the fact that PRMT1 binds to miRNA-451 as an RNA-binding protein and that PRMT1 is involved in its biogenesis suggests a link between PRMTs and the regulation of miRNA expression. Therefore, the increased expression pattern of miRNA-451 in PDAC may substantially correlate with PRMT1 expression, which can be further expanded experimentally (Treiber *et al.*, 2017).

PRMT1 interacts in a similar way as CARM1 with the C-terminal activator domain 2 (AD2) of p160 proteins. In this transcription regulated by nuclear hormone receptors, the binding of CARM1 and PRMT1 to AD2 is essential for their coactivator function (Koh *et al.*, 2001).

### **3.3.2 PRMT4 as a novel therapeutic target in PDAC - paper in review**

PRMT4, also referred to as coactivator-associated arginine methyltransferase 1 (CARM1), acts as a co-activator for estrogen receptor alpha (ER $\alpha$ ) mediated transcriptional activation in a ligand-independent manner (Xu *et al.*, 2004). According to the substrate, PRMT4 can function as a transcriptional activator but also as a suppressor in pancreatic cancer (Kim *et al.*, 2016; Wang *et al.*, 2016). It has been experimentally demonstrated that CARM1 is active for histone H3 methylation *in vitro* (Schurter *et al.*, 2001).

Mice expressing catalytically inactive CARM1 survive pregnancy, are smaller in size than their wild type siblings and die soon after birth (Kim *et al.*, 2010). CARM1-deficient embryos show differentiation defects in T cells (Kim *et al.*, 2004), adipose tissue (Yadav *et al.*, 2008), chondrocytes (Ito *et al.*, 2009), muscle (Dacwag *et al.*, 2009) and lung (O'Brien *et al.*, 2010). A number of studies have described the functions of CARM1 in a variety of cellular processes, for instance transcriptional regulation (Chen *et al.*, 1999), cell cycle progression (El Messaoudi *et al.*, 2006), mRNA splicing (Cheng *et al.*, 2007) and DNA damage response (Lee and Stallcup, 2011). Although Kim *et al.* 2020 published that PRMT4 is highly expressed in cancer (Kim and Ze'ev, 2020), others report that the PRMT4 protein expression is significantly down-regulated in pancreatic cancer cells (Wang *et al.*, 2016).

However, CARM1 has also been shown to positively influence the expression of matrix metalloproteinases (MMP), which are thought to play a role in the metastasis of degenerated cells by altering the TME (Fauquier *et al.*, 2008). This study established a connection between the MMP member, like ADAM8 (Schlomann *et al.*, 2015) and PRMTs. Therefore, the focus of this work has been set on the investigation of role of ADAM8 and PRMTs in tumor-stroma interactions in PDAC, among others.

### 3.3.3 Determination of serum ADMA levels in PDAC - paper in review

Asymmetric arginine dimethylation is catalyzed by type I PRMTs like PRMT1 and PRMT4 (Bedford and Richard, 2005). From a number of previous studies, it is known that serum ADMA level serves as a good diagnostic marker in cardiovascular disease and pulmonary dysfunction by demonstrating increased PRMT1 activity (Sibal *et al.*, 2010; Zakrzewicz and Eickelberg, 2009; Zakrzewicz *et al.*, 2012; Pullamsetti *et al.*, 2005). The current knowledge of the role of ADMA in PDAC pathogenesis, however, it remains not clearly understood because ADMA containing proteins in pancreatic cancer cells have not been extensively characterized (Pan *et al.*, 2002).

As the main goal of this research project addresses to find good diagnostic markers to detect PDAC in early stages, a further objective was to test whether serum ADMA could also serve as potential diagnostic markers in PDAC by measuring increased PRMT1 activity. Based on the measurement method of Teerlink *et al.* 2002, our clinical research group at Marburg University Hospital VTG-Chirurgie have already started an ongoing project to determine serum ADMA levels by the HPLC method in PDAC in collaborating with the research groups of AG Bartsch and AG Bauer (Teerlin *et al.*, 2002).

Preliminary results, which are currently being optimized, suggest that an increase in serum ADMA levels correlates with increased PRMT1 activity in PDAC. For this ongoing research we use PRMT1-positive and -negative sera from the same set of PDAC patients previously used for publications 2.2 and 2.3.

In order to further investigate the function of type I PRMT in tumor stroma cross-talk or immune escape mechanisms *in vitro*, single and co-culture assays such as the Boyden Chamber assay could be performed with stromal and tumor cells to monitor proliferation, migration, invasion and cytokine synthesis.



## 4 Summary

The search for new potential biomarkers is a major challenge for oncology, and early detection is key to reducing disease and mortality. Pancreatic ductal adenocarcinoma (PDAC) is a cancer entity with a very poor survival rate. However, its diagnosis in early stages and the interaction partners in tumor stroma cross-talk remains still elusive. Therefore, the main aim of this study is to identify potential diagnostic biomarkers to detect PDAC at early stages.

In this context, extracellular vesicles (EVs) are promising candidates for early PDAC diagnosis. They are released by virtually all cell types but play a poorly understood role in cell communication.

A disintegrin and metalloprotease 8 (ADAM8) which was detected on the surface of serum-EVs by FACS analysis is highly expressed in PDAC and correlates negatively with patient survival. While the function of ADAM8 in PDAC cells is already known, its role in tumor-associated cells remains elusive and no information is available on the expression profile of ADAM8 in cells of TME. Thus, the goal of this study was to analyze the ability of ADAM8-positive EVs isolated from the serum of PDAC patients and miRNAs as cargo of serum EVs, also involving PRMT1 and PRMT4, to distinguish precursor lesions or PDAC from healthy controls.

Firstly, to describe the stromal cell types expressing ADAM8 in PDAC, immunohistochemical staining was performed on human PDAC tissue and the results were evaluated. ADAM8 was found to be significantly expressed in macrophages (6 %), natural killer cells (40 %), and neutrophils (63 %), which, among other stromal cells, have the highest percentage of stromal cells expressing ADAM8 in PDAC tissue. From these data, it can be concluded that ADAM8 is not only present in PDAC cells but also in tumor-associated stromal macrophages, NK cells, and neutrophils in the TME and that ADAM8-expressing stromal cells may be a promising parameter that can serve for the early diagnosis of PDAC.

A total cohort of 72 PDAC patients and 20 healthy individuals as a comparison was used in this entire study. All experiments were performed with the same cohort of patients to build an information network about PDAC and its potential biomarkers.

Then, a set of miRNAs as cargo of ADAM8-positive serum EVs, which were differentially expressed in PDAC, were investigated. A downregulation was

significantly observed for miRNA-720 and an elevated expression profile for miRNA-451 in PDAC compared to healthy controls to distinguish PDAC from healthy controls. Thus, the detection of miR-720 and miR-451 cargo from ADAM8-positive EVs could provide a specific biomarker and thus a positive contribution to the screening of individuals at risk of PDAC.

To investigate the role of PRMT-1 and 4 on TME in PDAC, immunohistochemical staining was performed with the same stromal cells on human PDAC tissue as previously used to build a network of correlation. The expression levels revealed that PRMT1 promotes the tumor-suppressing effect of p14ARF, a tumor suppressor protein, and a correlation between patient survival and PRMT1 was observed suggesting that PRMT1 is a promising diagnostic marker. Research on PRMT4, which has already been carried out in this work, will be published in a project that has already been started.

## 5 Zusammenfassung

Die Suche nach neuen potenziellen Biomarkern ist eine große Herausforderung für die Onkologie, und die Früherkennung ist der Schlüssel zur Reduzierung von Krankheit und Sterblichkeit. Das duktales Adenokarzinom der Bauchspeicheldrüse (PDAC) ist eine Krebsart mit einer sehr schlechten Überlebensrate. Über seine Diagnose in frühen Stadien ist jedoch nur wenig bekannt. Ziel dieser Studie ist es daher, potenzielle diagnostische Biomarker zu finden, um PDAC in frühen Stadien zu erkennen.

In diesem Zusammenhang sind extrazelluläre Vesikel (EVs) vielversprechende Kandidaten für die PDAC-Frühd Diagnose. Sie werden von nahezu allen Zelltypen freigesetzt, spielen aber eine wenig verstandene Rolle in der Zellkommunikation. ADAM8, das mittels FACS-Analyse auf der Oberfläche von Serum-EVs nachgewiesen wurde, ist in PDAC stark exprimiert und korreliert negativ mit dem Überleben von PDAC-Patienten. Während die Funktion von ADAM8 in PDAC-Zellen bereits bekannt ist, bleibt seine Rolle in tumorassoziierten Zellen schwer fassbar und es liegen keine Informationen über das Expressionsprofil von ADAM8 in Zellen der TME vor.

Ziel dieser Studie war es daher, die Fähigkeit von ADAM8-positiven EVs, die aus dem Serum von PDAC-Patienten isoliert wurden und von miRNAs als Ladung von Serum-EVs zu analysieren, wobei auch PRMT1 und PRMT4 einbezogen wurden, um Vorläuferläsionen oder PDAC von gesunden Patienten abzugrenzen.

Um die Stromazelltypen zu beschreiben, die ADAM8 in PDAC exprimieren, wurde zunächst eine immunhistochemische Färbung von menschlichem PDAC-Gewebe durchgeführt und die Ergebnisse ausgewertet. Es zeigte sich, dass ADAM8 signifikant in Makrophagen (6 %), natürlichen Killerzellen (40 %) und Neutrophilen (63 %) exprimiert wird, die unter den anderen Stromazellen den höchsten Prozentsatz an Stromazellen aufweisen, die ADAM8 in PDAC-Gewebe exprimieren. Aus diesen Daten lässt sich schließen, dass ADAM8 nicht nur in PDAC-Zellen, sondern auch in tumorassoziierten stromalen Makrophagen, NK-Zellen und Neutrophilen im TME vorkommt und dass ADAM8-exprimierende Stromazellen ein vielversprechender Parameter sein können, der zur Frühd Diagnose von PDAC-Patienten dienen kann.

Für die gesamte Studie wurde eine Kohorte von 72 PDAC-Patienten und 20 gesunden Personen als Vergleich herangezogen. Alle Experimente wurden mit der

gleichen Patientenkohorte durchgeführt, um ein Informationsnetzwerk über PDAC und seine potenziellen Biomarker aufzubauen.

Anschließend wurde eine Reihe von miRNAs als „Cargo“ von ADAM8-positiven Serum-EVs untersucht, die bei PDAC unterschiedlich exprimiert wurden. Als Ergebnis wurde eine signifikante Herabregulierung der miRNA-720 und ein erhöhtes Expressionsprofil der miRNA-451 bei PDAC im Vergleich zu gesunden Kontrollen beobachtet, um PDAC von gesunden Kontrollen zu unterscheiden. Somit könnte der Nachweis von miR-720 und miR-451 aus ADAM8-positiven EVs einen spezifischen Biomarker darstellen und auf diese Weise einen positiven Beitrag zum Screening von Personen mit PDAC-Risiko leisten.

Um die Rolle von PRMT1 und PRMT4 im TME bei PDAC zu untersuchen, wurde eine immunhistochemische Färbung mit denselben Stromazellen auf menschlichem PDAC-Gewebe durchgeführt, die zuvor zum Aufbau eines Korrelationsnetzes verwendet wurde. Die Expressionswerte zeigten, dass PRMT1 die tumorsuppressive Wirkung von p14<sup>ARF</sup>, einem Tumorsuppressorprotein, fördert, und es wurde eine Korrelation zwischen dem Überleben der Patienten und PRMT1 beobachtet, was darauf hindeutet, dass PRMT1 ein vielversprechender diagnostischer Marker ist. Die Forschung zu PRMT4, die im Rahmen dieser Arbeit bereits durchgeführt wurde, wird in einem bereits begonnenen Projekt veröffentlicht.

## 6 References

- Akers, J. C., Gonda, D., Kim, R., Carter, B. S., & Chen, C. C. (2013). Biogenesis of extracellular vesicles (EV): exosomes, microvesicles, retrovirus-like vesicles, and apoptotic bodies. *Journal of neuro-oncology*, 113(1), 1-11.
- Andreola, G., Rivoltini, L., Castelli, C., Huber, V., Perego, P., Deho, P., ... & Fais, S. (2002). Induction of lymphocyte apoptosis by tumor cell secretion of FasL-bearing microvesicles. *The Journal of experimental medicine*, 195(10), 1303-1316.
- Balkwill, F., & Mantovani, A. (2001). Inflammation and cancer: back to Virchow? *The lancet*, 357(9255), 539-545.
- Bartsch, D. K., Gercke, N., Strauch, K., Wieboldt, R., Matthäi, E., Wagner, V., ... & Slater, E. P. (2018). The combination of MiRNA-196b, LCN2, and TIMP1 is a potential set of circulating biomarkers for screening individuals at risk for familial pancreatic cancer. *Journal of clinical medicine*, 7(10), 295.
- Bedford, M. T., & Richard, S. (2005). Arginine methylation: an emerging regulator of protein function. *Molecular cell*, 18(3), 263-272.
- Black, R. A., Rauch, C. T., Kozlosky, C. J., Peschon, J. J., Slack, J. L., Wolfson, M. F., ... & Cerretti, D. P. (1997). A metalloproteinase disintegrin that releases tumour-necrosis factor- $\alpha$  from cells. *Nature*, 385(6618), 729-733.
- Bosire, E. M., Nyamache, A. K., Gicheru, M. M., Khamadi, S. A., Lihana, R. W., & Okoth, V. (2013). Population specific reference ranges of CD3, CD4 and CD8 lymphocyte subsets among healthy Kenyans. *AIDS research and therapy*, 10(1), 1-7.
- Bui, J. D., & Schreiber, R. D. (2007). Cancer immunosurveillance, immunoediting and inflammation: independent or interdependent processes? *Current opinion in immunology*, 19(2), 203-208.
- Burnet, M. (1970). *Immunological surveillance*. Oxford Pergamon Press.
- Chakraborty, S., Kaur, S., Guha, S., & Batra, S. K. (2012). The multifaceted roles of neutrophil gelatinase associated lipocalin (NGAL) in inflammation and cancer. *Biochimica et Biophysica Acta (BBA)-Reviews on Cancer*, 1826(1), 129-169.
- Chen, D., Ma, H., Hong, H., Koh, S. S., Huang, S. M., Schurter, B. T., ... & Stallcup, M. R. (1999). Regulation of transcription by a protein methyltransferase. *Science*, 284(5423), 2174-2177.
- Cheng, D., Côté, J., Shaaban, S., & Bedford, M. T. (2007). The arginine methyltransferase CARM1 regulates the coupling of transcription and mRNA processing. *Molecular cell*, 25(1), 71-83.
- Chiarugi, P., & Cirri, P. (2016). Metabolic exchanges within tumor microenvironment. *Cancer letters*, 380(1), 272-280.
- Christmann, Dr. Daniela: Bauchspeicheldrüsenkrebs (September 2015), URL: <https://www.krebsgesellschaft.de/onko-internetportal/basis-informationen-krebs/krebsarten/bauchspeicheldruesenkrebs/bauchspeicheldruesenkrebs-basis-infos-fuer-pati.html> (as of June 25, 2021).

- Chu, G. C., Kimmelman, A. C., Hezel, A. F., & DePinho, R. A. (2007). Stromal biology of pancreatic cancer. *Journal of cellular biochemistry*, 101(4), 887-907.
- Clark, C. E., Hingorani, S. R., Mick, R., Combs, C., Tuveson, D. A., & Vonderheide, R. H. (2007). Dynamics of the immune reaction to pancreatic cancer from inception to invasion. *Cancer research*, 67(19), 9518-9527.
- Colombo, M., Raposo, G., & Théry, C. (2014). Biogenesis, secretion, and intercellular interactions of exosomes and other extracellular vesicles. *Annual review of cell and developmental biology*, 30, 255-289.
- Costa-Silva, B., Aiello, N. M., Ocean, A. J., Singh, S., Zhang, H., Thakur, B. K., ... & Lyden, D. (2015). Pancreatic cancer exosomes initiate pre-metastatic niche formation in the liver. *Nature cell biology*, 17(6), 816-826.
- Coussens, L. M., & Werb, Z. (2002). Inflammation and cancer. *Nature*, 420(6917), 860-867.
- Croce, C. M. (2009). Causes and consequences of microRNA dysregulation in cancer. *Nature reviews genetics*, 10(10), 704-714.
- Dacwag, C. S., Bedford, M. T., Sif, S., & Imbalzano, A. N. (2009). Distinct protein arginine methyltransferases promote ATP-dependent chromatin remodeling function at different stages of skeletal muscle differentiation. *Molecular and cellular biology*, 29(7), 1909-1921.
- Das, S. G., Romagnoli, M., Mineva, N. D., Barillé-Nion, S., Jézéquel, P., Campone, M., & Sonenshein, G. E. (2016). miR-720 is a downstream target of an ADAM8-induced ERK signaling cascade that promotes the migratory and invasive phenotype of triple-negative breast cancer cells. *Breast Cancer Research*, 18(1), 1-19.
- Detlefsen, S., Sipos, B., Feyerabend, B., & Klöppel, G. (2005). Pancreatic fibrosis associated with age and ductal papillary hyperplasia. *Virchows Archiv*, 447(5), 800-805.
- Edwards, D. R., Handsley, M. M., & Pennington, C. J. (2008). The ADAM metalloproteinases. *Molecular aspects of medicine*, 29(5), 258-289.
- Ehrlich, P. (1909). Ueber den jetzigen stand der karzinomforschung. vortrag gehalten vor den studenten der amsterdamer universitaet, vereinigung fuer wissenschaftliche arbeit 1 june 1908. printed in: P. ehrlich. Beitrage zur Experimentellen Pathologie und Chemotherapie, Akademische Verlagsgesellschaft, Leipzig, 118-164.
- El Messaoudi, S., Fabbriozio, E., Rodriguez, C., Chuchana, P., Fauquier, L., Cheng, D., ... & Sardet, C. (2006). Coactivator-associated arginine methyltransferase 1 (CARM1) is a positive regulator of the Cyclin E1 gene. *Proceedings of the National Academy of Sciences*, 103(36), 13351-13356.
- Escrevente, C., Keller, S., Altevogt, P., & Costa, J. (2011). Interaction and uptake of exosomes by ovarian cancer cells. *BMC cancer*, 11(1), 1-10.
- Eposito, I., Menicagli, M., Funel, N., Bergmann, F., Boggi, U., Mosca, F., ... & Campani, D. (2004). Inflammatory cells contribute to the generation of an angiogenic phenotype in pancreatic ductal adenocarcinoma. *Journal of Clinical Pathology*, 57(6), 630-636.
- Fauquier, L., Duboé, C., Joré, C., Trouche, D., & Vandiel, L. (2008). Dual role of the arginine methyltransferase CARM1 in the regulation of c Fos target genes. *The FASEB Journal*, 22(9), 3337-3347.

- Fujii, N., Shomori, K., Shiomi, T., Nakabayashi, M., Takeda, C., Ryoke, K., & Ito, H. (2012). Cancer associated fibroblasts and CD163-positive macrophages in oral squamous cell carcinoma: their clinicopathological and prognostic significance. *Journal of oral pathology & medicine*, 41(6), 444-451.
- Fukunaga A, Miyamoto M, Cho Y, Murakami S, Kawarada Y, Oshikiri T, Kato K, Kurokawa T, Suzuoki M, Nakakubo Y, Hiraoka K, Garcia-Lora, A., Algarra, I., & Garrido, F. (2003). MHC class I antigens, immune surveillance, and tumor immune escape. *Journal of cellular physiology*, 195(3), 346-355.
- Gjorgjeviski, M., Hannen, R., Carl, B., Li, Y., Landmann, E., Buchholz, M., ... & Nimsky, C. (2019). Molecular profiling of the tumor microenvironment in glioblastoma patients: correlation of microglia/macrophage polarization state with metalloprotease expression profiles and survival. *Bioscience reports*, 39(6).
- Grage-Griebenow, E., Schäfer, H., & Sebens, S. (2014). The fatal alliance of cancer and T cells: How pancreatic tumor cells gather immunosuppressive T cells. *Oncoimmunology*, 3(6), e29382.
- Graner, M. W., Alzate, O., Dechkovskaia, A. M., Keene, J. D., Sampson, J. H., Mitchell, D. A., & Bigner, D. D. (2009). Proteomic and immunologic analyses of brain tumor exosomes. *The FASEB Journal*, 23(5), 1541-1557.
- Grivennikov, S. I., Greten, F. R., & Karin, M. (2010). Immunity, inflammation, and cancer. *Cell*, 140(6), 883-899.
- Grover, S., & Syngal, S. (2010). Hereditary pancreatic cancer. *Gastroenterology*, 139(4), 1076-1080.
- Guo, R., Gu, J., Zhang, Z., Wang, Y., & Gu, C. (2017). MiR-451 promotes cell proliferation and metastasis in pancreatic cancer through targeting CAB39. *BioMed research international*, 2017.
- H Rashed, M., Bayraktar, E., K Helal, G., Abd-Allah, M. F., Amero, P., Chavez-Reyes, A., & Rodriguez-Aguayo, C. (2017). Exosomes: from garbage bins to promising therapeutic targets. *International journal of molecular sciences*, 18(3), 538.
- Harding, C., & Stahl, P. (1983). Transferrin recycling in reticulocytes: pH and iron are important determinants of ligand binding and processing. *Biochemical and biophysical research communications*, 113(2), 650-658.
- He, L., & Hannon, G. J. (2004). MicroRNAs: small RNAs with a big role in gene regulation. *Nature reviews genetics*, 5(7), 522-531.
- Helm, O., Held Feindt, J., Grage Griebenow, E., Reiling, N., Ungefroren, H., Vogel, I., ... & Sebens, S. (2014). Tumor associated macrophages exhibit pro and anti inflammatory properties by which they impact on pancreatic tumorigenesis. *International journal of cancer*, 135(4), 843-861.
- Helm, O., Mennrich, R., Petrick, D., Goebel, L., Freitag-Wolf, S., Röder, C., ... & Sebens, S. (2014). Comparative characterization of stroma cells and ductal epithelium in chronic pancreatitis and pancreatic ductal adenocarcinoma. *PloS one*, 9(5), e94357.
- Hernandez, Y. G., & Lucas, A. L. (2016). MicroRNA in pancreatic ductal adenocarcinoma and its

- precursor lesions. *World journal of gastrointestinal oncology*, 8(1), 18.).
- Herrmann, Richard: Pankreaskarzinom (Oktober 2018), URL: <https://www.onkopedia.com/de/onopedia/guidelines/pankreaskarzinom/@@guideline/html/index.html> (as of June 25, 2021).
- Hingorani, S. R., Petricoin III, E. F., Maitra, A., Rajapakse, V., King, C., Jacobetz, M. A., ... & Tuveson, D. A. (2003). Preinvasive and invasive ductal pancreatic cancer and its early detection in the mouse. *Cancer cell*, 4(6), 437-450.
- Hiraoka, N., Onozato, K., Kosuge, T., & Hirohashi, S. (2006). Prevalence of FOXP3+ regulatory T cells increases during the progression of pancreatic ductal adenocarcinoma and its premalignant lesions. *Clinical Cancer Research*, 12(18), 5423-5434.
- Hruban, R. H., Maitra, A. und Goggins, M. (2008) „Update on pancreatic intraepithelial neoplasia“, *International journal of clinical and experimental pathology*. e-Century Publishing Corporation, 1(4), S. 306.
- Hu, C., Hart, S. N., Polley, E. C., Gnanaolivu, R., Shimelis, H., Lee, K. Y., ... & Couch, F. J. (2018). Association between inherited germline mutations in cancer predisposition genes and risk of pancreatic cancer. *Jama*, 319(23), 2401-2409.
- Huber, M., Brehm, C. U., Gress, T. M., Buchholz, M., Alashkar Alhamwe, B., von Strandmann, E. P., ... & Lauth, M. (2020). The immune microenvironment in pancreatic cancer. *International Journal of Molecular Sciences*, 21(19), 7307.
- Ino, Y., Oguro, S., Yamazaki-Itoh, R., Hori, S., Shimada, K., & Hiraoka, N. (2019). Reliable evaluation of tumor-infiltrating lymphocytes in pancreatic cancer tissue biopsies. *Oncotarget*, 10(10), 1149.
- Ino, Y., Yamazaki-Itoh, R., Shimada, K., Iwasaki, M., Kosuge, T., Kanai, Y., & Hiraoka, N. (2013). Immune cell infiltration as an indicator of the immune microenvironment of pancreatic cancer. *British journal of cancer*, 108(4), 914-923.
- Ishikawa, N., Daigo, Y., Yasui, W., Inai, K., Nishimura, H., Tsuchiya, E., ... & Nakamura, Y. (2004). ADAM8 as a novel serological and histochemical marker for lung cancer. *Clinical Cancer Research*, 10(24), 8363-8370.
- Ito, T., Yadav, N., Lee, J., Furumatsu, T., Yamashita, S., Yoshida, K., ... & Asahara, H. (2009). Arginine methyltransferase CARM1/PRMT4 regulates endochondral ossification. *BMC developmental biology*, 9(1), 1-10.
- Itoh T, Morikawa T, Okushiba S, Kondo S, Katoh H (2004) CD8+ tumor-infiltrating lymphocytes together with CD4+tumor-infiltrating lymphocytes and dendritic cells improve the prognosis of patients with pancreatic adenocarcinoma. *Pancreas* 28 (1): e26–e31.
- Jahan, S., & Davie, J. R. (2015). Protein arginine methyltransferases (PRMTs): role in chromatin organization. *Advances in biological regulation*, 57, 173-184.
- Janeway, C., & Murphy, K. P. (2009). *Janeway Immunologie*. Heidelberg: Spektrum, Akad. Verl.
- Jarrold, J., & Davies, C. C. (2019). PRMTs and arginine methylation: cancer's best-kept secret? *Trends in molecular medicine*, 25(11), 993-1009.
- Johnston, R. M. (1992). The Jeanne Manery-Fisher Memorial Lecture 1991. Maturation of reticulocytes: formation of exosome as a mechanism for shedding membrane proteins. *Biochem Cell Biol.*, 70, 179-190.



- Johnstone, R. M., Adam, M., Hammond, J. R., Orr, L., & Turbide, C. (1987). Vesicle formation during reticulocyte maturation. Association of plasma membrane activities with released vesicles (exosomes). *Journal of Biological Chemistry*, 262(19), 9412-9420.
- Karin, M. (2006). Nuclear factor- $\kappa$ B in cancer development and progression. *Nature*, 441(7092), 431-436.
- Katsuda, T., Kosaka, N., Takeshita, F., & Ochiya, T. (2013). The therapeutic potential of mesenchymal stem cell-derived extracellular vesicles. *Proteomics*, 13(10-11), 1637-1653.
- Kawahara, A., Hattori, S., Akiba, J., Nakashima, K., Taira, T., Watari, K., ... & Ono, M. (2010). Infiltration of thymidine phosphorylase-positive macrophages is closely associated with tumor angiogenesis and survival in intestinal type gastric cancer. *Oncology reports*, 24(2), 405-415.
- Kim, D., Lee, J., Cheng, D., Li, J., Carter, C., Richie, E., & Bedford, M. T. (2010). Enzymatic activity is required for the in vivo functions of CARM1. *Journal of Biological Chemistry*, 285(2), 1147-1152.
- Kim, H., & Ze'ev, A. R. (2020). PRMT5 function and targeting in cancer. *Cell Stress*, 4(8), 199.
- Kim, H., Yoon, B. H., Oh, C. M., Lee, J., Lee, K., Song, H., ... & Kim, H. (2020). PRMT1 is required for the maintenance of mature  $\beta$ -cell identity. *Diabetes*, 69(3), 355-368.
- Kim, J. H., Yoo, B. C., Yang, W. S., Kim, E., Hong, S., & Cho, J. Y. (2016). The role of protein arginine methyltransferases in inflammatory responses. *Mediators of Inflammation*, 2016.
- Kim, J., Lee, J., Yadav, N., Wu, Q., Carter, C., Richard, S., ... & Bedford, M. T. (2004). Loss of CARM1 results in hypomethylation of thymocyte cyclic AMP-regulated phosphoprotein and deregulated early T cell development. *Journal of Biological Chemistry*, 279(24), 25339-25344.
- King, H. W., Michael, M. Z., & Gleadle, J. M. (2012). Hypoxic enhancement of exosome release by breast cancer cells. *BMC cancer*, 12(1), 1-10.
- Kleinschmidt, M. A., Streubel, G., Samans, B., Krause, M., & Bauer, U. M. (2008). The protein arginine methyltransferases CARM1 and PRMT1 cooperate in gene regulation. *Nucleic acids research*, 36(10), 3202-3213.
- Klimstra, D. S., Longnecker, D. S., Hruban, R. H., DiGiuseppe, J. A. und Offerhaus, G. J. A. (1994) „K-ras mutation in pancreatic ductal proliferative lesions“, *American Journal of Pathology*, 145(6), S. 1547–1550.
- Koh, S. S., Chen, D., Lee, Y. H., & Stallcup, M. R. (2001). Synergistic enhancement of nuclear receptor function by p160 coactivators and two coactivators with protein methyltransferase activities. *Journal of Biological Chemistry*, 276(2), 1089-1098.
- Komura, T., Sakai, Y., Harada, K., Kawaguchi, K., Takabatake, H., Kitagawa, H., ... & Kaneko, S. (2015). Inflammatory features of pancreatic cancer highlighted by monocytes/macrophages and CD 4+ T cells with clinical impact. *Cancer science*, 106(6), 672-686.
- Kosaka, N., Iguchi, H., Yoshioka, Y., Takeshita, F., Matsuki, Y., & Ochiya, T. (2010). Secretory Mechanisms and Intercellular Transfer of MicroRNAs in Living Cells\* $\diamond$ . *Journal of Biological Chemistry*, 285(23), 17442-17452.

- Kowal, J., Arras, G., Colombo, M., Jouve, M., Morath, J. P., Primdal-Bengtson, B., ... & Théry, C. (2016). Proteomic comparison defines novel markers to characterize heterogeneous populations of extracellular vesicle subtypes. *Proceedings of the National Academy of Sciences*, 113(8), E968-E977.
- Kurahara, H., Shinchii, H., Mataka, Y., Maemura, K., Noma, H., Kubo, F., ... & Takao, S. (2011). Significance of M2-polarized tumor-associated macrophage in pancreatic cancer. *Journal of Surgical Research*, 167(2), e211-e219.
- Kurahara, H., Takao, S., Maemura, K., Mataka, Y., Kuwahata, T., Maeda, K., ... & Natsugoe, S. (2013). M2-polarized tumor-associated macrophage infiltration of regional lymph nodes is associated with nodal lymphangiogenesis and occult nodal involvement in pN0 pancreatic cancer. *Pancreas*, 42(1), 155-159.
- Lee, E. J., Gusev, Y., Jiang, J., Nuovo, G. J., Lerner, M. R., Frankel, W. L., ... & Schmittgen, T. D. (2007). Expression profiling identifies microRNA signature in pancreatic cancer. *International journal of cancer*, 120(5), 1046-1054.
- Lee, K., Kim, H., Lee, J., Oh, C. M., Song, H., Kim, H., ... & Kim, H. (2019). Essential role of protein arginine methyltransferase 1 in pancreas development by regulating protein stability of neurogenin 3. *Diabetes & metabolism journal*, 43(5), 649-658.
- Lee, R. C., Feinbaum, R. L., & Ambros, V. (1993). *C. elegans* heterochronic gene lin-4 encodes small RNAs with antisense complementarity to lin-14. *Cell*, 75, 843-854.
- Lee, Y. H., & Stallcup, M. R. (2011). Roles of protein arginine methylation in DNA damage signaling pathways: Is CARM1 a life-or-death decision point?. *Cell cycle*, 10(9), 176-188.
- Leek, R. D., Lewis, C. E., Whitehouse, R., Greenall, M., Clarke, J., & Harris, A. L. (1996). Association of macrophage infiltration with angiogenesis and prognosis in invasive breast carcinoma. *Cancer research*, 56(20), 4625-4629.
- Li, L. Z., Zhang, C. Z., Liu, L. L., Yi, C., Lu, S. X., Zhou, X., ... & Yun, J. P. (2014). miR-720 inhibits tumor invasion and migration in breast cancer by targeting TWIST1. *Carcinogenesis*, 35(2), 469-478.
- Lissbrant, I. F., Stattin, P., Wikstrom, P., Damber, J. E., Egevad, L. A. R. S., & Bergh, A. N. D. E. R. S. (2000). Tumor associated macrophages in human prostate cancer: relation to clinicopathological variables and survival. *International journal of oncology*, 17(3), 445-496.
- Liu, X., Xu, J., Zhang, B., Liu, J., Liang, C., Meng, Q., ... & Shi, S. (2019). The reciprocal regulation between host tissue and immune cells in pancreatic ductal adenocarcinoma: new insights and therapeutic implications. *Molecular cancer*, 18(1), 1-14.
- Liyanage, U. K., Moore, T. T., Joo, H. G., Tanaka, Y., Herrmann, V., Doherty, G., ... & Linehan, D. C. (2002). Prevalence of regulatory T cells is increased in peripheral blood and tumor microenvironment of patients with pancreas or breast adenocarcinoma. *The Journal of Immunology*, 169(5), 2756-2761.
- Lodish, H., Berk, A., & Kaiser, A. C. (2013). Regulation of pre-mRNA processing In: *Molecular Cell Biology*.

- Mäkitie, T., Summanen, P., Tarkkanen, A., & Kivelä, T. (2001). Tumor-infiltrating macrophages (CD68+ cells) and prognosis in malignant uveal melanoma. *Investigative ophthalmology & visual science*, 42(7), 1414-1421.
- Mantovani, A., Allavena, P., Sica, A., & Balkwill, F. (2008). Cancer-related inflammation. *nature*, 454(7203), 436-444.ISO 690.
- Melo, S. A., Luecke, L. B., Kahlert, C., Fernandez, A. F., Gammon, S. T., Kaye, J., ... & Kalluri, R. (2015). Glypican-1 identifies cancer exosomes and detects early pancreatic cancer. *Nature*, 523(7559), 177-182.
- Miller, M. A., Barkal, L., Jeng, K., Herrlich, A., Moss, M., Griffith, L. G., & Lauffenburger, D. A. (2011). Proteolytic Activity Matrix Analysis (PrAMA) for simultaneous determination of multiple protease activities. *Integrative Biology*, 3(4), 422-438.
- Mitchell, P. J., Welton, J., Staffurth, J., Mason, M. D., Tabi, Z., & Clayton, A. (2009). Can urinary exosomes act as treatment response markers in prostate cancer?. *Journal of translational medicine*, 7(1), 1-13.
- Mittelbrunn, M., Gutiérrez-Vázquez, C., Villarroya-Beltri, C., González, S., Sánchez-Cabo, F., González, M. Á., ... & Sánchez-Madrid, F. (2011). Unidirectional transfer of microRNA-loaded exosomes from T cells to antigen-presenting cells. *Nature communications*, 2(1), 1-10.
- Mochizuki, S., & Okada, Y. (2007). ADAMs in cancer cell proliferation and progression. *Cancer science*, 98(5), 621-628.
- Moretting, A., Baldwin, R. M., & Côté, J. (2015). Arginine methyltransferases as novel therapeutic targets for breast cancer. *Mutagenesis*, 30(2), 177-189.
- Mowen, K. A., Schurter, B. T., Fathman, J. W., David, M., & Glimcher, L. H. (2004). Arginine methylation of NIP45 modulates cytokine gene expression in effector T lymphocytes. *Molecular cell*, 15(4), 559-571.
- Murphy, G. (2008). The ADAMs: signalling scissors in the tumour microenvironment. *Nature Reviews Cancer*, 8(12), 932-941.
- Naus, S., Blanchet, M. R., Gossens, K., Zaph, C., Bartsch, J. W., McNagny, K. M., & Ziltener, H. J. (2010). The metalloprotease-disintegrin ADAM8 is essential for the development of experimental asthma. *American journal of respiratory and critical care medicine*, 181(12), 1318-1328.
- Nicholson, T. B., Chen, T., & Richard, S. (2009). The physiological and pathophysiological role of PRMT1-mediated protein arginine methylation. *Pharmacological research*, 60(6), 466-474.
- Nilsson, J., Skog, J., Nordstrand, A., Baranov, V., Mincheva-Nilsson, L., Breakefield, X. O., & Widmark, A. (2009). Prostate cancer-derived urine exosomes: a novel approach to biomarkers for prostate cancer. *British journal of cancer*, 100(10), 1603-1607.
- O'Brien, K. B., Alberich-Jordà, M., Yadav, N., Kocher, O., DiRuscio, A., Ebralidze, A., ... & Kobayashi, S. (2010). CARM1 is required for proper control of proliferation and differentiation of pulmonary epithelial cells. *Development*, 137(13), 2147-2156.
- Ochi, A., Graffeo, C. S., Zambirinis, C. P., Rehman, A., Hackman, M., Fallon, N., ... & Miller, G.

- (2012). Toll-like receptor 7 regulates pancreatic carcinogenesis in mice and humans. *The Journal of clinical investigation*, 122(11), 4118-4129.
- Orth, M., Metzger, P., Gerum, S., Mayerle, J., Schneider, G., Belka, C., ... & Lauber, K. (2019). Pancreatic ductal adenocarcinoma: biological hallmarks, current status, and future perspectives of combined modality treatment approaches. *Radiation Oncology*, 14(1), 1-20.
- Otandault, A., Anker, P., Dache, Z. A. A., Guillaumon, V., Meddeb, R., Pastor, B., ... & Thierry, A. R. (2019). Recent advances in circulating nucleic acids in oncology. *Annals of Oncology*, 30(3), 374-384.
- Pan, B. T., & Johnstone, R. M. (1983). Fate of the transferrin receptor during maturation of sheep reticulocytes in vitro: selective externalization of the receptor. *Cell*, 33(3), 967-978.
- Pan, S., Brentnall, T. A., & Chen, R. (2020). Proteome alterations in pancreatic ductal adenocarcinoma. *Cancer letters*, 469, 429-436.
- Pegtel, D. M., Cosmopoulos, K., Thorley-Lawson, D. A., van Eijndhoven, M. A., Hopmans, E. S., Lindenberg, J. L., ... & Middeldorp, J. M. (2010). Functional delivery of viral miRNAs via exosomes. *Proceedings of the National Academy of Sciences*, 107(14), 6328-6333.
- Petersen, G. M., Amundadottir, L., Fuchs, C. S., Kraft, P., Stolzenberg-Solomon, R. Z., Jacobs, K. B., ... & Chanock, S. J. (2010). A genome-wide association study identifies pancreatic cancer susceptibility loci on chromosomes 13q22. 1, 1q32. 1 and 5p15. 33. *Nature genetics*, 42(3), 224-228.
- Pihlak R, Valle JW, McNamara MG. Germline mutations in pancreatic cancer and potential new therapeutic options. *Oncotarget*. 2017;8(42):73240–57.
- Protti, M. P., & De Monte, L. (2013). Immune infiltrates as predictive markers of survival in pancreatic cancer patients. *Frontiers in physiology*, 4, 210.
- Pullamsetti, S., Kiss, L., Ghofrani, H. A., Voswinckel, R., Haredza, P., Klepetko, W., ... & Schermuly, R. T. (2005). Increased levels and reduced catabolism of asymmetric and symmetric dimethylarginines in pulmonaryhypertension. *The FASEB journal*, 19(9), 1175-1177.
- Rabinowits, G., Gerçel-Taylor, C., Day, J. M., Taylor, D. D., & Kloecker, G. H. (2009). Exosomal microRNA: a diagnostic marker for lung cancer. *Clinical lung cancer*, 10(1), 42-46.
- Raposo, G., & Stoorvogel, W. (2013). Extracellular vesicles: exosomes, microvesicles, and friends. *Journal of Cell Biology*, 200(4), 373-383.
- Raposo, G., Nijman, H. W., Stoorvogel, W., Liejendekker, R., Harding, C. V., Melief, C. J., & Geuze, H. J. (1996). B lymphocytes secrete antigen-presenting vesicles. *Journal of Experimental Medicine*, 183(3), 1161-1172.
- Ratajczak, J., Miekus, K., Kucia, M., Zhang, J., Reca, R., Dvorak, P., & Ratajczak, M. Z. (2006). Embryonic stem cell-derived microvesicles reprogram hematopoietic progenitors: evidence for horizontal transfer of mRNA and protein delivery. *Leukemia*, 20(5), 847-856.
- Rhim, A. D., Mirek, E. T., Aiello, N. M., Maitra, A., Bailey, J. M., McAllister, F., ... & Stanger, B. Z. (2012). EMT and dissemination precede pancreatic tumor formation. *Cell*, 148(1-2), 349-361.
- Ribatti, D. (2017). The concept of immune surveillance against tumors: the first theories. *Oncotarget*, 8(4), 7175.

- Roemer, A., Schwettmann, L., Jung, M., Stephan, C., Roigas, J., Kristiansen, G., ... & Jung, K. (2004). The membrane proteases adam8 and hepsin are differentially expressed in renal cell carcinoma. Are they potential tumor markers?. *The Journal of urology*, 172(6 Part 1), 2162-2166.
- Savina, A., Furlán, M., Vidal, M., & Colombo, M. I. (2003). Exosome release is regulated by a calcium-dependent mechanism in K562 cells. *Journal of Biological Chemistry*, 278(22), 20083-20090.
- Schlomann, U., Koller, G., Conrad, C., Ferdous, T., Golfi, P., Garcia, A. M., ... & Bartsch, J. W. (2015). ADAM8 as a drug target in pancreatic cancer. *Nature communications*, 6(1), 1-16.
- Schlomann, U., Wildeboer, D., Webster, A., Antropova, O., Zeuschner, D., Knight, C. G., ... & Bartsch, J. W. (2002). The metalloprotease disintegrin ADAM8: processing by autocatalysis is required for proteolytic activity and cell adhesion. *Journal of biological chemistry*, 277(50), 48210-48219.
- Schultz, N. A., Dehlendorff, C., Jensen, B. V., Bjerregaard, J. K., Nielsen, K. R., Bojesen, S. E., ... & Johansen, J. S. (2014). MicroRNA biomarkers in whole blood for detection of pancreatic cancer. *Jama*, 311(4), 392-404.
- Schurter, B. T., Koh, S. S., Chen, D., Bunick, G. J., Harp, J. M., Hanson, B. L., ... & Aswad, D. W. (2001). Methylation of histone H3 by coactivator-associated arginine methyltransferase 1. *Biochemistry*, 40(19), 5747-5756.
- Sheldon, H., Heikamp, E., Turley, H., Dragovic, R., Thomas, P., Oon, C. E., ... & Harris, A. L. (2010). New mechanism for Notch signaling to endothelium at a distance by Delta-like 4 incorporation into exosomes. *Blood, The Journal of the American Society of Hematology*, 116(13), 2385-2394.
- Shimoda, M., & Khokha, R. (2017). Metalloproteinases in extracellular vesicles. *Biochimica et Biophysica Acta (BBA)-Molecular Cell Research*, 1864(11), 1989-2000.
- Sibal, L., C Agarwal, S., D Home, P., & H Boger, R. (2010). The role of asymmetric dimethylarginine (ADMA) in endothelial dysfunction and cardiovascular disease. *Current cardiology reviews*, 6(2), 82-90.
- Siegel, R. L., Miller, K. D., Goding Sauer, A., Fedewa, S. A., Butterly, L. F., Anderson, J. C., ... & Jemal, A. (2020). Colorectal cancer statistics, 2020. *CA: a cancer journal for clinicians*, 70(3), 145-164.
- Silva, J., Garcia, V., Rodriguez, M., Compte, M., Cisneros, E., Veguillas, P., ... & Bonilla, F. (2012). Analysis of exosome release and its prognostic value in human colorectal cancer. *Genes, chromosomes and cancer*, 51(4), 409-418.
- Skog, J., Würdinger, T., Van Rijn, S., Meijer, D. H., Gainche, L., Curry, W. T., ... & Breakefield, X. O. (2008). Glioblastoma microvesicles transport RNA and proteins that promote tumour growth and provide diagnostic biomarkers. *Nature cell biology*, 10(12), 1470-1476.
- Slater, E. P., Fendrich, V., Strauch, K., Rospleszcz, S., Ramaswamy, A., Mätthai, E., ... & Bartsch, D. K. (2013). LCN2 and TIMP1 as potential serum markers for the early detection of familial pancreatic cancer. *Translational oncology*, 6(2), 99-103.

- Slater, E. P., Strauch, K., Rospleszcz, S., Ramaswamy, A., Esposito, I., Klöppel, G., ... & Bartsch, D. K. (2014). MicroRNA-196a and-196b as potential biomarkers for the early detection of familial pancreatic cancer. *Translational oncology*, 7(4), 464-471.
- Song, C., Chen, T., He, L., Ma, N., Li, J., ang, Rong, Y. F., Fang, Y., Liu, M., Xie, D. und Lou, W. (2020) „PRMT1promotes pancreatic cancer growth and predicts poor prognosis“, *Cellular Oncology*, 43(1), S. 51–62.
- Springer Medizin. (2019). Therapie des Pankreaskarzinoms: Die Anstrengungen werden belohnt!. *InFo Hämatologie+ Onkologie*, 22, 3-3.
- Steidl, C., Lee, T., Shah, S. P., Farinha, P., Han, G., Nayar, T., ... & Gascoyne, R. D. (2010). Tumor-associated macrophages and survival in classic Hodgkin's lymphoma. *New England Journal of Medicine*, 362(10), 875-885.
- Sumrin, A., Moazzam, S., Khan, A. A., Ramzan, I., Batool, Z., Kaleem, S., ... & Bilal, M. (2018). Exosomes as biomarker of cancer. *Brazilian Archives of Biology and Technology*, 61.
- Szafarska, A. E., Davison, T. S., John, J., Cannon, T., Sipos, B., Maghnoij, A., ... & Hahn, S. A. (2007). MicroRNA expression changes are associated with tumorigenesis and non-neoplastic processes in pancreatic ductal adenocarcinoma. *Oncogene*, 26(30), 4442-4452.
- Tang, J., Frankel, A., Cook, R. J., Kim, S., Paik, W. K., Williams, K. R., ... & Herschman, H. R. (2000). PRMT1 is the predominant type I protein arginine methyltransferase in mammalian cells. *Journal of Biological Chemistry*, 275(11), 7723-7730.
- Teerlink, T., Nijveldt, R. J., De Jong, S., & Van Leeuwen, P. A. (2002). Determination of arginine, asymmetric dimethylarginine, and symmetric dimethylarginine in human plasma and other biological samples by high-performance liquid chromatography. *Analytical biochemistry*, 303(2), 131-137.
- Théry, C., Zitvogel, L., & Amigorena, S. (2002). Exosomes: composition, biogenesis and function. *Nature reviews immunology*, 2(8), 569-579.
- Thomas, L., & Lawrence, H. (1959). Cellular and humoral aspects of the hypersensitive states. New York: Hoeber-Harper, 529-32.
- Treiber, T., Treiber, N., Plessmann, U., Harlander, S., Daiß, J. L., Eichner, N., ... & Meister, G. (2017). A compendium of RNA-binding proteins that regulate microRNA biogenesis. *Molecular cell*, 66(2), 270-284.
- Ungefroren, H., Sebens, S., Seidl, D., Lehnert, H., & Hass, R. (2011). Interaction of tumor cells with the microenvironment. *Cell Communication and Signaling*, 9(1), 1-8.
- Valkovskaya, N., Kayed, H., Felix, K., Hartmann, D., Giese, N. A., Osinsky, S. P., ... & Kleeff, J. (2007). ADAM8 expression is associated with increased invasiveness and reduced patient survival in pancreatic cancer. *Journal of cellular and molecular medicine*, 11(5), 1162-1174.
- Van Goor, H., Melenhorst, W. B., Turner, A. J., & Holgate, S. T. (2009). Adamalysins in biology and disease. *The Journal of Pathology: A Journal of the Pathological Society of Great Britain and Ireland*, 219(3), 277-286.
- Van Niel, G., d'Angelo, G., & Raposo, G. (2018). Shedding light on the cell biology of



- extracellular vesicles. *Nature reviews Molecular cell biology*, 19(4), 213-228.
- Vasievich, E. A., & Huang, L. (2011). The suppressive tumor microenvironment: a challenge in cancer immunotherapy. *Molecular pharmaceuticals*, 8(3), 635-641.
- Wang, H., Huang, Z. Q., Xia, L., Feng, Q., Erdjument-Bromage, H., Strahl, B. D., ... & Zhang, Y. (2001). Methylation of histone H4 at arginine 3 facilitating transcriptional activation by nuclear hormone receptor. *Science*, 293(5531), 853-857.
- Wang, Y. P., Zhou, W., Wang, J., Huang, X., Zuo, Y., Wang, T. S., ... & Lei, Q. Y. (2016). Arginine methylation of MDH1 by CARM1 inhibits glutamine metabolism and suppresses pancreatic cancer. *Molecular cell*, 64(4), 673-687.
- Weinberg, R. A. (2014). Coming full circle from endless complexity to simplicity and back again. *Cell*, 157(1), 267-271.
- Welton, J. L., Khanna, S., Giles, P. J., Brennan, P., Brewis, I. A., Staffurth, J., ... & Clayton, A. (2010). Proteomics analysis of bladder cancer exosomes. *Molecular & cellular proteomics*, 9(6), 1324-1338.
- Wienholds, E., & Plasterk, R. H. (2005). MicroRNA function in animal development. *FEBS letters*, 579(26), 5911-5922.
- Wolfers, J., Lozier, A., Raposo, G., Regnault, A., They, C., Masurier, C., ... & Zitvogel, L. (2001). Tumor-derived exosomes are a source of shared tumor rejection antigens for CTL cross-priming. *Nature medicine*, 7(3), 297-303.
- Xu, W., Cho, H., Kadam, S., Banayo, E. M., Anderson, S., Yates, J. R., ... & Evans, R. M. (2004). A methylation-mediator complex in hormone signaling. *Genes & development*, 18(2), 144-156.
- Yadav, N., Cheng, D., Richard, S., Morel, M., Iyer, V. R., Aldaz, C. M., & Bedford, M. T. (2008). CARM1 promotes adipocyte differentiation by coactivating PPAR $\gamma$ . *EMBO reports*, 9(2), 193-198.
- Yamagata, K., Daitoku, H., Takahashi, Y., Namiki, K., Hisatake, K., Kako, K., ... & Fukamizu, A. (2008). Arginine methylation of FOXO transcription factors inhibits their phosphorylation by Akt. *Molecular cell*, 32(2), 221-231.
- Yáñez-Mó, M., Siljander, P. R. M., Andreu, Z., Bedina Zavec, A., Borràs, F. E., Buzas, E. I., ... & De Wever, O. (2015). Biological properties of extracellular vesicles and their physiological functions. *Journal of extracellular vesicles*, 4(1), 27066.
- Yee, N. S., Zhang, S., He, H. Z., & Zheng, S. Y. (2020). Extracellular vesicles as potential biomarkers for early detection and diagnosis of pancreatic cancer. *Biomedicines*, 8(12), 581.
- Yoshida, S., Setoguchi, M., Higuchi, Y., Akizuki, S. I., & Yamamoto, S. (1990). Molecular cloning of cDNA encoding MS2 antigen, a novel cell surface antigen strongly expressed in murine monocytic lineage. *International Immunology*, 2(6), 585-591.
- Zakrzewicz, D., & Eickelberg, O. (2009). From arginine methylation to ADMA: a novel mechanism with therapeutic potential in chronic lung diseases. *BMC pulmonary medicine*, 9(1), 1-7.
- Zakrzewicz, D., Zakrzewicz, A., Preissner, K. T., Markart, P., & Wygrecka, M. (2012). Protein

- arginine methyltransferases (PRMTs): promising targets for the treatment of pulmonary disorders. *International journal of molecular sciences*, 13(10), 12383-12400.
- Zhang, B. C., Gao, J., Wang, J., Rao, Z. G., Wang, B. C., & Gao, J. F. (2011). Tumor-associated macrophages infiltration is associated with peritumoral lymphangiogenesis and poor prognosis in lung adenocarcinoma. *Medical Oncology*, 28(4), 1447-1452.
- Zhang, Y., Liu, D., Chen, X., Li, J., Li, L., Bian, Z., ... & Zhang, C. Y. (2010). Secreted monocytic miR-150 enhances targeted endothelial cell migration. *Molecular cell*, 39(1), 133-144.
- Zhang, Y., Su, Y., Zhao, Y., Lv, G., & Luo, Y. (2017). MicroRNA-720 inhibits pancreatic cancer cell proliferation and invasion by directly targeting cyclin D1. *Molecular medicine reports*, 16(6), 9256-9262.
- Zitvogel, L., Regnault, A., Lozier, A., Wolfers, J., Flament, C., Tenza, D., ... & Amigorena, S. (1998). Eradication of established murine tumors using a novel cell-free vaccine: dendritic cell derived exosomes. *Nature medicine*, 4(5), 594-600.



Article

## Cohort Analysis of ADAM8 Expression in the PDAC Tumor Stroma

Christian Jaworek <sup>1,†</sup>, Yesim Verel-Yilmaz <sup>2,†</sup>, Sarah Driesch <sup>2</sup>, Sarah Ostgathe <sup>1</sup>, Lena Cook <sup>1</sup>, Steffen Wagner <sup>3</sup> , Detlef K. Bartsch <sup>2</sup>, Emily P. Slater <sup>2,†</sup> and Jörg W. Bartsch <sup>1,\*</sup> 

- <sup>1</sup> Department of Neurosurgery, Philipps University Marburg, Baldingerstrasse, 35033 Marburg, Germany; christian@jaworek.org (C.J.); sarah.ostgathe@googlemail.com (S.O.); cookl@staff.uni-marburg.de (L.C.)  
<sup>2</sup> Department of Visceral Surgery, Philipps University Marburg, Baldingerstrasse, 35033 Marburg, Germany; yesimverel@hotmail.de (Y.V.-Y.); sarahdriesch@hotmail.de (S.D.); bartsch@med.uni-marburg.de (D.K.B.); slater@med.uni-marburg.de (E.P.S.)  
<sup>3</sup> Head and Neck Surgery, Department of Otorhinolaryngology, Justus Liebig University Giessen, Aulweg 128 (ForMED), 35392 Giessen, Germany; Steffen.Wagner@hno.med.uni-giessen.de  
 \* Correspondence: jwbartsch@med.uni-marburg.de; Tel.: +49-6421-58-61173  
 † Equal contribution.



**Citation:** Jaworek, C.; Verel-Yilmaz, Y.; Driesch, S.; Ostgathe, S.; Cook, L.; Wagner, S.; Bartsch, D.K.; Slater, E.P.; Bartsch, J.W. Cohort Analysis of ADAM8 Expression in the PDAC Tumor Stroma. *J. Pers. Med.* **2021**, *11*, 113. <https://doi.org/10.3390/jpm11020113>

Academic Editor: Lisa Salvatore  
 Received: 26 January 2021  
 Accepted: 7 February 2021  
 Published: 10 February 2021

**Publisher's Note:** MDPI stays neutral with regard to jurisdictional claims in published maps and institutional affiliations.



**Copyright:** © 2021 by the authors. Licensee MDPI, Basel, Switzerland. This article is an open access article distributed under the terms and conditions of the Creative Commons Attribution (CC BY) license (<https://creativecommons.org/licenses/by/4.0/>).

**Abstract:** Pancreatic ductal adenocarcinoma (PDAC) is a cancer type with one of the highest mortalities. The metalloprotease-disintegrin ADAM8 is highly expressed in pancreatic cancer cells and is correlated with an unfavorable patient prognosis. However, no information is available on ADAM8 expression in cells of the tumor microenvironment. We used immunohistochemistry (IHC) to describe the stromal cell types expressing ADAM8 in PDAC patients using a cohort of 72 PDAC patients. We found ADAM8 expressed significantly in macrophages (6%), natural killer cells (40%), and neutrophils (63%), which showed the highest percentage of ADAM8 expressing stromal cells. We quantified the amount of ADAM8<sup>+</sup> neutrophils in post-capillary venules in PDAC sections by IHC. Notably, the amount of ADAM8<sup>+</sup> neutrophils could be correlated with post-operative patient survival times. In contrast, neither the total neutrophil count in peripheral blood nor the neutrophil-to-lymphocyte ratio showed a comparable correlation. We conclude from our data that ADAM8 is, in addition to high expression levels in tumor cells, present in tumor-associated stromal macrophages, NK cells, and neutrophils and, in addition to functional implications, the ADAM8-expressing neutrophil density in post-capillary venules is a diagnostic parameter for PDAC patients when the numbers of ADAM8<sup>+</sup> neutrophils are quantified.

**Keywords:** pancreatic cancer; tumor microenvironment; tumor stroma; neutrophils; ADAM8 protease

### 1. Introduction

Pancreatic ductal adenocarcinoma (PDAC) is a highly heterogeneous tumor entity with a grim prognosis with a 5-year survival rate of less than 8% [1]. Desmoplastic reaction is very common in PDAC and accounts for a massive activation of stroma and stromal cells in the tumor microenvironment. The PDAC tumor microenvironment (TME) with its inflammatory nature activates many immune cell types in response to tumor cell derived signals (reviewed in [2]). As creators of and responders to signals in the tumor microenvironment, ADAM proteases (A disintegrin and metalloprotease) have been found to be associated with numerous functions ranging from immune cell migration and invasion [3], degradation of extracellular matrix molecules (Collagens I, IV) [4] to proteolytic inactivation of immune checkpoint inhibitors such as PD-L1 [5,6]. With their multidomain structures, ADAM proteases are capable of multiple physiological functions associated with cell adhesion, cell fusion, cell signaling, and proteolysis. Proteolysis of membrane-anchored precursor proteins by ADAMs is a key event for the generation of signaling cascades within the TME. In PDAC, a significant contribution of ADAM

proteases to tumor progression was reported for ADAM8 [4], ADAM9 [7,8], ADAM10 [9], ADAM12 [10], and ADAM17 [11]. Notably, higher expression levels of these ADAM proteases were reported to be associated with a poor patient prognosis in PDAC. Similar to other solid cancers, shedding of EGF-ligands and EGFR by ADAM10 and 17 are clearly relevant for tumor signaling in pancreatic cancer [11,12]. Furthermore, there are a number of ADAM proteases lacking phenotypes in knockout mice but with a possible role in different tumor entities and specifically in PDAC, which applies for ADAM8 and ADAM9 [8]. In particular, high expression levels of ADAM8 and 9 are associated with a worsened patient prognosis [13]. In previous studies, ADAM8 in particular was described in tumor cells and functional analyses revealed a tumor-promoting effect of ADAM8 in pancreatic cancer cells [4], so that inhibition of ADAM8 in pancreatic cancer (KPC) mice using a cyclic ADAM8 inhibiting peptide (BK-1361) leads to prolonged survival and improved metrics of pathological parameters (metastasis formation, invasion of tumor cells, acinar structures). However, since ADAM8 was reported to be highly expressed in tumor-associated immune cells as shown in glioblastoma [14], the goal of the present study was to analyze the presence of ADAM8 in tumor stroma of PDAC in a cohort of 72 in-house patients.

## 2. Materials and Methods

### 2.1. Patients and Tissue Samples

A total of 72 patients with PDAC who underwent a pancreas resection in the Department of Visceral Surgery at the University Hospital Marburg were enrolled in our study (see Table 1). All tumors were histologically staged by an experienced pathologist according to UICC-TNM (Union for International Cancer Control; tumor, node, metastasis) classification 2017 [15]. All samples were obtained from the tumor bank of the Department of Pathology. Ethical approval was obtained by the local ethics committee at Marburg University, Faculty of Medicine (File Nr. 5/03). All patients provided written informed consent prior to participating in this study.

**Table 1.** Clinical data on pancreatic ductal adenocarcinoma (PDAC) patient cohort used in this study ( $n = 72$ ); abbreviations used: \*: NLR: neutrophil-to-lymphocyte ratio; UICC: Union for International Cancer Control.

<b>Gender</b>	Males (%)	37 (51%)
	Females (%)	35 (49%)
<b>Median Age at Surgery, Years (Range)</b>		68 (47 to 85)
<b>UICC Stage, Number of Patients (%)</b>	I	11 (15.3%)
	II	10 (13.9%)
	III	46 (63.9%)
	IV	5 (6.9%)
<b>Median Survival, Months (Range)</b>		22 (1 to 92)
<b>Location</b>	head	65 (90%)
	body or tail	7 (10%)
<b>Median NLR * (Range)</b>		3.14 (1.53 to 31.67)

### 2.2. Immunohistochemistry (IHC)

For ADAM8 immunostaining, formalin-fixed and paraffin-embedded archived tumor samples and corresponding normal tissues were stained as follows. Paraffin sections (4  $\mu$ m thickness) from PDAC patients were stained for ADAM8 using a polyclonal anti-ADAM8 antibody and a standard VectaStain Protocol. For double-staining of PDAC sections, sections were stained for ADAM8 and the respective markers for T cell markers CD3, CD4, and CD8, stellate cell marker SMA, macrophage marker CD68, natural killer cell marker CD56, and neutrophil marker myeloperoxidase (MPO). Antibodies, concentrations,

and sources of primary antibodies are listed below (Table 2). Briefly, slides were heated to 60 °C for 1 h, deparaffinized using xylene, and hydrated by a graded series of ethanol washes. Antigen retrieval was accomplished by steam-heating in Target Retrieval Solution, pH9 (Agilent Dako, Waldbronn, Germany) for 30 min. For immunohistochemistry, endogenous peroxidase activity was quenched by 5 min incubation in 3% H<sub>2</sub>O<sub>2</sub>. Sections were then incubated with primary antibodies for 45 min at RT followed by biotinylated secondary antibodies for 20 min also at RT. Bound antibodies were detected using the avidin-biotin complex (ABC) peroxidase method (ABC Elite Kit; Vector Labs, Burlingame, CA, USA). Final staining was developed with the Dako DAB peroxidase substrate kit. For double staining, HRP Magenta Substrate Chromogen System was employed. Counterstaining was performed using hematoxylin. All steps following the antigen retrieval were performed using the DakoCytomation Autostainer Plus.

**Table 2.** Concentrations and sources of primary antibodies.

Antibody	Species	Working Dilution	Source
ADAM8	rabbit	1:200	R&D Systems (AF1031)
CD3	mouse	1:50	Dako (M7254)
CD56	mouse	1:10	Monosan (MON 9006)
CD68	mouse	1:200	Novus Biologicals (NB100-683)
CD163	mouse	1:50	ThermoFisher (MA5-11458)
CD4	mouse	1:100	Dako (M7310)
CD8	mouse	1:200	R&D Systems (MAB3801)
α Smooth muscle actin	mouse	1:2000	R&D Systems (MAB1420)
MPO	mouse	1:50	R&D systems (MAB3174)

### 2.3. Selection of Patient Samples for Double-Staining

A total of 10 patients were selected for double-staining that reflect our total cohort by having 7 stage III (among them 2 R0) and 3 stage II samples and from these 5 patients with survival times of less than 18 months and 5 patients with survival time longer than 18 months (one patient alive with disease).

### 2.4. Quantitation

The quantitation of ADAM8-positive and marker-positive cells in paraffin-embedded and stained sections was performed using the virtual software programs Fiji Image J [16].

### 2.5. Cell Counting and Scoring of Neutrophils in PDAC Patients

Samples from 51 patients were included in neutrophil analyses and none of these patients received a neoadjuvant therapy. Planimetry measurements of three venous blood vessels on each ADAM8-stained section were performed. Later, the number of ADAM8<sup>+</sup> neutrophils in the lumen of the blood vessels was scored and a ratio was calculated (cells per area). The sum of the three data sets of each patient are listed in the last column of Table A1. The blood vessels analyzed fulfilled the following criteria. The vessels were located in the center of tumor with a minimal luminal area of 2000 μm<sup>2</sup>. The distance between the vessels was such that three different areas of the tumor could be analyzed randomly. Blood vessels displaying fixation-related artifacts were excluded. Only cells that could be identified clearly as neutrophils with a positive staining for ADAM8 were counted.

### 2.6. Statistical Analysis

Two-way ANOVA was used for stroma cell quantifications and survival analyses. For neutrophil/survival analyses, a Pearson correlation coefficient was determined in conjunction with *t* statistics and *p*-value. Analyses were performed using Prism 6 for

Mac OSX from GraphPad, San Diego, CA, USA. A value of  $p < 0.05$  was considered to be significant.

### 3. Results

#### 3.1. ADAM8 Expression in PDAC

The PDAC patient cohort (tumor, stromal cells, co-localization) consists of patients who were clinically diagnosed with PDAC in the department of visceral surgery and included in the study (see Materials and Methods section for information on exclusion criteria). From all tumor patients, paraffin-embedded sections were stained and scored for ADAM8 expression (Figure 1).

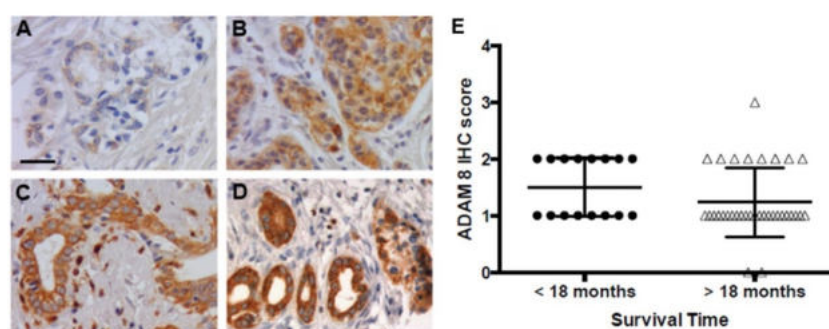


**Figure 1.** Correlation of ADAM8 staining scores with survival in patients of the PDAC cohort ( $n = 50$ ). Four exemplary images illustrating varying levels of ADAM8 staining in patient samples. The scale bar is 25  $\mu\text{m}$ . Staining intensities were determined for each section based on analysis of 5 viewing fields per section and were between 0 and 3 with no (0; (A)), low (1; (B)), moderate (2; (C)) and strong (3; (D)) ADAM8 staining. (E): Patients in the cohort were split into 2 groups with group 1, survival less than 18 months ( $\bullet$ ;  $n = 16$ ) and group 2 ( $\Delta$ ;  $n = 34$ ), patient survival longer than 18 months. Note that only two PDAC sections were almost negative for ADAM8. Difference is not significant.

Staining intensities in tumor cells were assessed by IHC score (0–3) according to earlier studies [17] in our in house cohort. Groups were separated into two according to median survival times either shorter or longer than 18 months. No significant differences were observed between the two groups with regard to ADAM8 IHC scores.

#### 3.2. Co-Localization of ADAM8 and Stromal Cell Markers in PDAC Tissue

In all PDAC sections stained for ADAM8, a notable expression was also observed in stromal cells (Figure 2A). To identify the stromal cell types expressing ADAM8 in PDAC, double staining of tissue with respective cell markers for T cells (CD3, CD4, CD8), natural killer (NK) cells (CD56), macrophages (CD68), neutrophils (MPO), and smooth muscle actin for stellate cells (SMA) was performed on a representative cohort of ten patients reflecting our total cohort (see Materials and Methods section for details).

We identified ADAM8-positive cells not only in the duct-like structures of the tumor area (Figure 2A), but also in the tumor microenvironment (Figure 2A–H). Stromal cells show moderate to high levels of ADAM8 staining. Significant co-staining of ADAM8 with markers for CD68 (macrophages, Figure 2B), for CD56 (NK cells, Figure 2F), and for MPO (neutrophils, Figure 2H) can be seen in Figure 2. Cells stained positively for both MPO and ADAM8 were identified to be neutrophils as evidenced by their granulocytic morphology.

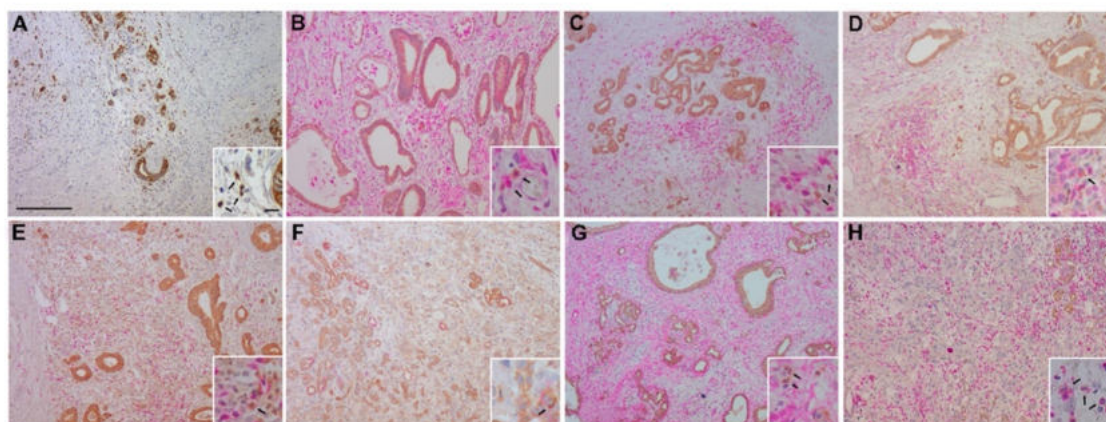


**Figure 2.** ADAM8 staining (A) in PDAC sections and co-localization of ADAM8 (brown) with markers (pink) for CD68 (macrophages, (B)), CD3 (CD3<sup>+</sup> T cells, (C)), CD4 (CD4<sup>+</sup> T cells, (D)), CD8 (CD8<sup>+</sup> T cells, (E)), CD56 (NK cells, (F)), SMA (stellate cells, (G)), and MPO (neutrophils, (H)). In (A), a control stain for ADAM8 alone is shown. Bar in A, 800 µm; bar in insert (A), 100 µm.

### 3.3. Quantitative Analysis of Co-Localization

ImageJ analysis on double-stained sections from a representative group of 10 patients was performed to quantify the number of specific stromal cells that were ADAM8 positive (Figure 3). Whereas T cells identified with distinct markers (CD3, CD4, and CD8) and pancreatic stellate cells (SMA) show a low percentage of co-localization, significant ADAM8-positive cell populations were observed for macrophages (CD68, 0–17%), NK cells (CD56, 18–75%), and neutrophils (MPO, 30–90%).

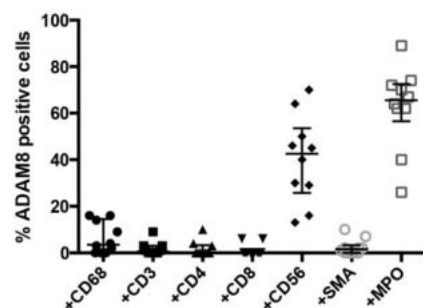


**Figure 3.** Scatter dot plot of the percentage of double-positive ADAM8/marker cells as analyzed in 10 representative PDAC sections stained for CD68 (●), CD3 (■), CD4 (▲), CD8 (▼), CD56 (◆), SMA (○) and MPO (□). Note that the frequency of ADAM8<sup>+</sup> stromal cells is highest for macrophages (CD68), NK cells (CD56), and neutrophils (MPO). For each section analyzed, data are derived from quantification of 5 viewing fields in the tumor proximal stroma areas. Median values with interquartile ranges are indicated. Note that the highest frequency of co-localization of ADAM8 with stromal markers is observed for MPO (neutrophils).

### 3.4. ADAM8 Expression in Neutrophils

We confirmed ADAM8 expression in neutrophils and their association with blood vessels in PDAC sections (Figure 3). Neutrophils enter the tissue from post-capillary venules in a process called leukodiapedesis. Thus, the likelihood of detecting neutrophils in these blood vessels is higher than in any other type of capillaries. Since post-capillary venules are large vessels, we sought to determine their frequency in PDAC sections.

To obtain comparable results, neutrophils were quantified in at least 3 independent post-capillary venules with an area of  $>2000 \mu\text{m}^2$  in the core tumor tissue (Figure 4 and Table A1 in Appendix A).

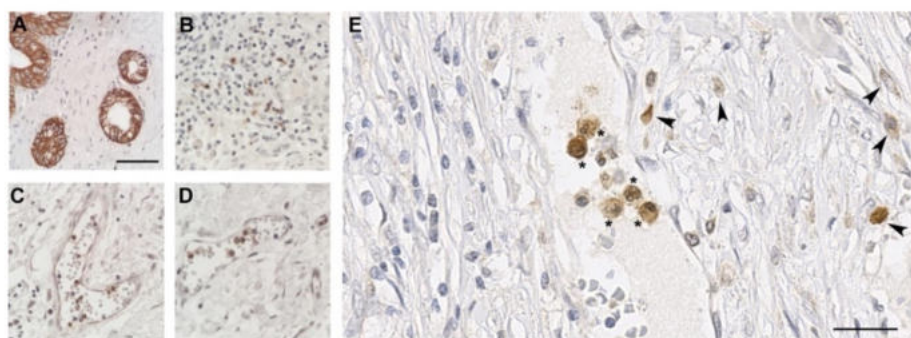


**Figure 4.** ADAM8 positive neutrophils located in tumor stromal post-capillary venules. (A), ADAM8 staining in duct-like structures; (B), ADAM8 staining in PDAC tumor stroma adjacent to duct-like structures reveals mainly ADAM8<sup>+</sup> neutrophils; (C) and (D) overview venules in tumor areas with ADAM8<sup>+</sup> neutrophils. (E), detailed view of venules with ADAM8<sup>+</sup> neutrophils in vessels (asterisks) and adjacent infiltrated neutrophils (arrowheads) in a representative PDAC section. Scale bar in (A), valid for (A–D), 120  $\mu\text{m}$ ; Scale bar in (E), 55  $\mu\text{m}$ .

Neutrophil numbers were correlated with patient survival data in the entire PDAC patient cohort (Figure 5A,B) where respective structures (venules) were analyzable. Moreover, we determined the neutrophil-to-leukocyte ratio (NLR) in PDAC patients where data were available and correlated these and the total blood neutrophil counts (Figure 5C,D) with survival data, respectively.

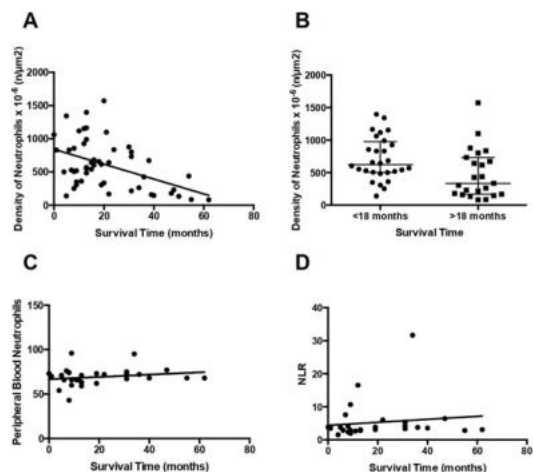


**Figure 5.** (A) Correlation analyses of ADAM8<sup>+</sup> neutrophil counts in post-capillary venules. Each data point is the average of 3 independent post-capillary venules of an area  $>2000 \mu\text{m}^2$  in the core tumor tissue ( $n = 50$ ). Pearson correlation revealed  $r = -0.463$  with  $p = 0.0006$ . (B) Neutrophil density diagram from our PDAC patient cohort split into survival time less than and greater than 18 months,  $p = 0.0128$ . (C) Neutrophil counts in peripheral blood of PDAC patients from the same cohort,  $p = 0.2797$ . (D) Neutrophil-to-lymphocyte ratio in the PDAC patient cohort,  $p = 0.5143$ . Note that only the ADAM8<sup>+</sup> neutrophil counts in post-capillary venules are significantly correlated with PDAC patient survival.

#### 4. Discussion

Due to high expression levels in PDAC tumor cells, ADAM8 was previously identified as a potential therapeutic target in PDAC [4,13]. Here we confirmed earlier results in our cohort that ADAM8 is expressed in almost all PDAC samples, but no significant correlation between ADAM8 expression in tumors and survival could be drawn. Interestingly, no previous study has mentioned expression of ADAM8 in stromal cells of PDAC. Given a distinct physiological expression profile of ADAM8 in immune cells such as macrophages and leukocytes, an ADAM8 expression in stromal cells of PDAC is likely and suggests an important role of ADAM8 in the tumor microenvironment of PDAC. However, the relatively low abundance of ADAM8-positive macrophages is unexpected as under physiological conditions, e.g., in the bone marrow, macrophages are constitutively expressing ADAM8 [14,18]. In macrophages, there is experimental evidence that ADAM8 can trigger their migratory behavior into the tissue under inflammatory conditions. This has been demonstrated in muscle regeneration when ADAM8-deficient macrophages are unable to remove muscle cell debris after muscle degeneration due to lack of motility [19]. A more general effect of ADAM8 on several immune related cells was observed in allergic asthma in mice where deficiency in ADAM8 caused a significantly reduced recruitment of macrophages, neutrophils, and eosinophils to the airway inflammation site to dampen the allergic response and the asthma severity [20]. By analyzing ADAM8 expression in neutrophils, we were able to show that an increased number of ADAM8-positive neutrophils particularly in venules of the tumor areas can be of prognostic value for PDAC patients. Mechanistically, this observation could point towards a detrimental effect of ADAM8-positive neutrophils in PDAC by regulating neutrophil transmigration from the vasculature to the tumor site. A neutrophil-to-lymphocyte ratio (NLR) has been reported to be a predictive parameter in clinical studies with PDAC patients. Higher ratios have been associated with poor outcome in some studies [21–23]. However, the value of this ratio in terms of prognosis is controversial [24]. In addition, whereas low tumor infiltration of neutrophils has been associated with poor prognosis [25], others report neutrophil infiltration to be observed in pancreatic tumors with the poorest prognosis [26]. It is interesting to note that the number of ADAM8-positive neutrophils in venules of PDAC patients shows a better correlation than either peripheral blood neutrophil count or the NLR. Although controversial, the general findings suggest that, in pretherapy PDAC patients, the NLR is not indicative for overall survival [24], which is in accordance with our findings.

#### 5. Conclusions

In PDAC, ADAM8 is significantly expressed in stromal cells, in particular in macrophages, NK cells, and neutrophils. Given the diagnostic value of neutrophil counts as reported previously [21–23], we propose that determination of neutrophil density in venules of tumor areas is a reliable indicator of disease progression and patient survival and could be used to stratify PDAC patients.

**Author Contributions:** Conceptualization, D.K.B., E.P.S. and J.W.B.; methodology, E.P.S. and J.W.B.; investigation, C.J., S.O., S.D. and Y.V.-Y.; resources, D.K.B. and E.P.S.; data curation, C.J., Y.V.-Y., S.O., S.W., L.C., E.P.S. and J.W.B.; writing—original draft preparation, C.J., J.W.B. and E.P.S.; writing—review and editing, C.J., D.K.B. and J.W.B.; supervision, D.K.B., E.P.S. and J.W.B.; project administration, E.P.S. and J.W.B.; funding acquisition, E.P.S. and J.W.B. All authors have read and agreed to the published version of the manuscript.

**Funding:** This research was funded by the DFG Clinical Research Unit (CRU) 325 (Clinical relevance of Tumor-microenvironment interactions in pancreatic cancer) grant number BA1606/4-1 and SL17/5-1. C.J. and S.D. received funding from the CRU 325 by a doctoral stipend; article processing charge was generously funded by Philipps University Marburg.

**Institutional Review Board Statement:** This study was conducted in accordance with the guidelines of the Declaration of Helsinki and approved by the local ethics committee, Medical Faculty of the Philipps University Marburg, file number 05/03.

**Informed Consent Statement:** Informed consent was obtained from all subjects involved in the study.

**Data Availability Statement:** Patient data can be made available upon request.

**Acknowledgments:** Authors would like to thank A. Ramaswamy for expert pathological advice, V. Wischmann for expert IHC staining, and N. Gercke for excellent technical assistance.

**Conflicts of Interest:** The authors declare no conflict of interest.

## Appendix A

**Table A1.** Summarizes clinical data and neutrophil counts in venules of PDAC patients in the cohort investigated. Abbreviations used: UICC: Union for International Cancer Control.; NLR: neutrophil-to-lymphocyte ratio.

Number	Gender	Age at Surgery (Years)	UICC Stage	Survival (Months)	Location	NLR	Density of Neutrophils (n/ $\mu\text{m}^2$ )
1	f	71	II	92	head	4.60	
2	m	85	IV	20	head	n.a.	$334 \times 10^6$
3	f	75	III	11	head	2.64	$360 \times 10^6$
4	m	65	III	31	head	4.29	$216 \times 10^6$
5	m	74	III	30	head	n.a.	$878 \times 10^6$
6	m	61	III	55	head	2.83	$84 \times 10^6$
7	m	56	III	62	head	3.09	$81 \times 10^6$
8	f	55	III	19	head	3.84	$305 \times 10^6$
9	m	73	III	6	body	2.87	$831 \times 10^6$
10	m	49	II	8	head	2.39	$856 \times 10^6$
11	m	67	III	5	head	n.a.	$139 \times 10^6$
12	f	51	III	40	head	3.58	$146 \times 10^6$
13	m	68	III	50	head	n.a.	$134 \times 10^6$
14	w	77	II	34	head	31.67	$260 \times 10^6$
15	f	85	II	0	head	3.84	$1061 \times 10^6$
16	m	52	IV	16	body	n.a.	$603 \times 10^6$
17	f	68	III	20	tail	n.a.	$1573 \times 10^6$
18	f	82	III	22	head	6.00	$643 \times 10^6$
19	f	53	III	35	head	n.a.	
20	f	69	IV	15	body	n.a.	$540 \times 10^6$
21	f	74	III	4	head	1.53	$501 \times 10^6$
22	m	68	III	4	head	n.a.	
23	f	78	III	39	head	n.a.	$159 \times 10^6$
24	m	56	III	30	head	n.a.	
25	f	65	III	38	head	n.a.	$672 \times 10^6$
26	f	50	III	13	head	2.81	$484 \times 10^6$
27	f	62	I	42	head	n.a.	
28	m	78	III	31	head	3.35	$800 \times 10^6$
29	f	75	I	32	head	n.a.	
30	m	68	I	1	head	3.50	$831 \times 10^6$
31	m	72	III	36	head	n.a.	
32	m	66	II	33	head	n.a.	
33	m	78	I	28	head	n.a.	
34	f	75	I	35	head	6.83	
35	f	79	III	22	head	n.a.	$168 \times 10^6$
36	m	60	III	9	head	2.87	$519 \times 10^6$
37	f	60	I	33	head	2.75	
38	f	58	III	27	head	2.79	
39	f	57	III	19	head	3.10	$616 \times 10^6$
40	m	67	III	28	head	n.a.	
41	m	64	III	24	head	n.a.	$836 \times 10^6$
42	f	68	I	29	head	n.a.	
43	m	60	I	n.a.	head	n.a.	
44	m	60	III	28	head	2.87	
45	f	51	III	16	head	n.a.	$682 \times 10^6$



Table A1. Cont.



Number	Gender	Age at Surgery (Years)	UICC Stage	Survival (Months)	Location	NLR	Density of Neutrophils (n/ $\mu\text{m}^2$ )
46	f	78	III	28	head	2.00	
47	f	79	I	26	head	n.a.	
48	m	47	III	10	head	n.a.	1117 $\times 10^6$
49	m	65	II	12	body	16.50	1154 $\times 10^6$
50	f	79	III	13	head	2.86	569 $\times 10^6$
51	m	72	III	13	head	2.86	1398 $\times 10^6$
52	m	58	III	48	head	n.a.	230 $\times 10^6$
53	f	71	II	75	head	2.67	
54	m	78	III	12	head	n.a.	926 $\times 10^6$
55	m	64	III	54	head	n.a.	438 $\times 10^6$
56	m	70	I	36	body	3.79	425 $\times 10^6$
57	f	61	III	31	head	5.36	733 $\times 10^6$
58	m	71	III	13	head	n.a.	1164 $\times 10^6$
59	m	68	III	21	head	n.a.	1099 $\times 10^6$
60	m	75	II	47	head	6.42	179 $\times 10^6$
61	f	77	III	57	head	3.14	
62	f	75	III	9	head	1.94	349 $\times 10^6$
63	m	80	II	8	head	4.11	252 $\times 10^6$
64	m	52	III	13	head	n.a.	991 $\times 10^6$
65	f	78	III	7	head	7.60	529 $\times 10^6$
66	m	80	II	9	head	10.67	308 $\times 10^6$
67	m	67	III	15	head	n.a.	643 $\times 10^6$
68	f	64	IV	13	body	3.09	553 $\times 10^6$
69	f	68	IV	18	head	n.a.	658 $\times 10^6$
70	f	73	III	5	head	3.74	1342 $\times 10^6$
71	f	72	III	8	head	n.a.	506 $\times 10^6$
72	m	77	I	16	head	n.a.	

## References

- Siegel, R.L.; Miller, K.D.; Jemal, A. Cancer statistics, 2020. *CA Cancer J. Clin.* **2020**, *70*, 7–30. [\[CrossRef\]](#)
- Huber, M.; Brehm, C.U.; Gress, T.M.; Buchholz, M.; Alhamwe, B.A.; von Strandmann, E.P.; Slater, E.P.; Bartsch, J.W.; Bauer, C.; Lauth, M. The immune microenvironment in pancreatic cancer. *Int. J. Mol. Sci.* **2020**, *21*, 7307. [\[CrossRef\]](#)
- Conrad, C.; Benzel, J.; Dorzweiler, K.; Cook, L.; Schlomann, U.; Zarbock, A.; Slater, E.P.; Nimsky, C.; Bartsch, J.W. ADAM8 in invasive cancers: Links to tumor progression, metastasis, and chemoresistance. *Clin. Sci. (London)* **2019**, *133*, 83–99. [\[CrossRef\]](#)
- Schlomann, U.; Koller, G.; Conrad, C.; Ferdous, T.; Golfi, P.; Garcia, A.M.; Höfling, S.; Parsons, M.; Costa, P.; Soper, R.; et al. ADAM8 as a drug target in pancreatic cancer. *Nat. Commun.* **2015**, *6*, 6175. [\[CrossRef\]](#) [\[PubMed\]](#)
- Romero, Y.; Wise, R.; Zolkiewska, A. Proteolytic processing of PD-L1 by ADAM proteases in breast cancer cells. *Cancer Immunol. Immunother.* **2020**, *69*, 43–55. [\[CrossRef\]](#)
- Orme, J.J.; Jazieh, K.A.; Xie, T.; Harrington, S.; Liu, X.; Ball, M.; Madden, B.; Charlesworth, M.C.; Azam, T.U.; Lucien, F.; et al. ADAM10 and ADAM17 cleave PD-L1 to mediate PD-(L)1 inhibitor resistance. *Oncimmunology* **2020**, *9*, 1744980. [\[CrossRef\]](#)
- Grützmann, R.; Lüttges, J.; Sipos, B.; Ammerpohl, O.; Dobrowolski, F.; Alldinger, I.; Kersting, S.; Ockert, D.; Koch, R.; Kalthoff, H.; et al. ADAM9 expression in pancreatic cancer is associated with tumour type and is a prognostic factor in ductal adenocarcinoma. *Br. J. Cancer* **2004**, *90*, 1053–1058. [\[CrossRef\]](#) [\[PubMed\]](#)
- Oria, V.O.; Lopatta, P.; Schmitz, T.; Preca, B.T.; Nyström, A.; Conrad, C.; Bartsch, J.W.; Kulemann, B.; Hoepfner, J.; Maurer, J.; et al. ADAM9 contributes to vascular invasion in pancreatic ductal adenocarcinoma. *Mol. Oncol.* **2019**, *13*, 456–479. [\[CrossRef\]](#)
- Gaida, M.M.; Haag, N.; Günther, F.; Tschaharganeh, D.F.; Schirmacher, P.; Friess, H.; Giese, N.A.; Schmidt, J.; Wente, M.N. Expression of A disintegrin and metalloprotease 10 in pancreatic carcinoma. *Int. J. Mol. Med.* **2010**, *26*, 281–288. [\[CrossRef\]](#) [\[PubMed\]](#)
- Veenstra, V.L.; Damhofer, H.; Waasdorp, C.; van Rijssen, L.B.; van de Vijver, M.J.; Dijk, F.; Wilmink, H.W.; Besselink, M.G.; Busch, O.R.; Chang, D.K.; et al. ADAM12 is a circulating marker for stromal activation in pancreatic cancer and predicts response to chemotherapy. *Oncogenesis* **2018**, *7*, 87. [\[CrossRef\]](#) [\[PubMed\]](#)
- Ardito, C.M.; Grüner, B.M.; Takeuchi, K.K.; Lubeseder-Martellato, C.; Teichmann, N.; Mazur, P.K.; Delgiorno, K.E.; Carpenter, E.S.; Halbrook, C.J.; Hall, J.C.; et al. EGF receptor is required for KRAS-induced pancreatic tumorigenesis. *Cancer Cell* **2012**, *22*, 304–317. [\[CrossRef\]](#)

12. Blobel, C.P. ADAMs: Key components in EGFR signalling and development. *Nat. Rev. Mol. Cell Biol.* **2005**, *6*, 32–43. [[CrossRef](#)] [[PubMed](#)]
13. Valkovskaya, N.; Kaye, H.; Felix, K.; Hartmann, D.; Giese, N.A.; Osinsky, S.P.; Friess, H.; Kleeff, J. ADAM8 expression is associated with increased invasiveness and reduced patient survival in pancreatic cancer. *J. Cell. Mol. Med.* **2007**, *11*, 1162–1174. [[CrossRef](#)] [[PubMed](#)]
14. Gjorgjevski, M.; Hannen, R.; Carl, B.; Li, Y.; Landmann, E.; Buchholz, M.; Bartsch, J.W.; Nimsy, C. Molecular profiling of the tumor microenvironment in glioblastoma patients: Correlation of microglia/macrophage polarization state with metalloprotease expression profiles and survival. *Biosci. Rep.* **2019**, *39*. [[CrossRef](#)]
15. Gospodarowicz, M.K.; Brierley, J.D. *TNM Classification of Malignant Tumors*; Wiley-Blackwell: Oxford, UK, 2017.
16. Schindelin, J.; Arganda-Carreras, I.; Frise, E.; Kaynig, V.; Longair, M.; Pietzsch, T.; Preibisch, S.; Rueden, C.; Saalfeld, S.; Schmid, B.; et al. Fiji: An open-source platform for biological-image analysis. *Nat. Methods* **2012**, *9*, 676–682. [[CrossRef](#)] [[PubMed](#)]
17. Conrad, C.; Götte, M.; Schlomann, U.; Roessler, M.; Pagenstecher, A.; Anderson, P.; Preston, J.; Pruessmeyer, J.; Ludwig, A.; Li, R.; et al. ADAM8 expression in breast cancer derived brain metastases: Functional implications on MMP-9 expression and transendothelial migration in breast cancer cells. *Int. J. Cancer* **2018**, *142*, 779–791. [[CrossRef](#)] [[PubMed](#)]
18. Li, Y.; Guo, S.; Zhao, K.; Conrad, C.; Driescher, C.; Rothbart, V.; Schlomann, U.; Guerreiro, H.; Bopp, M.H.; König, A.; et al. ADAM8 affects glioblastoma progression by regulating osteopontin-mediated angiogenesis. *Biol. Chem.* **2020**. [[CrossRef](#)]
19. Nishimura, D.; Sakai, H.; Sato, T.; Sato, F.; Nishimura, S.; Toyama-Sorimachi, N.; Bartsch, J.W.; Sehara-Fujisawa, A. Roles of ADAM8 in elimination of injured muscle fibers prior to skeletal muscle regeneration. *Mech. Dev.* **2015**, *135*, 58–67. [[CrossRef](#)]
20. Naus, S.; Blanchet, M.R.; Gossens, K.; Zaph, C.; Bartsch, J.W.; McNagny, K.; Ziltener, H.J. The metalloprotease-disintegrin ADAM8 is essential for the development of experimental asthma. *Am. J. Respir. Crit. Care Med.* **2010**, *181*, 1318–1328. [[CrossRef](#)]
21. Arima, K.; Okabe, H.; Hashimoto, D.; Chikamoto, A.; Tsuji, A.; Yamamura, K.; Kitano, Y.; Inoue, R.; Kaida, T.; Higashi, T.; et al. The diagnostic role of the neutrophil-to-lymphocyte ratio in predicting pancreatic ductal adenocarcinoma in patients with pancreatic diseases. *Int. J. Clin. Oncol.* **2016**, *21*, 940–945. [[CrossRef](#)] [[PubMed](#)]
22. Ben, Q.; An, W.; Wang, L.; Wang, W.; Yu, L.; Yuan, Y. Validation of the pretreatment neutrophil-lymphocyte ratio as a predictor of overall survival in a cohort of patients with pancreatic ductal adenocarcinoma. *Pancreas* **2015**, *44*, 471–477. [[CrossRef](#)]
23. Tao, L.; Zhang, L.; Peng, Y.; Tao, M.; Li, G.; Xiu, D.; Yuan, C.; Ma, C.; Jiang, B. Preoperative neutrophil-to-lymphocyte ratio and tumor-related factors to predict lymph node metastasis in patients with pancreatic ductal adenocarcinoma (PDAC). *Oncotarget* **2016**, *7*, 74314–74324. [[CrossRef](#)] [[PubMed](#)]
24. Chawla, A.; Huang, T.L.; Ibrahim, A.M.; Hardacre, J.M.; Siegel, C.; Ammori, J.B. Pretherapy neutrophil to lymphocyte ration and platelet to lymphocyte ratio do not predict survival in resectable pancreatic cancer. *HPB (Oxford)* **2018**, *20*, 398–404. [[CrossRef](#)]
25. Naso, J.R.; Topham, J.T.; Karasinska, J.M.; Lee, M.K.C.; Kalloger, S.E.; Wong, H.L.; Nelson, J.; Moore, R.A.; Mungall, A.J.; Jones, S.J.M.; et al. Tumor infiltrating neutrophils and gland formation predict overall survival and molecular subgroups in pancreatic ductal adenocarcinoma. *Cancer Med.* **2020**. [[CrossRef](#)] [[PubMed](#)]
26. Steele, C.W.; Karim, S.A.; Leach, J.D.G.; Bailey, P.; Upstill-Goddard, R.; Rishi, L.; Foth, M.; Bryson, S.; McDaid, K.; Wilson, Z.; et al. CXCR2 inhibition profoundly suppresses metastases and augments immunotherapy in pancreatic ductal adenocarcinoma. *Cancer Cell* **2016**, *29*, 832–845. [[CrossRef](#)] [[PubMed](#)]

# PRMT1 promotes the tumor suppressor function of p14<sup>ARF</sup> and is indicative for pancreatic cancer prognosis

Antje Repenning<sup>1,†</sup>, Daniela Happel<sup>1,†</sup>, Caroline Bouchard<sup>1</sup>, Marion Meixner<sup>1</sup>, Yesim Verel-Yilmaz<sup>2</sup>, Hartmann Raifer<sup>3,4</sup>, Lena Holembowski<sup>1</sup>, Eberhard Krause<sup>5</sup>, Elisabeth Kremmer<sup>6</sup>, Regina Feederle<sup>7</sup> , Corinna U Keber<sup>8</sup>, Michael Lohoff<sup>4</sup>, Emily P Slater<sup>2</sup>, Detlef K Bartsch<sup>2</sup> & Uta-Maria Bauer<sup>1,\*</sup> 

## Abstract

The p14<sup>ARF</sup> protein is a well-known regulator of p53-dependent and p53-independent tumor-suppressive activities. In unstressed cells, p14<sup>ARF</sup> is predominantly sequestered in the nucleoli, bound to its nucleolar interaction partner NPM. Upon genotoxic stress, p14<sup>ARF</sup> undergoes an immediate redistribution to the nucleolar and cytoplasm, where it promotes activation of cell cycle arrest and apoptosis. Here, we identify p14<sup>ARF</sup> as a novel interaction partner and substrate of PRMT1 (protein arginine methyltransferase 1). PRMT1 methylates several arginine residues in the C-terminal nuclear/nucleolar localization sequence (NLS/NoLS) of p14<sup>ARF</sup>. In the absence of cellular stress, these arginines are crucial for nucleolar localization of p14<sup>ARF</sup>. Genotoxic stress causes augmented interaction between PRMT1 and p14<sup>ARF</sup>, accompanied by arginine methylation of p14<sup>ARF</sup>. PRMT1-dependent NLS/NoLS methylation promotes the release of p14<sup>ARF</sup> from NPM and nucleolar sequestration, subsequently leading to p53-independent apoptosis. This PRMT1-p14<sup>ARF</sup> cooperation is cancer-relevant and indicative for PDAC (pancreatic ductal adenocarcinoma) prognosis and chemotherapy response of pancreatic tumor cells. Our data reveal that PRMT1-mediated arginine methylation is an important trigger for p14<sup>ARF</sup>'s stress-induced tumor-suppressive function.

**Keywords** apoptosis; arginine methylation; pancreatic cancer; post-translational modification; tumor suppression

**Subject Categories** Autophagy & Cell Death; Cell Cycle; Post-translational Modifications & Proteolysis

**DOI** 10.15252/emboj.2020106777 | Received 12 September 2020 | Revised 31 March 2021 | Accepted 1 April 2021 | Published online 17 May 2021

**The EMBO Journal (2021) 40: e106777**

## Introduction

The INK4a/ARF (CDKN2A) gene locus on human chromosome 9p21 encodes two structurally unrelated proteins with distinct tumor suppressor functions, p14<sup>ARF</sup> and p16<sup>INK4a</sup>. While p16<sup>INK4a</sup> blocks the kinase activity of CDK4/CDK6, thus preventing Rb phosphorylation and subsequently S-phase entry, p14<sup>ARF</sup> exerts p53-dependent and p53-independent cell cycle arrest and apoptosis (Kim & Sharpless, 2006). Consistent with these functions, the *INK4a/ARF* locus is frequently mutated in human malignancies, e.g., in ≥ 80% of sporadic pancreatic ductal adenocarcinomas (PDACs; Hezel *et al.*, 2006), indicating that inactivation of this locus is essential for abnormal cell proliferation and loss of genomic stability.

p14<sup>ARF</sup> is an important sensor of different types of cellular stress and hence positively regulated in response to oncogenic signals and genotoxic stress (Ozanne *et al.*, 2010). In unstressed healthy cells, p14<sup>ARF</sup> is usually expressed at low levels as a result of efficient N-terminal ubiquitination and subsequent proteasomal degradation (Kuo *et al.*, 2004; Chen *et al.*, 2010). Moreover, in the absence of DNA damage, p14<sup>ARF</sup> is sequestered in the nucleoli due to its interaction with the abundant nucleolar protein NPM (nucleophosmin) leading to a functionally inactive, but more stable protein fraction (Rodway *et al.*, 2004; Korgaonkar *et al.*, 2005). Upon genotoxic stress, p14<sup>ARF</sup> redistributes from the nucleolus to the nucleolar and cytoplasm, where it, among others, promotes activation of the p53 pathway by inhibiting the E3 ubiquitin ligase MDM2 (Lee *et al.*, 2005; Sherr, 2006). Importantly, p14<sup>ARF</sup> governs also tumor-suppressive activities independent of p53 and interacts with a variety of proteins, such as TIP60, TOPO I, and p32 (C1QBP), thereby regulating their function in DNA damage signaling, DNA repair, and

1 Institute for Molecular Biology and Tumor Research (IMT), Philipps-University Marburg, Marburg, Germany

2 Department of Visceral, Thoracic and Vascular Surgery, University Hospital Marburg, Philipps-University Marburg, Marburg, Germany

3 Core Facility Flow Cytometry, University Hospital Marburg, Philipps-University Marburg, Marburg, Germany

4 Institute for Med. Microbiology & Hospital Hygiene, University Hospital Marburg, Philipps-University Marburg, Marburg, Germany

5 Leibniz Institute of Molecular Pharmacology, Berlin, Germany

6 Institute of Molecular Immunology, Helmholtz Zentrum München, German Research Center for Environmental Health, München, Germany

7 Monoclonal Antibody Core Facility, Institute for Diabetes and Obesity, Helmholtz Zentrum München, German Research Center for Environmental Health, Neuherberg, Germany

8 Institute for Pathology, University Hospital Marburg, Philipps-University Marburg, Marburg, Germany

\*Corresponding author. Tel: +49 6421 2865325; Fax: +49 6421 2865196; E-mail: bauer@imt.uni-marburg.de

†These authors contributed equally to this work.

apoptosis (Karayan *et al.*, 2001; Ayrault *et al.*, 2003; Eymin *et al.*, 2006; Itahana & Zhang, 2008). Enforced nucleolar retention of p14<sup>ARF</sup> inhibits these tumor-suppressive activities (Korgaonkar *et al.*, 2005). The molecular mechanisms, which lead to the stress-induced redistribution of p14<sup>ARF</sup>, have not been elucidated.

Targeting of p14<sup>ARF</sup> to the nucleus and nucleolus is mediated by an arginine-rich sequence motif (amino acids 85–101) in its C-terminus (Zhang & Xiong, 1999; Rizos *et al.*, 2000). Tumor-associated mutations of several arginine residues within this nuclear/nucleolar localization sequence (NLS/NoLS) have been reported to cause an altered subcellular localization of the protein. These NLS/NoLS mutations disrupt the p53-independent pro-apoptotic functions of p14<sup>ARF</sup>, for example, attenuating p32-mediated apoptosis (Itahana & Zhang, 2008). The fact that p14<sup>ARF</sup> is a highly basic protein, overall composed of 20% arginine residues, raises the question whether arginine methylation participates in the functional regulation of p14<sup>ARF</sup>. The enzymes responsible for this post-translational modification are the protein arginine methyltransferases (PRMTs), which constitute a family of nine members in mammals (Yang & Bedford, 2013). They transfer methyl groups from the ubiquitous methyl-group donor S-adenosyl-L-methionine (SAM) to the terminal guanidino nitrogens of arginine residues, catalyzing monomethyl arginine (MMA), asymmetric dimethyl-arginine (ADMA), or symmetric dimethyl-arginine (SDMA). A multitude of nuclear and cytoplasmic proteins are post-translationally modified by arginine methylation. Thereby, PRMTs regulate a wide range of essential cellular processes, for example, signal transduction, nucleo-cytoplasmic transport, transcriptional regulation, and RNA splicing (Yang & Bedford, 2013).

In the present study, we investigated the potential impact of arginine methylation on the function of p14<sup>ARF</sup>. We show that p14<sup>ARF</sup> is arginine-methylated *in vivo* and that PRMT1 is responsible for the generation of ADMA-modified p14<sup>ARF</sup>. Using mass spectrometry, we identified four arginine residues (R87/88/96/99) within the NLS/NoLS of p14<sup>ARF</sup> as the major methylation sites of PRMT1. Overexpression or depletion of PRMT1 leads to perturbed subcellular localization and turnover of endogenous p14<sup>ARF</sup> and defects in apoptosis signaling. Moreover, mutation of these PRMT1 methylation sites to amino acids that do not preserve the basic charge causes relocalization of the mutant p14<sup>ARF</sup> proteins from the nucleoli to the nucleolar and cytoplasm. Genotoxic stress, such as UVC irradiation, results in an enhanced interaction between PRMT1 and p14<sup>ARF</sup> and concomitantly increased levels of arginine-methylated p14<sup>ARF</sup>, which contribute to the release from its nucleolar binding partner NPM. In addition, arginine methylation of p14<sup>ARF</sup> enforces its interaction with the pro-apoptotic factor p32 and promotes apoptosis. Our data suggest that PRMT1-mediated arginine methylation causes crucial changes in the interaction network of p14<sup>ARF</sup> and triggers stress-induced relocalization and tumor-suppressive functions of p14<sup>ARF</sup>. Finally, we find that the PRMT1-p14<sup>ARF</sup> cooperation is cancer-relevant and indicative for PDAC prognosis and chemotherapy response of pancreatic tumor cells.

## Results

### Arginine residues in p14<sup>ARF</sup> are methylated by PRMT1 and PRMT5

Given that cancer-associated mutations of certain arginine residues within p14<sup>ARF</sup> disclose an important role in the regulation of

apoptosis (Itahana & Zhang, 2008), we raised the question whether p14<sup>ARF</sup> is arginine methylated and whether this post-translational modification is relevant for its tumor suppressor function. To this end, we analyzed the occurrence of *in vivo* methylation of p14<sup>ARF</sup> by metabolic labeling. EGFP-tagged p14<sup>ARF</sup> and empty vector (control) expressing HEK293 cells (Appendix Fig S1A) were cultured in the presence of L-[<sup>3</sup>H-methyl]-methionine, which is intracellularly metabolized to SAM. Additionally, cells were treated with translational inhibitors to avoid incorporation of radiolabelled methionine by *de novo*-protein biosynthesis (Liu & Dreyfuss, 1995). Subsequent to immunoprecipitation and SDS-PAGE, p14<sup>ARF</sup> methylation was detected by fluorography, as depicted in Fig 1A (upper panel). Treatment with the global methyltransferase inhibitor adenosine dialdehyde (AdOx) resulted in hypomethylated cell extracts and in the loss of detection of methylated p14<sup>ARF</sup> (Appendix Fig S1B, Fig 1A, upper panel). The overexpression and precipitation of EGFP-tagged p14<sup>ARF</sup>, which typically occurred in a doublet band, were verified by Western blot analysis (Fig 1A, lower panel). Since p14<sup>ARF</sup> does not contain any lysine residues, but a high number of arginines, this result indicates that p14<sup>ARF</sup> is methylated at arginine residues *in vivo*.

To identify responsible PRMTs, we performed *in vitro* methyltransferase (MT) assays using bacterially expressed and purified GST-tagged p14<sup>ARF</sup> and PRMTs (expressed/purified either from E.coli, mammalian cells or Sf9 cells) in the presence of radiolabeled methyl-group donor SAM. Here, PRMT1 and PRMT5 were found to methylate p14<sup>ARF</sup>, whereas PRMT4 did not modify the protein (Fig 1B and C). PRMT1 and PRMT5 are known to share common substrates, but deposit different dimethylation marks, ADMA, and SDMA, respectively, which elicit diverse functional properties (Favia *et al.*, 2019). In the present study, we focussed on the role of PRMT1-mediated methylation of p14<sup>ARF</sup>. Using recombinant GST-tagged p14<sup>ARF</sup> deletion constructs, we mapped the methylation sites of PRMT1 within the C-terminus of p14<sup>ARF</sup> (aa 65–132), which encompasses an arginine-rich NoLS/NLS, whereas the N-terminal region (aa 1–64) also containing a basic charged NoLS/NLS was not modified by PRMT1 (Fig 1D). Mass-spectrometric analysis of *in vitro* methylated full-length GST-tagged p14<sup>ARF</sup> protein was performed to identify the specific arginine residues that are modified by PRMT1. After tryptic digestion, LC-MS/MS identified two arginine residues (R96/R99) within the NoLS/NLS of p14<sup>ARF</sup> as the major mono- and dimethylation sites (Fig 1E). In addition, fragment ion spectra provided some evidence of methylation of arginine 87 and 88 (R87/R88) with a lower degree of modification (data not shown). Remarkably, these four amino acid positions overlap with published cancer-associated mutations within the C-terminus of p14<sup>ARF</sup> (Zhang & Xiong, 1999). Mutation of the four arginines to glycines in the full-length p14<sup>ARF</sup> protein (p14<sup>ARF</sup> RG) abolished *in vitro* methylation by PRMT1 and confirmed that PRMT1 predominantly modifies these four arginines in p14<sup>ARF</sup> (Fig 1F). Furthermore, co-immunoprecipitation experiments showed that overexpressed Myc-tagged PRMT1 and Flag-tagged p14<sup>ARF</sup> interact in U2OS cell extracts (Fig 1G). These results identify p14<sup>ARF</sup> as a novel substrate and interaction partner of PRMT1.

### PRMT1 regulates the cellular localization of p14<sup>ARF</sup>

Given that p14<sup>ARF</sup> is arginine methylated within its C-terminal NLS/NoLS by PRMT1, we investigated the subcellular localization

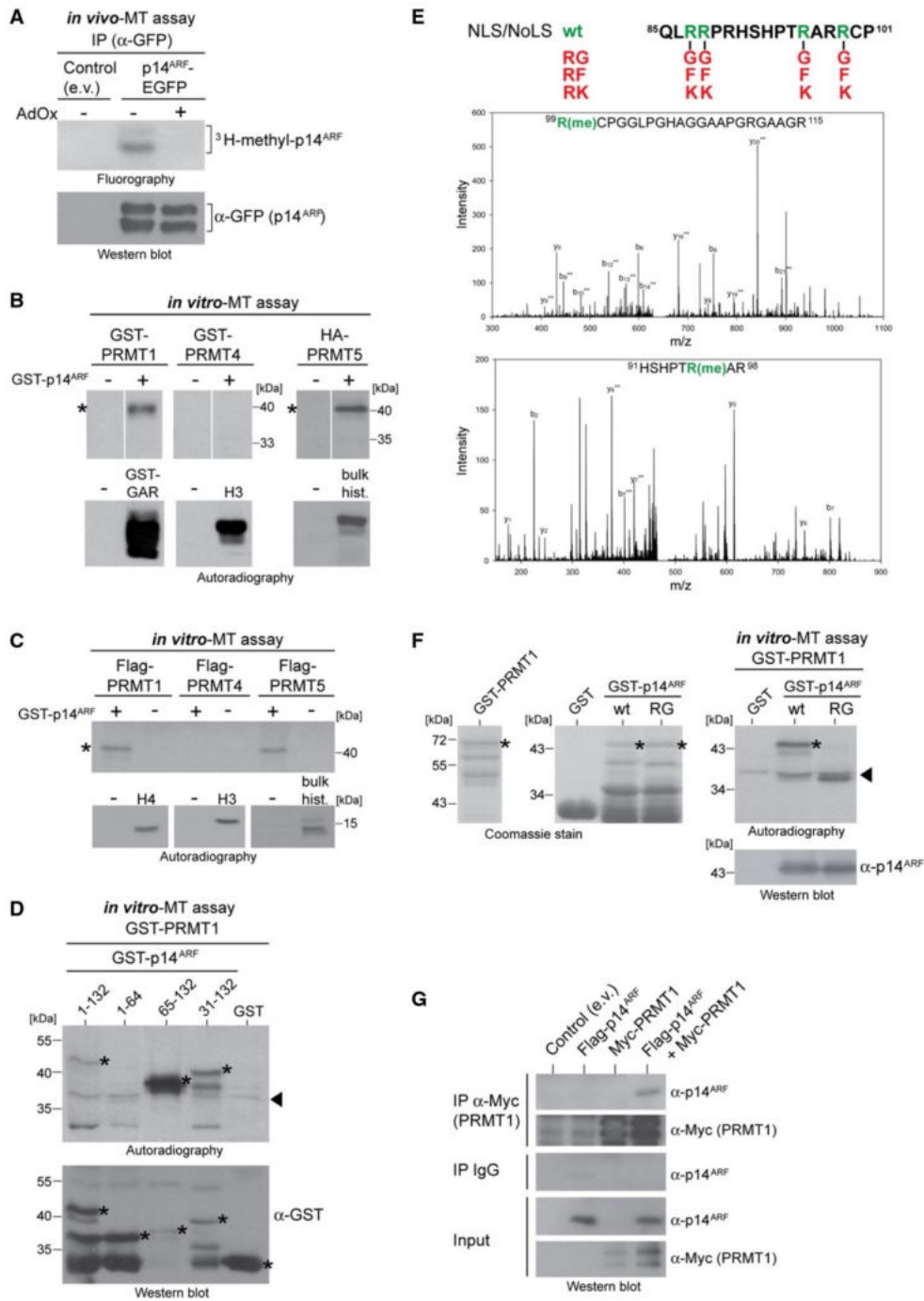


Figure 1.

**Figure 1. Arginine methylation of p14<sup>ARF</sup> by PRMT1.**

- A For *in vivo* methyltransferase (MT) assay, HEK293 cells were transfected with either empty vector (e.v., control) or EGFP-tagged p14<sup>ARF</sup>-containing plasmid. Subsequently, cells were treated with the global methyltransferase inhibitor adenosine dialdehyde, AdOx (+) or left untreated (-) for 72 h and then cultured in the presence of L-[<sup>3</sup>H-methyl]-methionine. Cell lysates were subjected to  $\alpha$ -GFP immunoprecipitation (IP) and then assayed by fluorography (upper panel) and immunoblotting using  $\alpha$ -GFP antibody (lower panel). EGFP-epitope tagged p14<sup>ARF</sup> typically migrated as a doublet band, indicated by the bracket. Corresponding Appendix Fig S1 confirms p14<sup>ARF</sup> overexpression in the cell lysates and hypomethylation caused by AdOx treatment.
- B Recombinant GST-tagged substrates (p14<sup>ARF</sup>, GAR) and PRMT1/PRMT4 enzyme purified from bacteria or PRMT5 overexpressed/immunoprecipitated from HeLa cells (HA-tagged PRMT5/Myc-tagged MEPS0) were subjected to *in vitro* methyltransferase (MT) assays in the presence of [<sup>14</sup>C-methyl]-SAM. Reactions were separated by SDS-PAGE, blotted, and assayed by autoradiography. GST-GAR, histone H3, and bulk histones served as a positive control for PRMT1, PRMT4, and PRMT5 activity, respectively. The two depicted negative controls (-) for PRMT1 are identical. The asterisks indicate the methylated p14<sup>ARF</sup> protein. Corresponding autoradiography results show representative images and derive from the same blots and exposure times with white lines indicating where tracks were cut. Size markers (in kDa) are shown on the right.
- C Recombinant GST-tagged p14<sup>ARF</sup> purified from bacteria and Flag-tagged PRMT1, PRMT4, or PRMT5 enzyme purified from baculoviral infected Sf9 cells were subjected to *in vitro* methyltransferase (MT) assays in the presence of [<sup>14</sup>C-methyl]-SAM. Reactions were separated by SDS-PAGE, blotted and assayed by autoradiography. Histone proteins H4, H3 and bulk histones served as a positive control for PRMT1, PRMT4 and PRMT5 activity, respectively. The asterisk indicates the methylated p14<sup>ARF</sup> protein. Size markers (in kDa) are shown on the right.
- D GST-tagged full-length ORF (aa 1–132) and deletion constructs (aa 1–64, aa 65–132, and aa 31–132) of p14<sup>ARF</sup> as well as GST alone were subjected to *in vitro* MT assays in the presence of GST-PRMT1 as described in (B). Methylation activities were detected by autoradiography (upper panel). Asterisks indicate methylated p14<sup>ARF</sup> proteins, whereas the arrowhead marks p14<sup>ARF</sup>-unrelated background signals (likely deriving from PRMT1 automethylation). Amounts of p14<sup>ARF</sup> proteins and GST alone were visualized by immunoblotting using  $\alpha$ -GST antibody (lower panel). Asterisks highlight the expected size and location of the different proteins. Size markers (in kDa) are shown on the left.
- E NLS/NoLS of p14<sup>ARF</sup> (aa 85–101) is depicted at the top, with the PRMT1-methylated arginine residues distinguished in green and mutations to glycine (G), phenylalanine (F), or lysine (K) in red. For mass spectrometry, GST-tagged p14<sup>ARF</sup> (full-length protein) was *in vitro* methylated by PRMT1, separated by SDS-PAGE, in-gel digested with trypsin and analyzed by LC-MS/MS. Fragment ion spectrum resulted from the doubly charged precursor ion of the R99-methylated (upper panel) and the R96-methylated (lower panel) p14<sup>ARF</sup> peptides showing y-ions and b-ions by consecutive fragmentation reactions. Relevant ions were labeled according to the accepted nomenclature. Dimethylation of R99 was confirmed by detection of methylated N-terminal b-ions and unmethylated C-terminal y-ions. Dimethylation of R96 was detected in the mass of the b7, y6 and y7 ions.
- F Full-length GST-tagged wild-type (wt) and RG mutant p14<sup>ARF</sup> protein, GST alone as well as GST-PRMT1 were purified from bacteria, as visualized by SDS-PAGE and Coomassie Blue staining (left and middle panel), with asterisks indicating the corresponding PRMT1 and p14<sup>ARF</sup> protein bands. GST and GST-p14<sup>ARF</sup> proteins (wt, RG) were subjected to *in vitro* MT assays in the presence of GST-PRMT1 as described in (B). Methylation activities were detected subsequent to protein blotting by autoradiography (upper right panel). The asterisk highlights the methylated p14<sup>ARF</sup> wt protein, whereas the arrowhead indicates p14<sup>ARF</sup>-unrelated background signals (likely deriving from PRMT1 automethylation). Amounts of p14<sup>ARF</sup> proteins were detected by immunostaining of the autoradiographed blot using  $\alpha$ -p14<sup>ARF</sup> antibody (lower right panel). Size markers (in kDa) are shown on the left.
- G U2OS cells were transfected with the indicated plasmids (e.v., empty vector/control). Immunoprecipitation (IP) from cell lysates was performed using  $\alpha$ -Myc antibody (exogenous PRMT1) or IgG as negative control. IP reactions and input lysates were analyzed by immunoblotting using the indicated antibodies.
- Source data are available online for this figure.

of endogenous p14<sup>ARF</sup> in different human cells upon ectopic expression of PRMT1 by immunofluorescence staining. In control transfected HeLa cells, endogenous p14<sup>ARF</sup> displayed predominantly nucleolar localization (\*) with rare detection in the nucleolar and cytoplasm (<), as illustrated in Fig 2A. Upon overexpression of PRMT1, p14<sup>ARF</sup> showed an altered cellular distribution, namely predominant localization in the nucleolar and cytoplasm (Fig 2A). This finding was further corroborated by cell counting, in which the cell number with exclusively nucleolar p14<sup>ARF</sup> staining was strongly reduced upon PRMT1 overexpression (Fig 2B). The PRMT1-dependent alteration of p14<sup>ARF</sup>'s localization was not due to nucleolar disruption, as staining of the nucleolar protein NPM indicates the regular presence of nucleoli also in PRMT1-overexpressing cells (Appendix Fig S2). Similar observations were obtained in U2OS cells, which do not endogenously express p14<sup>ARF</sup> (Stott *et al*, 1998). Exogenous p14<sup>ARF</sup> was primarily found in the nucleoli of U2OS cells (Fig 2C and D). Overexpression of PRMT1 coincided with a redistribution of p14<sup>ARF</sup> to the nucleolar and cytoplasm, whereas this redistribution was diminished upon overexpression of catalytically inactive PRMT1 (Fig 2C–E). Moreover, siRNA-mediated depletion of PRMT1 resulted in a more pronounced, exclusively nucleolar localization of p14<sup>ARF</sup> (Fig 2F–I). In the PRMT1 depletion analysis, p14<sup>ARF</sup>'s relocation into the nucleoli was subtle due to the already predominant nucleolar localization of p14<sup>ARF</sup> in the siControl transfected HeLa cells

(Fig 2H and I). Altogether, these results indicate that PRMT1 regulates the cellular localization of p14<sup>ARF</sup> and that its methyltransferase activity contributes to this function.

#### The basic charge of the PRMT1-targeted arginine residues is important for the nucleolar localization of p14<sup>ARF</sup>

To investigate whether the PRMT1-targeted arginine residues within the NLS/NoLS are important for mediating the cellular localization of p14<sup>ARF</sup>, we established several methyl-deficient mutant p14<sup>ARF</sup> proteins. To this end, the four arginines (R87/88/96/99) were either mutated to glycines (RG) or phenylalanines (RF), which do not preserve the basic charge, or to lysines (RK), which retain the basic charge, but cannot be methylated by PRMTs (Fig 1E). EGFP-tagged p14<sup>ARF</sup> wild-type and mutant proteins were overexpressed in U2OS cells and their cellular distribution (either exclusively nucleolar, not-exclusively nucleolar but additionally nucleolar/cytoplasmic or exclusively cytoplasmic) was investigated. Mutation of the four arginines to lysines resulted in a mutant protein (p14<sup>ARF</sup> RK) with predominant, exclusively nucleolar localization similar to the wild-type protein (Fig 3A and B). In contrast, p14<sup>ARF</sup> RG- and RF-mutant proteins showed a significant redistribution from the nucleolus to the nucleolar and cytoplasm, with the p14<sup>ARF</sup> RF mutant displaying the highest cell number with exclusive localization in the cytoplasm (Fig 3A and B). Our results conform with the literature (Rizos *et al*,

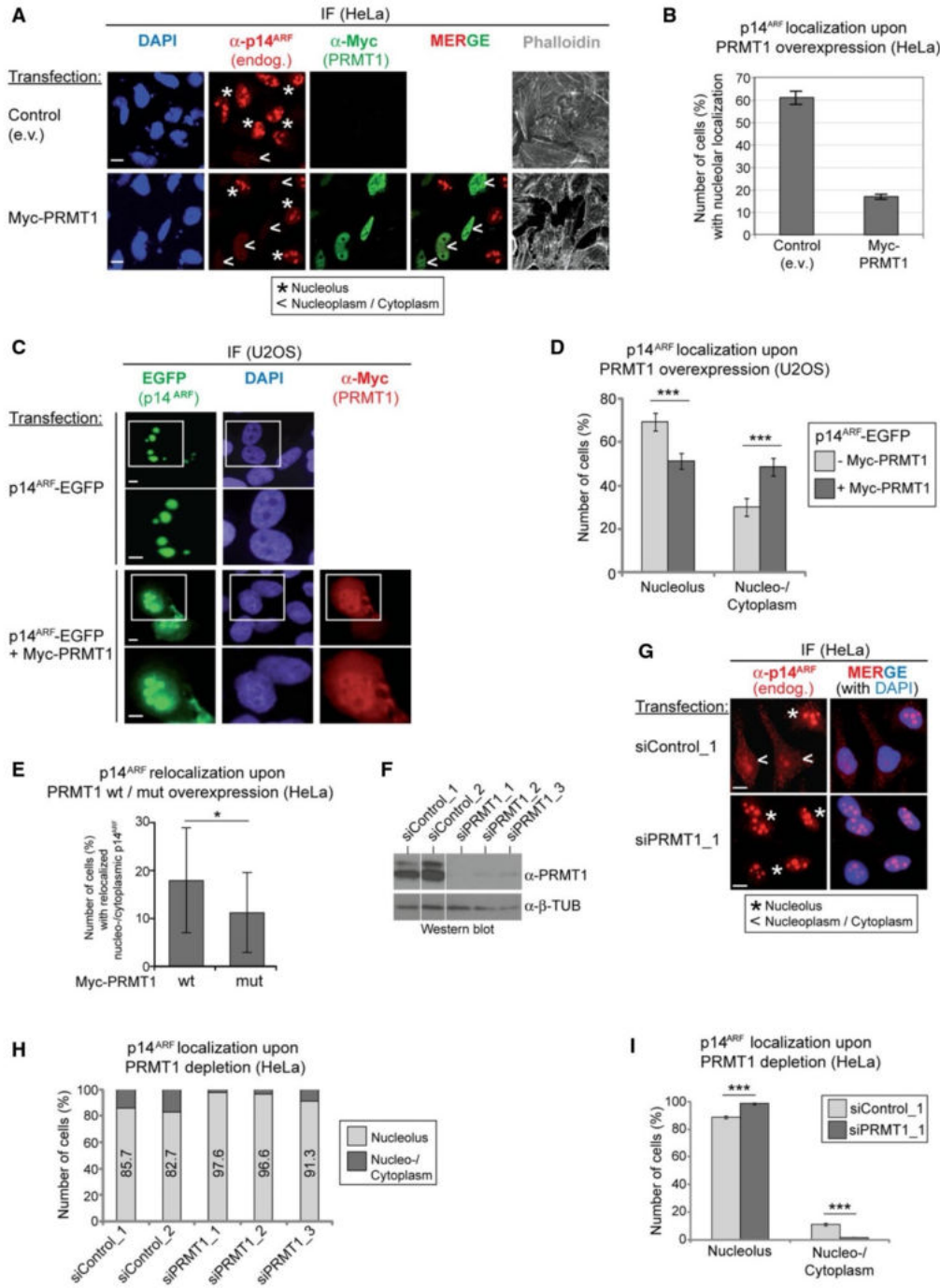


Figure 2.

**Figure 2. PRMT1-dependent redistribution of nucleolar p14<sup>ARF</sup>.**

- A, B HeLa cells were transfected with empty vector (e.v., control) or Myc-tagged wild-type PRMT1-containing plasmid. Immunofluorescence (IF) staining was performed using  $\alpha$ -p14<sup>ARF</sup> (red, endogenous p14<sup>ARF</sup>),  $\alpha$ -Myc (green, exogenous PRMT1) antibodies, DAPI (blue, nuclei/DNA), and Phalloidin (gray, cytoplasm/F-actin). In (A), representative IF results are shown, with asterisks indicating cells with exclusive nucleolar and arrowheads indicating cells with predominantly nucleo-/cytoplasmic p14<sup>ARF</sup> localization. The merge displays the combination of p14<sup>ARF</sup> and PRMT1 staining. Scale bars: 15  $\mu$ m. The quantification of exclusive nucleolar p14<sup>ARF</sup> was performed by cell counting (percentage of cells) and is shown for three independent experiments in (B) (mean  $\pm$  SD).
- C, D U2OS cells were transfected with EGFP-tagged p14<sup>ARF</sup> alone or in combination with Myc-tagged wild-type PRMT1-containing plasmids. p14<sup>ARF</sup>-EGFP (green), DAPI (blue, nuclei/DNA), and PRMT1 (red, using  $\alpha$ -Myc antibody) were visualized by fluorescence microscopy, for which representative results are shown in (C), with the lower images displaying a magnification as indicated in the upper images by the rectangles. Scale bars: 10  $\mu$ m. The subcellular distribution of p14<sup>ARF</sup>-EGFP (exclusively nucleolar or not-exclusively nucleolar but predominantly nucleo-/cytoplasmic) was quantified in p14<sup>ARF</sup>-positive and p14<sup>ARF</sup>/Myc-PRMT1-double-positive cells by cell counting (percentage of cells) for three independent experiments in (D) (mean  $\pm$  SD, \*\*\* $P$   $\leq$  0.001 using Welch's t-test).
- E U2OS cells were transfected with EGFP-tagged p14<sup>ARF</sup> alone or in combination with Myc-tagged wild-type (wt) or catalytically inactive (mut) PRMT1-containing plasmids. The cellular distribution of p14<sup>ARF</sup>-EGFP was quantified as in (D). The relocalization of p14<sup>ARF</sup> out of the nucleolus upon overexpression of PRMT1 (wt or mut) was determined by cell counting (percentage of cells) for four independent experiments (mean  $\pm$  SD, \* $P$   $\leq$  0.05 using the paired t-test).
- F–I HeLa cells were transfected with the indicated siRNAs (two control/non-targeting siRNAs and three PRMT1-specific siRNAs). PRMT1 depletion was verified by immunoblotting using  $\alpha$ -PRMT1 and  $\alpha$ - $\beta$ -TUBULIN (loading control) antibodies ((F); depicted staining results derive from the same blot as well as exposure times with white lines indicating where tracks were cut). The cellular p14<sup>ARF</sup> distribution was determined by immunofluorescence staining (IF) using  $\alpha$ -p14<sup>ARF</sup> antibody. Representative IF images for the siControl\_1 and siPRMT1\_1 condition are shown in (G) (endogenous p14<sup>ARF</sup> in red and the merge additionally with DAPI in blue for nuclei/DNA). Scale bars: 15  $\mu$ m. The subcellular localization of p14<sup>ARF</sup> (exclusively nucleolar or not-exclusively nucleolar but predominantly nucleo-/cytoplasmic) was quantified by cell counting (percentage of cells) for all used siRNAs in (H) and for siControl\_1/siPRMT1\_1 from three independent experiments in (I) (mean  $\pm$  SD, \*\*\* $P$   $\leq$  0.001 using Welch's t-test).

2000) that the basic charge of these arginine residues is crucial for the predominant nucleolar localization of p14<sup>ARF</sup>.

To answer the question whether the four arginines R87/88/96/99 and their potential to be methylated are pivotal for the influence of PRMT1 on the p14<sup>ARF</sup> localization, we determined the effect of PRMT1 overexpression on the relocalization of wild-type p14<sup>ARF</sup> into the nucleolar and cytoplasm compared to p14<sup>ARF</sup> RK. Thereby, exogenous PRMT1 caused a higher cell fraction with predominant nucleo-/cytoplasmic localization of wild-type p14<sup>ARF</sup> compared to the RK mutant (Fig 3C). Thus, our results suggest that these specific arginines in the NLS/NoLS are important for the PRMT1-mediated redistribution of nucleolar p14<sup>ARF</sup> into the nucleolar and cytoplasm, possibly due to their capability to be methylated.

Given that the nucleolar protein NPM has been reported to sequester p14<sup>ARF</sup> in the nucleoli (Korgaonkar *et al.*, 2005), we examined next whether the association of p14<sup>ARF</sup> with NPM is influenced by PRMT1. Co-immunoprecipitation analyses showed that upon overexpression of PRMT1, endogenous p14<sup>ARF</sup> interacts less efficiently with endogenous NPM in HeLa cell extracts, which was also confirmed in reciprocal precipitations (Fig 3D). Interestingly, NPM has previously been found to associate with multiple protein regions of p14<sup>ARF</sup>, including also the C-terminus encompassing the arginine methylation sites of PRMT1 (Moulin *et al.*, 2008). Therefore, we raised the question whether methylation of these arginines directly influences the interaction between p14<sup>ARF</sup> and NPM. We performed peptide pull-down assays using two NLS/NoLS peptides of p14<sup>ARF</sup> (aa 91–99 and aa 92–103) comprising the adjacent methylation sites R96 and R99, either unmodified or premodified by asymmetric dimethylation (single-modified R96me2a in peptide aa 91–99 and double-modified R96/R99me2a in peptide aa 92–103). Recombinant NPM protein displayed a binding preference for the unmodified NLS/NoLS peptides, whereas the single R96me2a and the double R96/R99me2a modification led to reduced NPM binding (Fig 3E). These data suggest that arginine methylation of the NLS/NoLS of p14<sup>ARF</sup> by PRMT1 contributes to the release from its nucleolar binding partner NPM.

### PRMT1 regulates p14<sup>ARF</sup> protein stability

Previously, several reports showed that redistribution of nucleolar p14<sup>ARF</sup> into the nucleolar and cytoplasm is accompanied by reduced protein stability (Rodway *et al.*, 2004; Moulin *et al.*, 2008). We therefore examined the protein levels of wild-type p14<sup>ARF</sup> versus mutant proteins by Western blot. Of note, the  $\alpha$ -p14<sup>ARF</sup> antibodies used in this study were able to equally efficiently recognize p14<sup>ARF</sup> wild-type and mutant (RG/RF/RK) proteins, as confirmed by Western blot analysis of recombinant GST-tagged p14<sup>ARF</sup> proteins (Fig 1F, Appendix Fig S3A). Upon overexpression of the different p14<sup>ARF</sup> proteins in various human cell lines, the p14<sup>ARF</sup> RG and RF mutants showed strongly reduced protein levels compared to wild-type p14<sup>ARF</sup> (Fig 4A), which was not due to diminished transcript levels of the RG and RF mutants (Fig 4B, Appendix Fig S3B and C). In contrast, the RK mutant displayed only moderately altered protein levels, which were not reflected by transcriptional changes in U2OS and HeLa cells, but in HEK293 cells. Furthermore, siRNA-mediated depletion of PRMT1 led to elevated endogenous p14<sup>ARF</sup> protein levels, while overexpression of PRMT1 caused a reduction in p14<sup>ARF</sup> protein levels (Fig 4C and D). Since these observations could also not be explained by an alteration of p14<sup>ARF</sup> gene transcription (Appendix Fig S3D), we investigated whether PRMT1 influences p14<sup>ARF</sup> protein stability. We applied doxycycline (Dox)-inducible shRNA to knock down endogenous PRMT1 in HeLa cells (Fig 4E) and monitored p14<sup>ARF</sup> protein turnover following addition of the translational inhibitor cycloheximide (CHX). Depletion of PRMT1 upon doxycycline addition caused an increase in the level and stability of p14<sup>ARF</sup> protein (Fig 4E–G). However, the interaction between p14<sup>ARF</sup> and its reported ubiquitin ligases ULF, MKRN, and SIVA1 was not influenced by PRMT1 (data not shown; Chen *et al.*, 2010; Ko *et al.*, 2012; Wang *et al.*, 2013). Together, these results indicate that PRMT1-mediated displacement of p14<sup>ARF</sup> from the nucleolus leads to a reduction in protein stability likely due to its release from nucleolar sequestration (Rodway *et al.*, 2004).



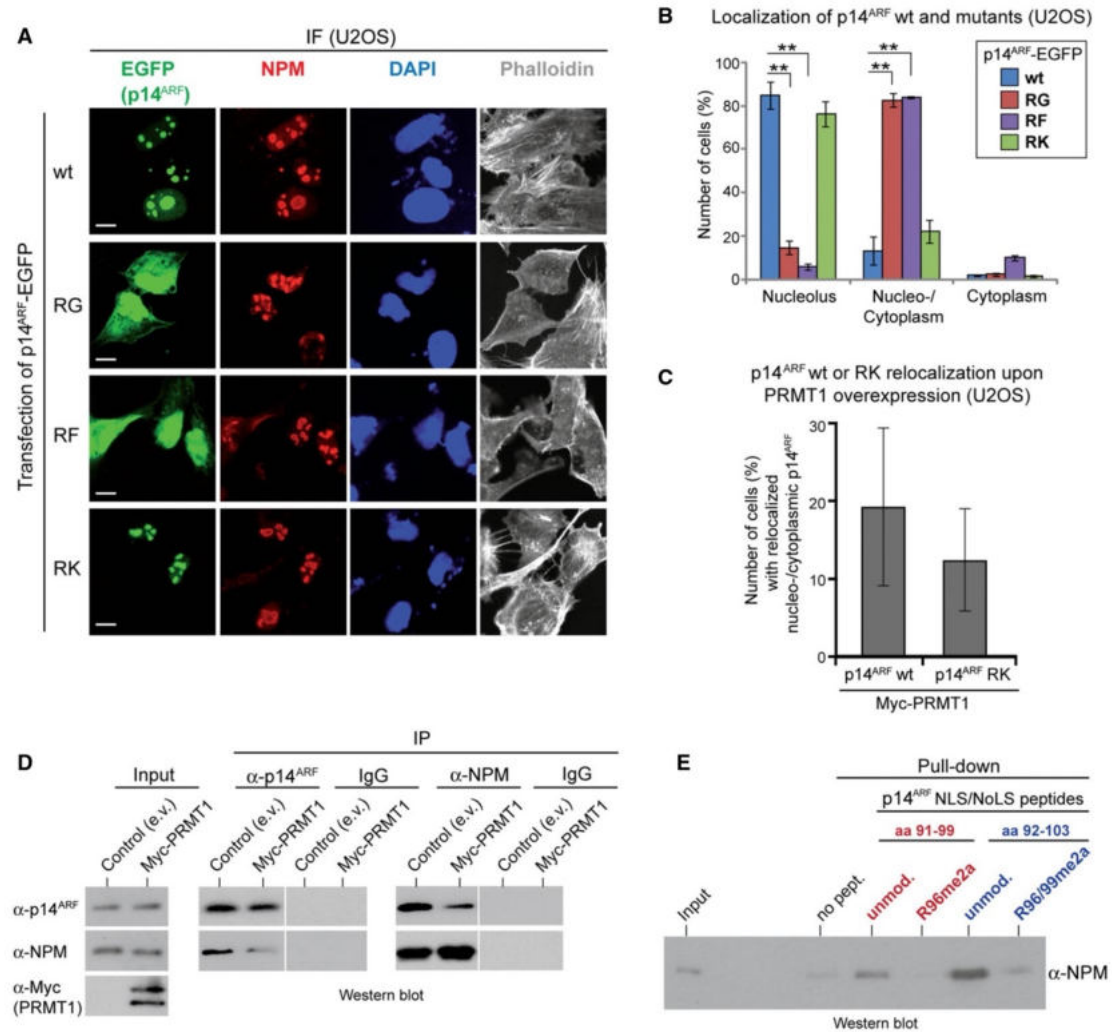


**Figure 3. Involvement of the PRMT1-targeted arginines in p14<sup>ARF</sup>'s nucleolar localization.**

**A, B** U2OS cells were transfected with EGFP-tagged wild-type (wt) or mutant (RG, RF, RK) p14<sup>ARF</sup>-containing plasmids. p14<sup>ARF</sup>-EGFP (green), endogenous NPM as a nucleolar marker (red, using  $\alpha$ -NPM antibody), DAPI (blue, nuclei/DNA), and Phalloidin (gray, cytoplasm/F-actin) were visualized by fluorescence microscopy, for which representative results are shown in (A). Scale bars: 10  $\mu$ m. The subcellular distribution of p14<sup>ARF</sup>-EGFP (exclusively nucleolar, not-exclusively nucleolar but additionally nucleo-/cytoplasmic or exclusively cytoplasmic) was quantified by cell counting (percentage of cells) for three independent experiments in (B) (mean  $\pm$  SD, \*\* $P$   $\leq$  0.005 using Welch's  $t$ -test).

**C** U2OS cells were transfected with EGFP-tagged wild-type (wt) or mutant (RK) p14<sup>ARF</sup>, either alone or in combination with Myc-tagged wild-type PRMT1-containing plasmids. Cells with predominant nucleo-/cytoplasmic localization of p14<sup>ARF</sup>-EGFP (for both wt and RK) were quantified in the absence or presence of PRMT1 overexpression, i.e., in p14<sup>ARF</sup>-positive as well as p14<sup>ARF</sup>/Myc-PRMT1-double-positive cells, by immunofluorescence staining and cell counting. Relocalization of p14<sup>ARF</sup> wt and RK into the nucleo/cytoplasm upon overexpression of PRMT1 was defined in percentage of cells for five independent experiments (mean  $\pm$  SD).

**D** HeLa cells were transfected with empty vector (e.v., control) or Myc-tagged wild-type PRMT1-containing plasmid. Immunoprecipitation (IP) of endogenous p14<sup>ARF</sup> or NPM was performed from cell lysates using the corresponding antibodies or IgG as negative control. IP reactions and input lysates were analyzed by immunoblotting using the indicated antibodies. Staining results of the IP reactions derive from the same blot and exposure times with the white lines indicating where tracks were cut.

**E** Indicated NLS/NoLS p14<sup>ARF</sup> peptides (aa 91–99 or aa 92–103) either unmodified or premodified (asymmetric dimethylation of R96 in peptide aa 91–99 and of R96/R99 in peptide aa 92–103) were covalently coupled to Sulfolink-beads and incubated with recombinant, baculoviral purified Flag-tagged NPM. Pull-down reactions and input of NPM protein were resolved by SDS-PAGE and analyzed by  $\alpha$ -NPM immunoblotting.

**DNA damage leads to PRMT1-dependent methylation of p14<sup>ARF</sup>**

Next, we investigated which cellular pathways might utilize the PRMT1-mediated regulation of p14<sup>ARF</sup>'s function. Interestingly, when cells encounter genotoxic stress, p14<sup>ARF</sup> has been described to

be activated, namely to redistribute from the nucleolar compartment to the nucleo- and cytoplasm, where it functions as a tumor suppressor, coinciding with decreased protein stability (Lee et al, 2005; Gallagher et al, 2006; Chen et al, 2013). To address whether stress-induced p14<sup>ARF</sup> activation is influenced by PRMT1, we

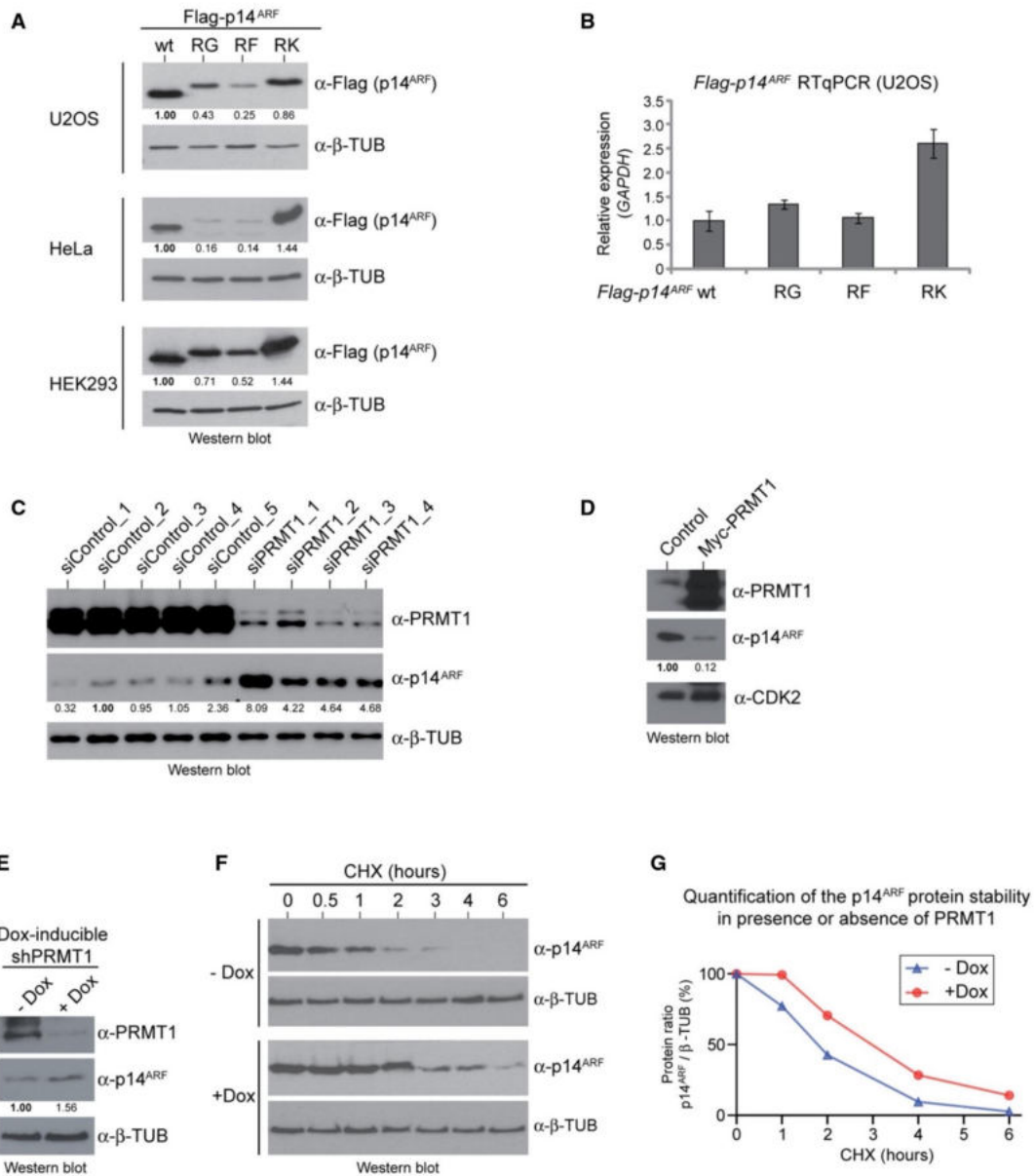


Figure 4.

**Figure 4. Influence of PRMT1 and PRMT1-targeted arginines on p14<sup>ARF</sup> protein stability.**

- A, B U2OS, HeLa, and HEK293 cells were transfected with Flag-tagged wild-type (wt) or mutant (RG, RF, RK) p14<sup>ARF</sup>-containing plasmids. Overexpression was analyzed by immunoblotting using  $\alpha$ -Flag (exogenous p14<sup>ARF</sup> proteins) and  $\alpha$ - $\beta$ -TUBULIN (loading control) antibodies (A). As visualized here, p14<sup>ARF</sup> with the Flag-epitope tagged reproducibly showed a clear migration difference between wt and mutant p14<sup>ARF</sup> proteins, with the mutants (especially the RK mutant) migrating slower than wt protein in the SDS-PAGE. The staining signals of the p14<sup>ARF</sup> bands were densitometrically quantified and normalized to the respective  $\beta$ -TUBULIN signal, as specified by the numbers below the blots, with the protein signals of p14<sup>ARF</sup> wt set to 1. Transcript levels of wt and mutant p14<sup>ARF</sup> were determined by RT-qPCR in U2OS cells (B) as well as in HeLa and HEK293 cells (Appendix Fig S3B and C). Values were normalized to *GAPDH* expression and presented relative to wt p14<sup>ARF</sup>, mean  $\pm$  SD of triplicates.
- C HeLa cells were transfected with the indicated siRNAs (five control/non-targeting siRNAs and four PRMT1-specific siRNAs). PRMT1 depletion and endogenous p14<sup>ARF</sup> protein levels were analyzed by immunoblotting using  $\alpha$ -PRMT1,  $\alpha$ -p14<sup>ARF</sup> and  $\alpha$ - $\beta$ -TUBULIN (loading control) antibodies. The p14<sup>ARF</sup> signals were densitometrically quantified and normalized to the respective  $\beta$ -TUBULIN signal, as specified by the numbers below the blot, with the siControl\_2 condition set to 1. Transcript levels of p14<sup>ARF</sup> were determined by RT-qPCR (Appendix Fig S3D).
- D HeLa cells were infected with recombinant adenovirus encoding GFP (control) or wild-type PRMT1. PRMT1 overexpression and endogenous p14<sup>ARF</sup> protein levels were analyzed by immunoblotting using  $\alpha$ -PRMT1,  $\alpha$ -p14<sup>ARF</sup>, and  $\alpha$ -CDK2 (loading control) antibodies. The p14<sup>ARF</sup> signals were densitometrically quantified and normalized to the respective CDK2 signal, as specified by the numbers below the blot, with the control condition set to 1.
- E-G HeLa cells expressing a doxycycline-inducible shRNA targeting PRMT1 were treated or not with doxycycline (Dox) for 6 days. PRMT1 depletion was monitored by immunoblotting using the indicated antibodies (E). The p14<sup>ARF</sup> signals were densitometrically quantified and normalized to the respective  $\beta$ -TUBULIN signal, as specified by the numbers below the blot, with the -Dox condition set to 1. PRMT1-proficient (-Dox) and PRMT1-depleted cells (+Dox) were further treated with the protein synthesis inhibitor cycloheximide (CHX) and harvested after 0, 0.5, 1, 2, 3, 4, and 6 h. Cell lysates were subjected to immunoblotting using  $\alpha$ -p14<sup>ARF</sup> and  $\alpha$ - $\beta$ -TUBULIN (loading control) antibodies and conventional ECL detection (F). For precise quantification of the p14<sup>ARF</sup> protein stability in the -/+ Dox conditions during the CHX time course, immunoblotting was performed with independent cell lysates and primary antibodies, as in (F), which were then detected using fluorescence dye-coupled secondary antibodies and the LI-COR Odyssey system. The quantitative p14<sup>ARF</sup> signals were normalized to the corresponding quantitative  $\beta$ -TUBULIN signals and displayed in (G). The CHX-untreated samples (0 h) were set to 100% for each condition.

irradiated wild-type and PRMT1-depleted HeLa cells with UVC and subsequently assessed p14<sup>ARF</sup> localization by immunofluorescence staining. Upon exposure to UVC radiation, nucleolar staining of p14<sup>ARF</sup> was strongly reduced in wild-type cells compared to the untreated condition (Fig 5A and B) in agreement with previous reports (Lee *et al*, 2005). However, PRMT1 depletion led to a higher accumulation of p14<sup>ARF</sup> in the nucleolar compartment of unstressed cells, as observed before (Fig 2G-I). This effect was even more pronounced in UVC-stressed cells (Fig 5A and B) indicating that PRMT1 depletion antagonizes the UVC-induced redistribution of p14<sup>ARF</sup> into the nucleolar and cytoplasm. Furthermore, PRMT1 knock-down increased the p14<sup>ARF</sup> protein levels also in UVC-treated cells, which was not due to enhanced p14<sup>ARF</sup> gene transcription (Fig 5C, Appendix Fig S4A). Similar results were obtained upon treatment with the DNA-damaging agent etoposide, where PRMT1 depletion counteracted the damage-stimulated relocalization and destabilization of p14<sup>ARF</sup> (Appendix Fig S4B and C). Together, these data suggest that PRMT1-mediated p14<sup>ARF</sup> regulation might be relevant for DNA damage-induced cellular responses.

To test this hypothesis, we screened commercially available pan-methyl-arginine antibodies, but could not identify any antibodies specifically binding methylated p14<sup>ARF</sup>. We therefore generated a monoclonal methyl-arginine-specific antibody ( $\alpha$ -me-p14<sup>ARF</sup>) that recognizes the PRMT1-dependent methylation of R96 and R99 in p14<sup>ARF</sup>, as validated by peptide dot blot analysis and Western blot analyses of *in vitro* MT assays, overexpressed wild-type p14<sup>ARF</sup> versus RK mutant and PRMT1-depleted cell extracts (Appendix Fig S5A and Fig 5D and E, Appendix Fig S5B). By using the anti-me-p14<sup>ARF</sup> antibody, we observed that UVC radiation caused an increase in the methylation of endogenous p14<sup>ARF</sup> protein compared to low methylation levels in unstressed HeLa cells (Fig 5F). Detection of this DNA damage-induced methylation coincided with decreased p14<sup>ARF</sup> protein levels indicating that p14<sup>ARF</sup> methylation and p14<sup>ARF</sup> protein stability counter-correlate. To address whether UVC-dependent arginine methylation of p14<sup>ARF</sup> is mediated by

PRMT1, we established PRMT1 knockout and control HeLa cell lines using the CRISPR/Cas9 technology (Appendix Fig S6). Control cells displayed UVC-dependent methylation and reduced protein levels of endogenous p14<sup>ARF</sup>, whereas PRMT1 knockout cells showed elevated p14<sup>ARF</sup> protein levels and no detectable methylation of p14<sup>ARF</sup> (Fig 5G). To ensure that this lower level of p14<sup>ARF</sup> detected in control cells is actually caused by reduced protein levels and not by impaired antibody recognition of the endogenous protein due to epitope masking, we investigated the behavior of N-terminally Flag-tagged p14<sup>ARF</sup> protein overexpressed in HeLa cells by  $\alpha$ -Flag and  $\alpha$ -p14<sup>ARF</sup> immunostaining. The exogenous p14<sup>ARF</sup> also exhibited an UVC-mediated reduction of its protein levels, similar to the endogenous p14<sup>ARF</sup> protein (Appendix Fig S7). Consistent with the observation of a stress-dependent role of PRMT1 in p14<sup>ARF</sup> regulation, the interaction between endogenous p14<sup>ARF</sup> and endogenous PRMT1 was enhanced in co-immunoprecipitation experiments using wild-type HeLa cells upon UVC irradiation and coincided with endogenous p14<sup>ARF</sup> methylation (Fig 5H). Altogether, these data suggest that genotoxic stress triggers the interaction between p14<sup>ARF</sup> and PRMT1 accompanied by methylation and nucleolar release of p14<sup>ARF</sup>, which results in a less stable but likely functionally active tumor suppressor protein.

#### Depletion of PRMT1 results in defects of apoptosis signaling

To assess whether PRMT1 influences the tumor suppressor activities of p14<sup>ARF</sup>, such as cell cycle arrest and apoptosis induction, we examined the cell cycle distribution by flow cytometry using propidium iodide staining (PI-FACS) in PRMT1-depleted HeLa cells. In unstressed cells, siRNA-mediated depletion of PRMT1 did not cause significant changes in the cell cycle distribution compared to control cells (Fig 6A and B, Appendix Fig S8). Likewise, overexpression of wild-type p14<sup>ARF</sup> and methyl-deficient mutant proteins (RG, RF, RK) caused a similar extent of G<sub>1</sub> phase arrest in U2OS cells (Appendix Fig S9A). Furthermore, wild-type p14<sup>ARF</sup> and mutants

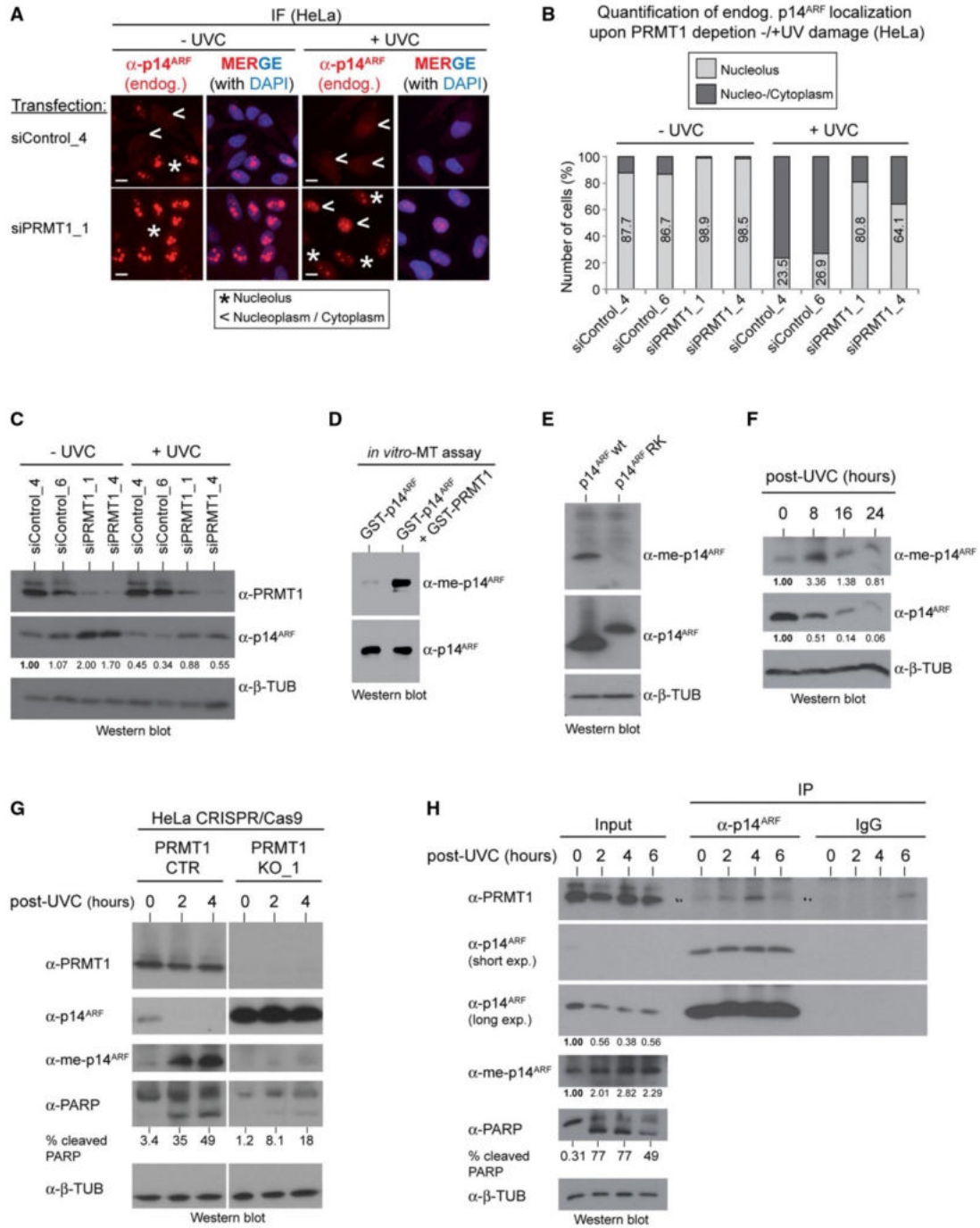


Figure 5.

◀ **Figure 5. PRMT1-dependent p14<sup>ARF</sup> methylation in response to DNA damage.**

- A–C HeLa cells were transfected with the indicated siRNAs (two control/non-targeting siRNAs and two PRMT1-specific siRNAs) and irradiated at 150 J/cm<sup>2</sup> UVC or not irradiated. After 24 h, the cellular distribution of endogenous p14<sup>ARF</sup> was determined by immunofluorescence (IF) staining using  $\alpha$ -p14<sup>ARF</sup> antibody (red, endogenous p14<sup>ARF</sup>) and in the merge additionally DAPI (blue, nuclei/DNA). Representative IF results are shown for two conditions (siControl\_4 and siPRMT1\_1) in (A), with asterisks indicating exclusively nucleolar and arrowheads indicating not-exclusively nucleolar but additionally or predominantly nucleolar/cytoplasmic p14<sup>ARF</sup> localization. Scale bars: 15  $\mu$ m. The subcellular distribution of p14<sup>ARF</sup>, as determined by IF, was quantified by cell counting (percentage of cells) for all conditions (B). PRMT1 depletion and p14<sup>ARF</sup> protein levels were analyzed by immunoblotting using the indicated antibodies (C). The p14<sup>ARF</sup> signals were densitometrically quantified and normalized to the respective  $\beta$ -TUBULIN signal, as specified by the numbers below the blot, with the siControl\_4 condition set to 1.
- D GST-tagged p14<sup>ARF</sup> and PRMT1 proteins purified from bacteria were subjected to an *in vitro* methyltransferase (MT) assay in the presence of SAM. Reactions were separated by SDS-PAGE and analyzed by immunoblotting using  $\alpha$ -me-p14<sup>ARF</sup> and  $\alpha$ -p14<sup>ARF</sup> antibodies.
- E U2OS cells were transfected with Flag-tagged wild-type (wt) or mutant (RK) p14<sup>ARF</sup>-containing plasmids. Methylation and overexpression of p14<sup>ARF</sup> were analyzed by immunoblotting using  $\alpha$ -me-p14<sup>ARF</sup>,  $\alpha$ -p14<sup>ARF</sup>, and  $\alpha$ - $\beta$ -TUBULIN (loading control) antibodies. The me-p14<sup>ARF</sup> antibody predominantly recognizes the p14<sup>ARF</sup> protein on the immunoblot, but weakly also other protein bands with higher molecular weights.
- F HeLa cells were irradiated at 150 J/cm<sup>2</sup> UVC. After 0, 8, 16, and 24 h, methylation of endogenous p14<sup>ARF</sup> was analyzed by immunoblotting using  $\alpha$ -me-p14<sup>ARF</sup>,  $\alpha$ -p14<sup>ARF</sup>, and  $\alpha$ - $\beta$ -TUBULIN (loading control) antibodies. The methylated p14<sup>ARF</sup> and the p14<sup>ARF</sup> signals were densitometrically quantified and normalized to the respective  $\beta$ -TUBULIN signal, as specified by the numbers below the blots, with the not irradiated condition (0 h) set to 1.
- G HeLa cells either CRISPR/Cas9 control (CTR) or PRMT1-deleted (KO\_1) were irradiated at 150 J/cm<sup>2</sup> UVC. After 0, 2, and 4 h, cell lysates were analyzed by immunoblotting using the indicated antibodies. Depicted staining results derive from the same blot and exposure times with white lines (between CTR and KO\_1) indicating where tracks were cut. The percentage of PARP cleavage was densitometrically quantified and is indicated below the blot.
- H HeLa cells were irradiated at 150 J/cm<sup>2</sup> UVC. After 0, 2, 4, and 6 h, immunoprecipitation (IP) of endogenous p14<sup>ARF</sup> was performed from cell lysates using  $\alpha$ -p14<sup>ARF</sup> antibody or IgG as negative control. IP reactions and input lysates were analyzed by immunoblotting using the indicated antibodies. Short and long exposure times are indicated. The p14<sup>ARF</sup> and the methylated p14<sup>ARF</sup> signals were densitometrically quantified and normalized to the respective  $\beta$ -TUBULIN signal, as specified by the numbers below the blots, with the not irradiated condition (0 h) set to 1. The percentage of PARP cleavage was also densitometrically quantified and is indicated below the blot.

equally stabilized p53 protein levels and showed the same capability to interact with the ubiquitin ligase MDM2 (Appendix Fig S9B–E). These results indicate that PRMT1-mediated arginine methylation of p14<sup>ARF</sup> does not impact the cell cycle distribution of unstressed cells or the arrest functions of p14<sup>ARF</sup> linked to p53 regulation.

Strikingly, upon UVC irradiation PRMT1-depleted HeLa cells displayed a significantly lower cell number in the subG<sub>1</sub> phase than control cells, as quantified by PI-FACS analysis (Fig 6A and B, Appendix Fig S8). Furthermore, in contrast to control cells, PRMT1-depleted cells showed no detectable increase of endogenous p14<sup>ARF</sup> methylation upon UVC treatment (Fig 6C). To corroborate the observation on the pro-apoptotic effect of PRMT1 upon genotoxic stress, we investigated additional apoptosis markers in the PRMT1 knockout HeLa cell lines, i.e., PARP cleavage by Western blotting and Annexin V staining by flow cytometry. Consistently, the knockout cell clones showed diminished PARP cleavage and Annexin V-positive cell numbers upon UVC treatment compared to control clones (Fig 6D and E, Appendix Fig S10). To address whether PRMT1 promotes apoptosis via its methylation sites in p14<sup>ARF</sup>, we overexpressed the nucleolar, basic charged p14<sup>ARF</sup> RK mutant and the non-nucleolar p14<sup>ARF</sup> RF mutant in PRMT1 knockout HeLa cells and exposed the cells to UVC irradiation. The apoptosis defect of PRMT1 knockout cells was more efficiently restored by the non-nucleolar RF mutant, which likely mimics functionally active p14<sup>ARF</sup>, than by the nucleolar RK mutant (Fig 6F). These results suggest that PRMT1 and arginine methylation of p14<sup>ARF</sup> contribute to the activation of apoptosis upon genotoxic stress.

Given that the PRMT1-mediated methylation of p14<sup>ARF</sup> did not result in p53 activation, we hypothesized that the p53-independent tumor suppressor functions of p14<sup>ARF</sup> are regulated by PRMT1. TIP60 and p32 have both been identified as direct interaction partners of p14<sup>ARF</sup> that cooperate with p14<sup>ARF</sup> to enable a p53-independent DNA damage response and apoptosis induction in cellular stress situations (Eymin *et al*, 2006; Itahana & Zhang, 2008). Using co-immunoprecipitation experiments, we found that the interaction between TIP60 and

p14<sup>ARF</sup> is not influenced by PRMT1 or the RF mutation (Appendix Fig S11A and B). Remarkably, R87, R88, and R99 in p14<sup>ARF</sup>, which we identified here as PRMT1 methylation sites, have been reported to mediate the interaction with the pro-apoptotic protein p32 (Itahana & Zhang, 2008). Cancer-derived mutations of these arginine residues disrupt the p14<sup>ARF</sup>-p32 association and the pro-apoptotic function of p14<sup>ARF</sup>. Using recombinant, purified proteins, we investigated in direct interaction assays whether the PRMT1-targeted arginines within p14<sup>ARF</sup> influence its binding capability toward p32. The corresponding pull-down experiments revealed that the p14<sup>ARF</sup> RF mutant, which *in vivo* seems to mimic functionally active p14<sup>ARF</sup> (Fig 6F), exhibits a stronger interaction with p32 than wild-type p14<sup>ARF</sup> (Fig 6G). Moreover, endogenous co-immunoprecipitation analyses showed that p14<sup>ARF</sup> interacts less efficiently with p32 in PRMT1 knockout HeLa cell lines than in control cell lines (Fig 6H). These results suggest that PRMT1, likely via methylation of p14<sup>ARF</sup>, enhances the interaction between p14<sup>ARF</sup> and its pro-apoptotic binding partner p32 and thereby promotes p53-independent apoptosis.

#### PRMT1 expression levels are indicative for clinical PDAC prognosis and chemotherapy response of pancreatic tumor cells

Altered expression levels of PRMT1 have been reported in many human cancer types (Yoshimatsu *et al*, 2011). Given that our findings disclosed a novel tumor-suppressive activity of PRMT1, we investigated the clinical relevance of the PRMT1-p14<sup>ARF</sup> connection in one of the most aggressive and lethal solid human tumors, namely PDAC. Initial survival analysis using the TCGA mRNA data set on PDAC (Anaya, 2016) indicated that high transcript levels of PRMT1 correlate with an extended long-term survival of PDAC patients (> 500 days), whereas this correlation was not observed for the short-term survival group (< 500 days, Fig 7A). To enable comparative expression analyses of PRMT1 and p14<sup>ARF</sup> on protein level in PDAC, we performed immunohistochemistry (IHC) stainings on surgical resection specimens of a cohort of 75 PDAC patients that

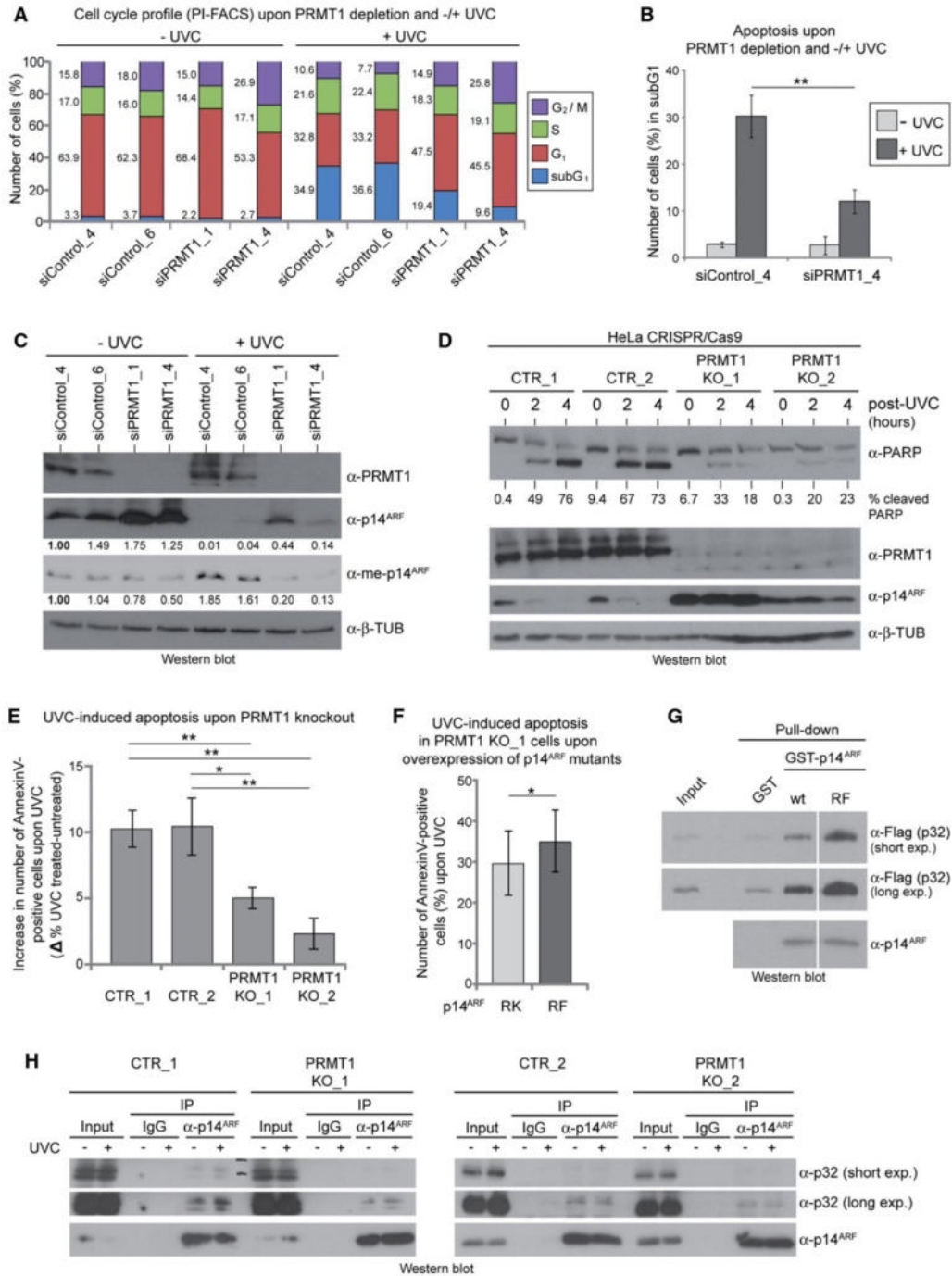


Figure 6.

**Figure 6. Apoptosis regulation by PRMT1-mediated arginine methylation of p14<sup>ARF</sup>.**

- A–C HeLa cells were transfected with the indicated siRNAs (two control/non-targeting siRNAs and two PRMT1-specific siRNAs) and irradiated at 150 J/cm<sup>2</sup> UVC or not irradiated. After 24 h, cell cycle distribution was analyzed by flow cytometry using propidium iodide (PI) DNA staining for a representative experiment ((A), Appendix Fig S8). The subG1 fraction of the siControl\_4 and siPRMT1\_4 condition was quantified for three independent experiments in (B) (mean ± SD, \*\*P ≤ 0.005 using Welch's t-test). PRMT1 depletion and p14<sup>ARF</sup> methylation of the samples (from (A)) were monitored by immunoblotting using the indicated antibodies (C). The p14<sup>ARF</sup> and the methylated p14<sup>ARF</sup> signals were densitometrically quantified and normalized to the respective β-TUBULIN signal, as specified by the numbers below the blots, with siControl\_4 condition set to 1.
- D CRISPR/Cas9 control (CTR\_1 and CTR\_2) or PRMT1-deleted (KO\_1 and KO\_2) HeLa cell lines were irradiated at 150 J/cm<sup>2</sup> UVC. After 0, 2, and 4 h, cell lysates were analyzed by immunoblotting using the indicated antibodies. The percentage of PARP cleavage was densitometrically quantified and is specified below the blot.
- E CRISPR/Cas9 control (CTR\_1 and CTR\_2) or PRMT1-deleted (KO\_1 and KO\_2) HeLa cell lines were irradiated at 150 J/cm<sup>2</sup> UVC. After 4 h, the apoptotic cell fraction was analyzed by flow cytometry using FITC-labeled Annexin V and propidium iodide (PI). The increase in the apoptotic cell fraction upon UVC irradiation was quantified for three independent experiments (mean ± SD, \*\*P ≤ 0.005 and \*P ≤ 0.05 using Welch's t-test).
- F HeLa CRISPR/Cas9 PRMT1 deleted (KO\_1) cells were transfected with Flag-tagged-mutant RK or RF p14<sup>ARF</sup>-containing plasmid and subsequently irradiated at 150 J/cm<sup>2</sup> UVC. After 4 h, the apoptotic cell fraction was quantified by flow cytometry using FITC-labeled Annexin V and propidium iodide (PI) for seven independent experiments (mean ± SD, \*P ≤ 0.05 using the paired t-test).
- G GST alone, GST-tagged wild-type (wt), and mutant (RF) p14<sup>ARF</sup> proteins were coupled to Glutathione beads and incubated with baculoviral expressed, purified Flag-tagged p32. Pull-down reactions and input of p32 protein were resolved by SDS-PAGE and analyzed by immunoblotting using α-Flag and α-p14<sup>ARF</sup> antibodies. Short and long exposure times are specified. Staining results derive from the same blot and exposure times with white lines indicating where tracks were cut.
- H CRISPR/Cas9 control (CTR\_1 and CTR\_2) or PRMT1-deleted (KO\_1 and KO\_2) HeLa cell lines were irradiated at 150 J/cm<sup>2</sup> UVC or not irradiated. After 4 h, immunoprecipitations (IP) of endogenous p14<sup>ARF</sup> were performed from cell lysates using α-p14<sup>ARF</sup> antibody or IgG as negative control. IP reactions and input lysates were analyzed by immunoblotting using the indicated antibodies. Short and long exposure times are specified.

all received post-operative adjuvant chemotherapy with gemcitabine. We scored the PRMT1 staining intensity in tumor cells of the PDAC tissues into three categories, namely highly elevated, moderately elevated and not elevated PRMT1 protein levels compared to the expression levels in normal pancreas tissue, which shows PRMT1 expression in pancreatic islet and acinar cells, but not in ductal cells (Fig 7B, Appendix Fig S12). In the present PDAC cohort, 45% of patients exhibited highly elevated, 32% moderately elevated, and 23% not elevated/normal PRMT1 protein levels (Fig 7C) indicating that the majority of PDAC patients (77%,  $n = 58$ ) revealed elevated PRMT1 expression in their tumor cells. Moreover, elevated PRMT1 protein levels were positively correlated with survival. Of the 31 patients who survived at least 24 months after surgery, 55% displayed a highly elevated PRMT1 expression and 26% a moderately elevated PRMT1 expression, whereas only 19% showed a normal and not elevated PRMT1 expression (Fig 7D). On the opposite, 60% of patients with shorter survival times, for example, less than 12 months, exhibited not elevated or moderately elevated PRMT1 levels and only 40% showed highly elevated PRMT1 expression. These results suggest that very high PRMT1 expression levels correlate with a favorable prognosis of PDAC patients after potentially curative resection.

Given the here identified p14<sup>ARF</sup>-mediated tumor-suppressive function of PRMT1, we hypothesized that PDAC patient survival might benefit from co-expression of p14<sup>ARF</sup> with very high levels of PRMT1, but not with PRMT1 co-expressed at lower or not elevated levels in tumor cells. To this end, we determined the p14<sup>ARF</sup> protein expression levels in the tumor cells of the PDAC cohort using immunofluorescence staining. We found that 29% of the patients exhibited a strong cytoplasmic/nuclear and pronounced nucleolar p14<sup>ARF</sup> staining in their pancreatic neoplastic cells, indicating high p14<sup>ARF</sup> expression levels similar to normal pancreas tissue (Fig 7E). Therefore, in this subgroup of PDAC patients, the tumor suppressor function of p14<sup>ARF</sup> is likely to be relevant for chemotherapy response. The remaining 71% of PDAC specimens were scored as p14<sup>ARF</sup>-negative, consistent with the literature reporting that the *CDKN2A* locus is very often inactivated in PDAC (Hezel *et al*, 2006).

Subsequent comparative analysis of the p14<sup>ARF</sup> and PRMT1 protein levels in the PDAC cohort revealed that the percentage of patients co-expressing p14<sup>ARF</sup> and highly elevated PRMT1 levels was considerably larger in the long-term survival group (35%, ≥ 24 months) than in the short-term survival group (12.5%, ≤ 12 months) (Fig 7F). In contrast, the percentage of p14<sup>ARF</sup>-positive patients co-expressing not elevated or only moderately elevated PRMT1 levels was rather equal in the short-term (21%) and long-term (25%) survival group. These correlation analyses confirm our hypothesis that the long-term survival of PDAC patients might benefit from co-expression of p14<sup>ARF</sup> with high PRMT1 levels, but not with low PRMT1 levels.

Given that PDAC patients generally undergo post-operative adjuvant chemotherapy with nucleoside analogues (gemcitabine or 5-fluorouracil as part of folfox) to eradicate remaining tumor cells, we questioned next whether DNA damage caused by gemcitabine also triggers p14<sup>ARF</sup> activation. Therefore, we initially examined several human pancreatic tumor cell lines for their p14<sup>ARF</sup> expression. In agreement with the literature and the observation of a high mutation and inactivation rate of p14<sup>ARF</sup> in primary PDACs (Hezel *et al*, 2006; Deer *et al*, 2010), we found that the majority of the tested cell lines do not express p14<sup>ARF</sup>, such as MiaPaCa-2, S2-007 and Panc1 cells, but PaTu8988 cells showed high expression levels of p14<sup>ARF</sup>, which was also predominantly localized in the nucleoli (Fig 8A, Appendix Fig S13). All PDAC cell lines tested expressed high levels of PRMT1 (Fig 8A). Remarkably, treatment of PaTu8988 cells with gemcitabine caused a redistribution of p14<sup>ARF</sup> from the nucleolar compartment into the nucleolar and cytoplasm (Appendix Fig S14). Furthermore, this resulted in decreased protein levels and in increased p14<sup>ARF</sup> methylation (Fig 8B and C), suggesting that p14<sup>ARF</sup> acts also as a stress sensor in response to this kind of chemotherapeutic drugs. Therefore, we hypothesized that PRMT1 influences the efficiency of anti-cancer drugs such as gemcitabine. To this end, we treated p14<sup>ARF</sup>-proficient (PaTu8988) and p14<sup>ARF</sup>-deficient (MiaPaCa-2) pancreatic tumor cell lines with gemcitabine in the absence or presence of the type I PRMT1 inhibitor MS023, which has been demonstrated to efficiently inhibit PRMT1 (Eram *et al*, 2016). Using Annexin V/propidium iodide staining and flow

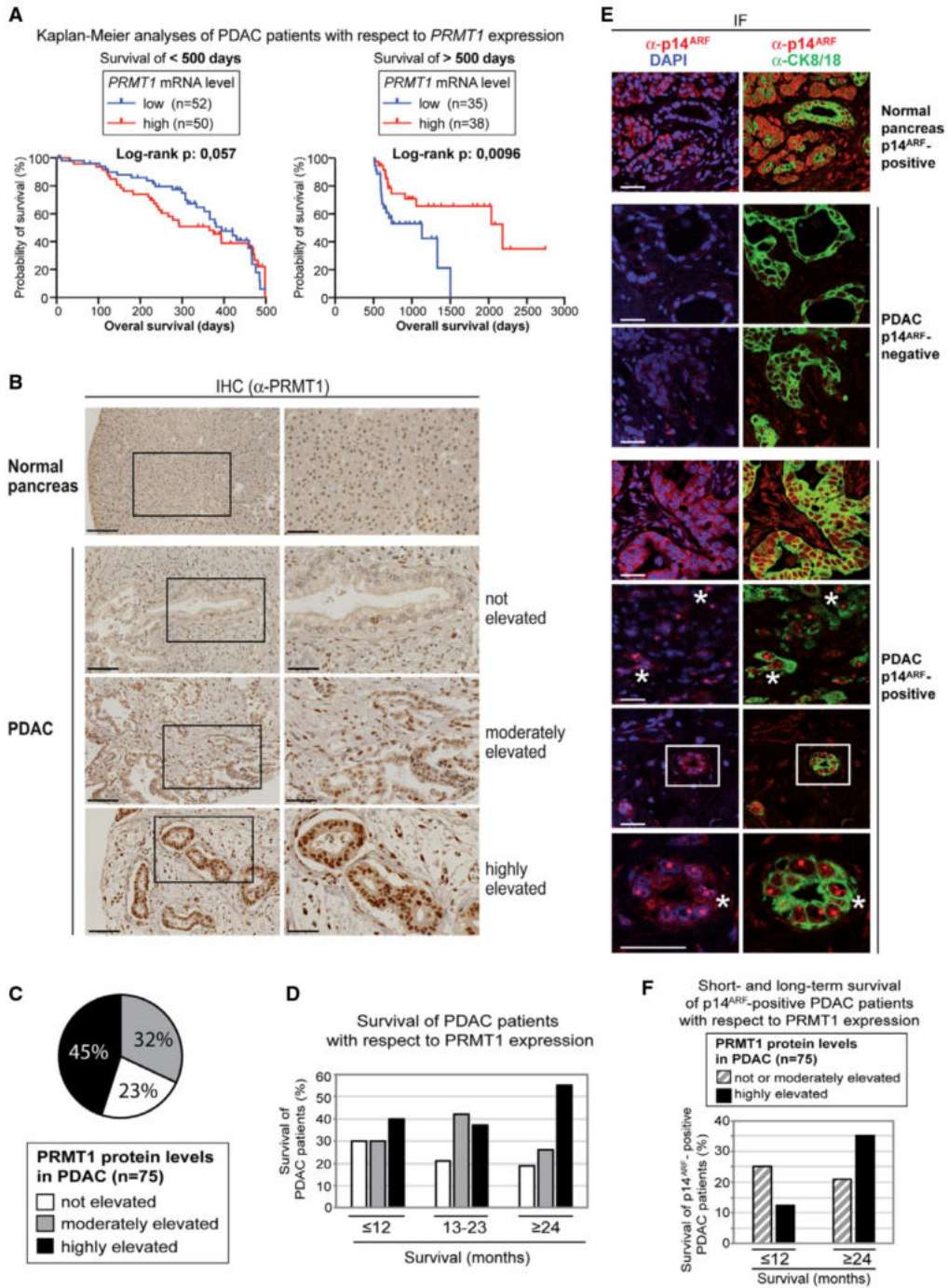


Figure 7.



**Figure 7. Prognostic relevance of PRMT1 for clinical PDAC outcome.**

- A Kaplan–Meier plot was generated using the transcriptome data set of PDAC from TCGA and OncoLnc to visualize the survival of PDAC patients with low or high PRMT1 transcript levels and short-term (< 500 days, left plot) and long-term survival (> 500 days, right plot).
- B Representative immunohistochemistry (IHC) stainings of PRMT1 (brown) are shown for normal human pancreatic tissue and three PDAC specimens deriving from the cohort of 75 patients. Based on the immunostaining intensity and the percentage of stained tumor cells, all specimens were divided into three PRMT1 expression scores: not elevated, moderately elevated, and highly elevated PRMT1 expression in tumor cells in comparison with normal pancreas. Right images are magnifications of the left images, as indicated by the black rectangles. Scale bars in the left images: 100  $\mu$ m. Scale bars in the right images: 50  $\mu$ m.
- C The pie chart depicts the percentage of patients of the PDAC cohort ( $n = 75$ ) belonging to the three PRMT1 expression scores: not elevated, moderately elevated, and highly elevated PRMT1 expression.
- D Patients of the PDAC cohort were grouped according to their survival time in months into three survival groups: short-term ( $\leq 12$  months), medium-term (13–23 months), and long-term survivors ( $\geq 24$  months). Subsequently, the percentage of patients belonging to the three different PRMT1 expression scores (legend as in C) are displayed for each survival group.
- E Immunofluorescence (IF) stainings of the 75 PDAC specimens were performed using  $\alpha$ -p14<sup>ARF</sup> (red),  $\alpha$ -CK8/18 (green, staining ductal cells in normal pancreas and neoplastic cells in PDAC) antibodies and DAPI (blue, nuclei/DNA). Representative IF images are shown for normal human pancreatic tissue, two PDAC specimens displaying no p14<sup>ARF</sup> expression and three PDAC specimens displaying strong p14<sup>ARF</sup> expression in tumor cells. Left and corresponding right images show the same tissue section. Asterisks indicate nucleolar p14<sup>ARF</sup> localization in neoplastic cells of PDAC. The last image pair shows a magnification of the image pair above (indicated by the rectangle). Scale bars: 35  $\mu$ m.
- F p14<sup>ARF</sup>-positive patients of the PDAC cohort were grouped according to their survival time in month into two survival groups: short-term ( $\leq 12$  months) and long-term survivors ( $\geq 24$  months). Subsequently, the percentages of patients with either not/moderately elevated PRMT1 expression or highly elevated PRMT1 expression are displayed for the two survival groups.

cytometry, we found that both p14<sup>ARF</sup>-proficient and p14<sup>ARF</sup>-deficient PDAC cells undergo cell death upon gemcitabine treatment (Fig 8D, Appendix Fig S15). However, co-treatment with MS023 resulted in diminished gemcitabine-induced cell death of PaTu8988t (p14<sup>ARF</sup>-proficient), but not of MiaPaCa-2 cells (p14<sup>ARF</sup>-deficient). Furthermore, addition of MS023 alone reduced the numbers of dead PaTu8988t cells compared to the untreated condition, which was not the case for MiaPaCa-2 cells. These observations in PaTu8988t cells were also corroborated by Western blot analysis of PARP cleavage, which was decreased upon co-treatment with gemcitabine and MS023 in comparison with single treatment with gemcitabine (Fig 8E). Moreover, MS023 treatment resulted in elevated p14<sup>ARF</sup> protein levels, reminiscent of the effect caused by PRMT1 depletion or deletion (Figs 5C and G, and 6C and D).

Given that PaTu8988t and MiaPaCa-2 cells have accumulated multiple mutations, which might contribute to their specific apoptotic behavior apart from their PRMT1 and p14<sup>ARF</sup> status, we generated PaTu8988t cells depleted for p14<sup>ARF</sup> (Fig 8F) and MiaPaCa-2 cells exogenously expressing p14<sup>ARF</sup> (Fig 8H). Both sets of isogenic cell lines were then analyzed for their ability to undergo gemcitabine-dependent apoptosis and for their response toward MS023 treatment. Control siRNA transfected PaTu8988t cells showed similarly to wild-type PaTu8988t cells (Fig 8D) that gemcitabine-induced apoptosis was diminished upon MS023 treatment (Fig 8G). In contrast, siRNA-mediated depletion of p14<sup>ARF</sup> led to unchanged or increased gemcitabine-induced apoptosis of PaTu8988t cells in the presence of MS023 (Fig 8G), reminiscent of the behavior of p14<sup>ARF</sup>-deficient MiaPaCa-2 cells (Fig 8D) indicating that p14<sup>ARF</sup> and PRMT1 cooperate in apoptosis induction of PaTu8988t cells. Overexpression of p14<sup>ARF</sup> in MiaPaCa-2 cells did not change the apoptotic rate in the untreated condition (Fig Appendix S16), but strikingly, resulted in reduced levels of MS023- and MS023/gemcitabine-mediated apoptosis compared to control transfected cells (Fig 8I), thereby converting the apoptotic behavior of these cells into that of p14<sup>ARF</sup>-proficient PDAC tumor cells. PRMT1 activity seems to contribute to an efficient chemotherapy response, at least in the context of certain cancer cell genome states, e.g., in the presence of wild-type p14<sup>ARF</sup>. Altogether, our results reveal that p14<sup>ARF</sup> and PRMT1 functionally cooperate in

their tumor-suppressive activities *in vivo* and that their synergy might be relevant for tumor prognosis and clinical outcome of PDAC.

## Discussion

In the present study, we identify the tumor suppressor protein p14<sup>ARF</sup> as a novel interaction partner and substrate of PRMT1. Our findings show that the interaction between PRMT1 and p14<sup>ARF</sup> is reinforced upon genotoxic stress leading to arginine methylation of the NoLS/NLS in p14<sup>ARF</sup> (Fig 9). This methylation event concomitantly causes crucial changes in the interaction network of p14<sup>ARF</sup>. On the one hand, p14<sup>ARF</sup> methylation weakens the association with its nucleolar interaction partner NPM and enables its release from the nucleolar compartment. Upon relocalization to the nucleolar and cytoplasm p14<sup>ARF</sup> becomes functionally active, albeit less stable. On the other hand, the stress-induced methylation of p14<sup>ARF</sup> seems to enforce its interaction with the pro-apoptotic factor p32 and promotes p53-independent apoptosis. Our data unravel PRMT1-mediated arginine methylation as an important trigger for the stress-induced tumor-suppressive function of p14<sup>ARF</sup> (Fig 9).

Given that nothing is known so far about the mechanism leading to stress-induced arginine methylation of p14<sup>ARF</sup>, we hypothesize that post-translational modifications, such as DNA damage-induced phosphorylation, might alter PRMT1's binding affinity and activity toward its substrate p14<sup>ARF</sup>. Phosphorylation of PRMT1 has been reported to regulate protein–protein interactions and substrate specificity (Rust *et al*, 2014; Bao *et al*, 2017). Recently, replication stress stimulated by cisplatin treatment and other agents has been shown to induce a PRMT1-dependent arginine methylome in ovarian cancer cells (Musiani *et al*, 2020). Cisplatin exposure triggers the interaction between PRMT1 and DNA-PK, a kinase required for NHEJ (non-homologous end joining)-mediated DNA repair, leading to phosphorylation and concomitant chromatin recruitment of PRMT1. This stress-induced redirection of the activity of PRMT1 enhances methylation of histone H4 at arginine 3 (H4R3me) in chromatin and promotes the activation of a pro-inflammatory and cell cycle arrest gene expression program (Musiani *et al*, 2020).

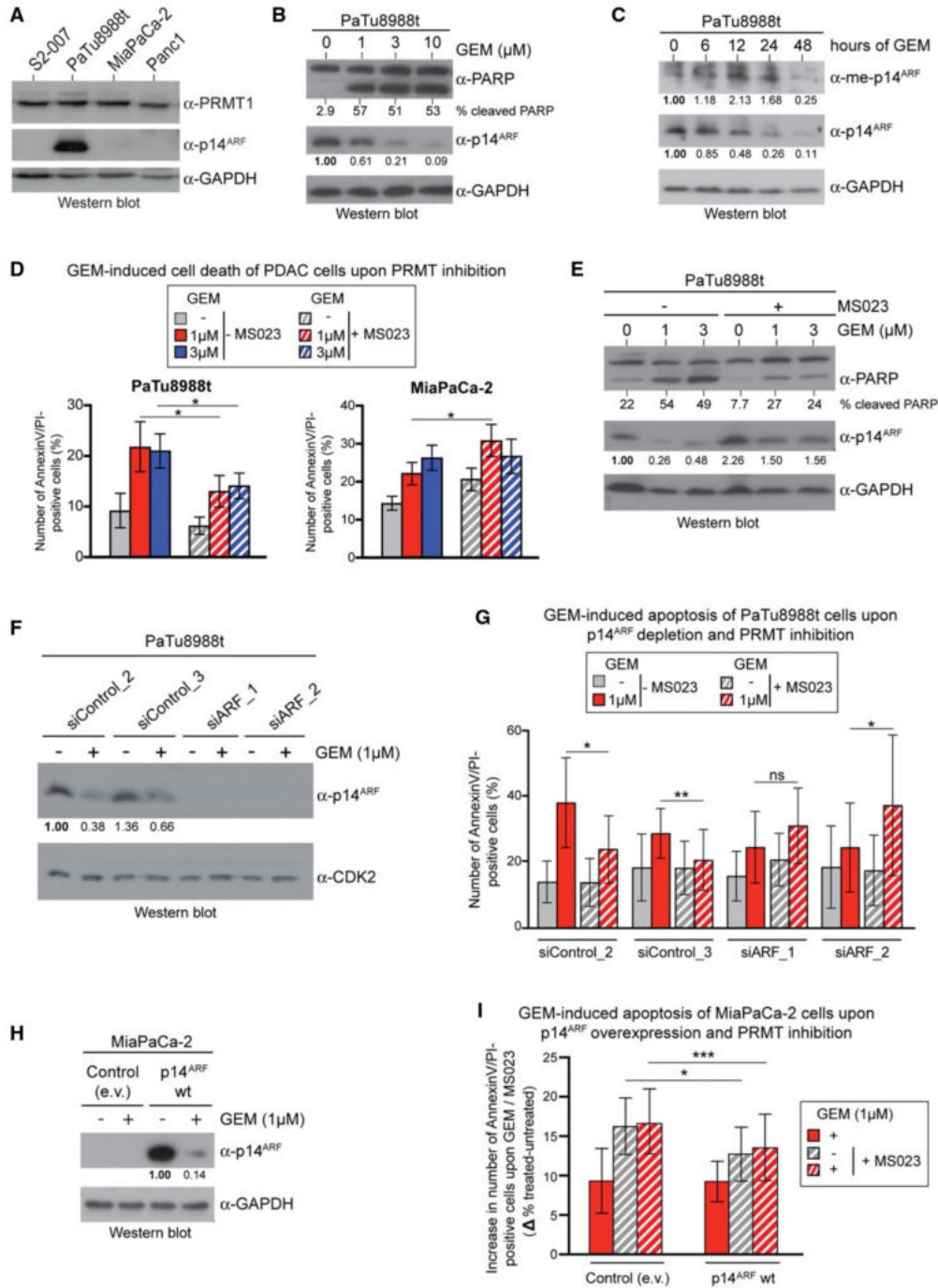
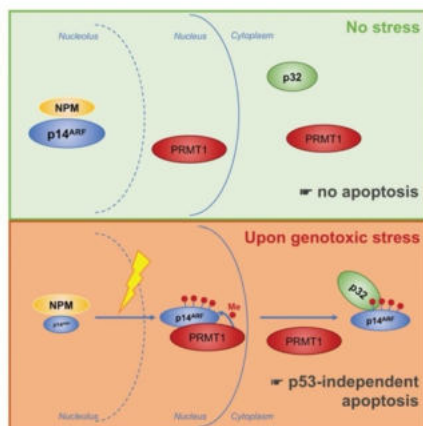


Figure 8.

**Figure 8. Impact of PRMT1 on chemotherapy response and apoptosis induction of PDAC cell lines.**

- A Cell lysates of the indicated human pancreatic tumor cell lines (S2-007, PaTu8988t, MiaPaCa-2, Panc1) were resolved by SDS-PAGE and analyzed by immunoblotting for p14<sup>ARF</sup> ( $\alpha$ -p14<sup>ARF</sup>) and PRMT1 ( $\alpha$ -PRMT1) protein levels. GAPDH staining served as loading control.
- B PaTu8988t cells were treated with 0, 1, 3, and 10  $\mu$ M gemcitabine (GEM). After 48 h, cell lysates were analyzed by immunoblotting using the indicated antibodies. The p14<sup>ARF</sup> signals were densitometrically quantified and normalized to the respective GAPDH signal, as specified by the numbers below the blots, with the untreated condition (– GEM) set to 1. The percentage of PARP cleavage was also densitometrically quantified and is indicated below the blot.
- C PaTu8988t cells were treated with 3  $\mu$ M gemcitabine (GEM) or left untreated (0 h). After 0, 6, 12, 24, and 48 h, methylation of endogenous p14<sup>ARF</sup> was analyzed by immunoblotting using  $\alpha$ -me-p14<sup>ARF</sup>,  $\alpha$ -p14<sup>ARF</sup>, and  $\alpha$ -GAPDH (loading control) antibodies. The methylated p14<sup>ARF</sup> and the p14<sup>ARF</sup> signals were densitometrically quantified and normalized to the respective GAPDH signal, as specified by the numbers below the blots, with the untreated condition (0 h) set to 1.
- D, E PaTu8988t and MiaPaCa-2 cells were treated (+) with 20  $\mu$ M MSO23 or left untreated (–) for 3 days. For the last 2 days, the cells were additionally exposed to 0, 1, or 3  $\mu$ M gemcitabine (GEM). Subsequently, cell death was quantified by flow cytometry (in (D)) using FITC-labeled Annexin V and propidium iodide (PI) for four independent experiments (mean  $\pm$  SD, \* $P$   $\leq$  0.05 using Welch's t-test). Additionally, PaTu8988t cell lysates were analyzed by immunoblotting using the indicated antibodies. A representative result is displayed in (E). The p14<sup>ARF</sup> signals were densitometrically quantified and normalized to the respective GAPDH signal, as specified by the numbers below the blots, with the untreated condition (– GEM, – MSO13) set to 1. The percentage of PARP cleavage was also densitometrically quantified and is indicated below the blot.
- F, G PaTu8988t were transfected with the indicated siRNAs (two control/non-targeting siRNAs and two p14<sup>ARF</sup>-specific siRNAs) and treated (+) with 20  $\mu$ M MSO23 or left untreated (–) for 3 days. For the last 2 days, the cells were additionally exposed 1  $\mu$ M gemcitabine (+ GEM) or not (– GEM). p14<sup>ARF</sup> depletion was monitored by immunoblotting using the indicated antibodies. A representative result is displayed in (F). The p14<sup>ARF</sup> signals in the siControl conditions were densitometrically quantified and normalized to the respective CDK2 signal, as specified by the numbers below the blot, with the untreated condition (– GEM) of the siControl\_2 sample set to 1. Apoptosis was quantified by flow cytometry (G) using FITC-labeled Annexin V and propidium iodide (PI) for six independent experiments (mean  $\pm$  SD, \*\* $P$   $\leq$  0.005, \* $P$   $\leq$  0.05, ns: not significant using Welch's t-test).
- H, I MiaPaCa-2 cells were transfected with empty vector (e.v., control) or Flag-tagged wild-type (wt) p14<sup>ARF</sup>-containing plasmid and treated (+) with 20  $\mu$ M MSO23 or left untreated (–) for 3 days. For the last 2 days, the cells were additionally exposed to 1  $\mu$ M gemcitabine (+ GEM) or not (– GEM). p14<sup>ARF</sup> overexpression was monitored by immunoblotting using the indicated antibodies. A representative result is displayed in (H). The p14<sup>ARF</sup> signals in the overexpression conditions were densitometrically quantified and normalized to the respective GAPDH signal, as specified by the numbers below the blot, with the untreated condition (– GEM) set to 1. Apoptosis was analyzed by flow cytometry (I) using FITC-labeled Annexin V and propidium iodide (PI). The increase in the apoptotic cell fraction upon gemcitabine and/or MSO23 was quantified for four independent experiments (mean  $\pm$  SD, \*\*\* $P$   $\leq$  0.001, \* $P$   $\leq$  0.05 using Welch's t-test).

**Figure 9. Model for the regulation of the tumor suppressor protein p14<sup>ARF</sup> by PRMT1.**

In unstressed cells, p14<sup>ARF</sup> is predominantly sequestered in the nucleoli, bound to its nucleolar interaction partner NPM. Upon genotoxic stress, the interaction between p14<sup>ARF</sup> and PRMT1 is reinforced and the C-terminal NLS/NoLS of p14<sup>ARF</sup> is methylated by PRMT1. This stress-induced arginine methylation promotes the release of p14<sup>ARF</sup> from NPM and nucleolar sequestration, leading to p53-independent apoptosis.

The relevance of the methylation sites in p14<sup>ARF</sup> is emphasized by the fact that these arginine residues are frequently mutated in cancer, thereby disrupting the pro-apoptotic function of p14<sup>ARF</sup> (Itahana & Zhang, 2008). Similarly, PRMT1 expression has been

reported to be altered, mostly upregulated, in many human tumors (Yoshimatsu *et al.*, 2011; Yang & Bedford, 2013). PRMT1 is the most abundant PRMT member and responsible for generating the majority of arginine-methylated residues in mammalian cells (Tang *et al.*, 2000). In agreement with its essential function in early embryonic development, PRMT1 regulates progenitor cell renewal and lineage commitment mainly on the level of transcriptional regulation by methylation of H4R3 and other chromatin proteins (Pawlak *et al.*, 2000; Zhao *et al.*, 2008; Bao *et al.*, 2017; Blanc *et al.*, 2017). On the one hand, in muscle stem cells, PRMT1 restricts the self-renewal capacity and promotes the myogenic differentiation program, whereas on the other hand the opposite is the case in epidermal stem cell, where PRMT1 is responsible for progenitor proliferation as well as maintenance and inhibits terminal differentiation (Bao *et al.*, 2017; Blanc *et al.*, 2017). Thus, depending on the cell lineage, PRMT1 executes opposing effects on proliferation and differentiation, either pro-proliferative and differentiation-blocking or anti-proliferative and differentiation-promoting activities. Consequently, in the context of carcinogenesis, it is conceivable that PRMT1 functions as an oncoprotein but also as a tumor suppressor protein. For example, in acute myeloid leukemia PRMT1 cooperates with cancer cell-specific transcription factors and coregulators, such as RUNX1 or oncogenic MLL-fusion proteins, leading to an aberrant pro-proliferative and tumor-promoting transcriptional response (Cheung *et al.*, 2007, 2016; Shia *et al.*, 2012).

Apart from affecting stem cell homeostasis and differentiation processes, PRMT1 is also involved in important cellular house-keeping functions, for example, in the maintenance of genome stability and DNA damage response, for example, by methylation of critical DNA repair proteins, such as MRE11, 53BP, and BRAC1 (Boisvert *et al.*, 2005a, 2005b; Yu *et al.*, 2009; Vadnais *et al.*, 2018; Montenegro *et al.*, 2020). In line with this protection function in

cellular stress situations, PRMT1 also regulates apoptosis by methylation of pro-apoptotic proteins, such as the transcription factor FOXO1 and the BCL-2 antagonist BAD. These methylation events inhibit AKT-dependent phosphorylation of FOXO1 and BAD, thereby enabling apoptosis induction (Yamagata *et al.*, 2008; Sakamaki *et al.*, 2011). Similarly, methylation of the transcription factor E2F-1 by PRMT1 stabilizes the protein during DNA damage and fosters E2F-1-dependent apoptosis (Zheng *et al.*, 2013). Our findings on the pro-apoptotic cooperation between PRMT1 and p14<sup>ARF</sup> integrate into the general perspective that the cellular activities of PRMT1 upon DNA damage are anti-proliferative and activate tumor suppressor functions.

In cancer cells, in which PRMT1 mainly acts as an oncoprotein by stimulating proliferation, blocking differentiation and apoptosis or enhancing DNA repair efficiency, pharmacological inhibition of PRMT1 will likely be therapeutically beneficial (Guccione & Richard, 2019). In these cases, PRMT1 inhibition in combination with classic chemotherapy can help to prevent the PRMT1-driven oncogenic transcriptional responses and cancer cells from evading apoptosis. However, in cancer cells, in which the dominating stress-induced function of PRMT1, e.g., during chemotherapy treatment, is pro-apoptotic by methylation of p14<sup>ARF</sup>, FOXO1, BAD, or E2F-1, PRMT1 inhibition is counterproductive and harmful. In the majority of human PDAC patients, we found elevated PRMT1 protein levels in agreement with recent reports (Wang *et al.*, 2016; Song *et al.*, 2020). Remarkably, PRMT1 expression levels positively correlated with an extended long-term survival of PDAC patients suggesting that the tumor-suppressive effects of PRMT1 might prevail in this tumor entity. Furthermore, PDAC patients benefited in their long-term survival from co-expression of p14<sup>ARF</sup> with high levels of PRMT1, but not with lower levels of PRMT1. In agreement, p14<sup>ARF</sup>-positive pancreatic tumor cells with high PRMT1 levels revealed increased gemcitabine-induced apoptosis rates compared to cells co-treated with a PRMT inhibitor, suggesting that here PRMT1 might contribute to an efficient chemotherapy response. Upregulation of PRMT1 during tumor cell evolution might be conducive to increase the tumor mass and malignancy, but PRMT1 inhibitor treatment should not be taken per se as a promising therapeutic strategy. Instead, further in-depth understanding of the molecular pathology and the accompanying genetic alterations of specific tumor entities is strictly necessary to decide on the advantage or disadvantage of pharmacological PRMT1 inhibition.

## Materials and Methods

### Cell lines and reagents

U2OS, HeLa, HEK293T, PaTu8988t, MiaPaCa-2, S2-007, and Panc1 cells were maintained in DMEM supplemented with 10% fetal calf serum (FCS, Gibco/BRL), 1% penicillin/streptomycin at 37°C and 5% CO<sub>2</sub>. Sf9 cells were cultured as described in (Berberich *et al.*, 2017). Detailed information on cell culture reagents, manipulations, plasmids, and antibodies (including the generation of  $\alpha$ -me-p14<sup>ARF</sup>) is supplied in the Appendix Supplementary Methods. Of note, all  $\alpha$ -p14<sup>ARF</sup> antibodies used in the present study were able to equally efficiently recognize unmethylated and methylated p14<sup>ARF</sup> wild-type (Fig 5C) and the p14<sup>ARF</sup>-mutant (RG/RF/RK) proteins (shown for  $\alpha$ -

p14<sup>ARF</sup> from Bethyl in Fig 1F, Appendix Fig S3A; data not shown for  $\alpha$ -p14<sup>ARF</sup> from Novus and Sigma).

### Human tissue

Patient material was obtained from the Department of Surgery at the University Hospital Marburg and pancreatic tissue blocks were archived in the Department of Pathology. All patients provided written informed consent, and the study was approved by the Ethics Committee of the Philipps-University Marburg (No. 05/2003).

### In vivo MT assay

For detection of *in vivo* methylation of p14<sup>ARF</sup>, metabolic labeling of HEK293 cells was conducted in the presence of radiolabeled methionine, of which the <sup>3</sup>H-labeled methyl-group is intracellularly metabolized and incorporated into the cofactor SAM, as described in (Liu & Dreyfuss, 1995). In detail, transfected HEK293 cells were initially cultured for 3 days in the absence or presence of AdOx (20  $\mu$ M). For translational block, cells were pretreated with 40  $\mu$ g/ml chloramphenicol (Sigma-Aldrich) and 100  $\mu$ g cycloheximide (AppliChem). After 30 min of pretreatment, L-[<sup>3</sup>H-methyl]-methionine (<sup>3</sup>H-methionine 10  $\mu$ Ci/ml; Perkin Elmer) was added in a methionine- and cysteine-free medium for 3 h. Cell extracts were prepared in RIPA buffer and subjected to benzonase treatment (0.25 U/ $\mu$ l in presence of 7.5 mM MgCl<sub>2</sub> for 1 h at 4°C). After centrifugation, 4–6 mg lysates were employed in immunoprecipitation of EGFP-tagged p14<sup>ARF</sup>. Immunoprecipitates were analyzed by SDS-PAGE followed either by immunoblotting or fluorography. For fluorography, gels were incubated with Enlight enhancing solution (Mo Bi Tec) and vacuum dried at 80°C. Radioactive signals were detected using X-ray films (Hyperfilm; Amersham) and intensifying screens (Kodak).

### In vitro MT assays

*In vitro* methylation assays were performed in the presence of radiolabeled SAM (<sup>14</sup>C-labeled methyl-group) using recombinant GST-tagged substrates and PRMT enzymes purified from bacteria or eukaryotic cells as described in (Hyllus *et al.*, 2007; Berberich *et al.*, 2017). Eluted GST-tagged or Flag-tagged PRMT enzymes or immunoprecipitated HA-tagged PRMT5/Myc-tagged MEP50 were incubated with substrates (either bead-bound GST-tagged proteins or histone H3, H4, or bulk histones from calf thymus; Sigma-Aldrich) in the presence of [<sup>14</sup>C-methyl]-S-adenosyl-methionine (<sup>14</sup>C-methyl-SAM 20  $\mu$ Ci/ml; Perkin Elmer) for 1–2 h at 37°C. Reactions were separated by SDS-PAGE and blotted on PVDF membrane for autoradiography and subsequent immunostaining. Radioactive signals were detected using X-ray films (Hyperfilm; Amersham) and intensifying screens (Kodak).

### Pull-down assays

Pull-down assays using bead-coupled peptides or GST-tagged proteins were performed as described in the Appendix Supplementary Methods. Unmodified and modified p14<sup>ARF</sup> NLS/NoLS peptides followed by a C-terminal cysteine residue were obtained from Peptide Specialty Laboratories (Heidelberg, Germany).

### Flow cytometry

For detection of cell cycle distribution and apoptosis/necrosis, flow cytometry was used as recently described in (Streubel *et al.*, 2013; Bouchard *et al.*, 2018). In detail, for quantification of cell cycle distribution, cells were harvested, washed in ice-cold PBS, and fixed in ice-cold 70% ethanol overnight. After complete permeabilization, cells were washed twice with FACS buffer. DNA was then stained with 54  $\mu$ M propidium iodide (PI, Sigma-Aldrich) in the presence of 38 mM sodium citrate and 250  $\mu$ g/ml RNase A for 30 min at 37°C in the dark. For quantification of phosphatidylserine on the surface of UVC-treated cells,  $0.5\text{--}1 \times 10^6$  unfixed cells were incubated with FITC-labeled Annexin-V and/or PI (BD Pharmingen) according to the manufacturer's instructions. All samples were analyzed using BD FACSCalibur flow cytometer (BD Bioscience). Data were processed using the CellQuestPro or FlowJo (FlowJo LLC) Software.

### Immunofluorescence (IF) stainings

Localization and expression levels of p14<sup>ARF</sup> and PRMT1 were detected in cell lines and human pancreatic tissue of PDAC patients by immunofluorescence stainings (IF) and immunohistochemistry stainings (IHC). For IF stainings of cells, cells were grown on glass coverslips and fixed with either 4% formaldehyde at RT or methanol at  $-20^{\circ}\text{C}$  for 10–15 min, permeabilized in PBS with 0.3% Triton X-100 for 5 min, and incubated with blocking solution (PBS; 0.1–0.3% Triton X-100 or without Triton X-100; 5% BSA) for 45–60 min. Incubation with primary antibodies (Appendix Supplementary Methods) was performed in blocking solution at RT for 2 h. Cells were washed three times in PBS, followed by incubation with fluorophore-linked secondary antibodies (Appendix Supplementary Methods) for 30–75 min. Subsequently, cells were stained with DAPI (0.15 mg/ml; Sigma-Aldrich) in PBS for 2–4 min, washed three times in PBS, once in water, and then embedded in mounting medium (Mowiol4-88 with DABCO, Roth). Stainings were analyzed using a Leica DMR fluorescence microscope and the Confocal Laser Scanning microscope Leica SP8i, followed by analysis with the Leica LAS AF and Fiji software. For quantification of subcellular p14<sup>ARF</sup> localization,  $\geq 200$  cells per condition and biological replicate were counted and grouped into exclusively nucleolar, not-exclusively nucleolar but additionally/predominantly nucleolar/cytoplasmic or exclusively cytoplasmic localization.

For IF staining of human tissue, formalin-fixed and paraffin-embedded PDAC samples and corresponding normal pancreas were deparaffinized and hydrated as for IHC. For antigen retrieval, tissue sections were steam-heated for 35 min in citrate buffer (pH 6.0) and then washed in PBS. For reducing the background staining, sections were incubated twice 5 min in 100 mM glycine, followed by rinsing three times in TBS with 0.1% Tween (TBS-T) and incubation in blocking solution (PBS; 10% chicken serum; 0.3% Triton X-100) at RT for 60 min. Incubation with primary antibodies (Appendix Supplementary Methods) was performed overnight at 4°C in blocking solution with 5% chicken serum. Subsequently, the sections were washed three times with TBS-T and blocked for 30 min in blocking solution followed by incubation with secondary antibodies (Appendix Supplementary Methods) and DAPI (0.15  $\mu$ g/ml; Sigma-Aldrich) for 90 min at RT. After 3 additional washing steps in TBS-T and one washing step in water, the sections were embedded

in mounting medium (Mowiol4-88 with DABCO, Roth) and stored at 4°C. Fluorescence images were captured using the Confocal Laser Scanning microscope Leica SP8i and analyzed using the Leica LAS AF software.

### Immunohistochemistry (IHC) stainings

Formalin-fixed and paraffin-embedded archived human PDAC samples and corresponding normal tissues were stained as follows. Tissue sections were heated to 60°C for 1 h, deparaffinized using xylene, and hydrated by a graded series of ethanol washes. Antigen retrieval was accomplished by steam-heating in target retrieval solution (pH 9.0, Dako) for 30 min. Endogenous peroxidase activity was quenched by 5-min incubation in 3% H<sub>2</sub>O<sub>2</sub>. Sections were then incubated with primary antibodies (Appendix Supplementary Methods) for 45 min at RT followed by biotinylated secondary antibodies for 20 min also at RT. Bound antibodies were detected using the avidin–biotin complex (ABC) peroxidase method (ABC Elite Kit; Vector Labs, Burlingame, California, USA). Final staining was developed with the Dako DAB peroxidase substrate kit. For double staining, HRP Magenta Substrate Chromogen System was employed. Counterstaining was performed using hematoxylin. All steps following the antigen retrieval were performed using the DakoCytomation Autostainer Plus. The quantitation of PRMT1 positive cells was performed using the virtual software programs Fiji ImageJ (Schindelin *et al.*, 2009) and ViewPoint software version 2018-02-05 from PreciPoint GmbH (Freising, Germany). Quantitative expression scores for PRMT1 were determined by counting of  $\geq 100$  tumor cells per specimen. Scores (not elevated, moderately elevated or highly elevated PRMT1 expression) are based on the immunostaining intensity and the percentage of stained tumor cells in PDAC tissues compared to normal pancreas.

### Protein and RNA isolation

Protein and RNA isolation for immunoblotting, immunoprecipitation, or reverse transcription quantitative PCR (RT-qPCR) was performed as described in the Appendix Supplementary Methods.

### Statistical analysis

All experiments were performed at least three times (biological replicates, n-values as indicated in the figure legends) and are represented as mean  $\pm$  SD. Reproducible and representative data sets are shown. Corresponding statistical tests are mentioned in the figure legends.

### Data availability

This study includes no data deposited in external repositories.

**Expanded View** for this article is available online.

### Acknowledgements

We thank present and former members of the U.M.B. laboratory, in particular Kaatje Heinelt, Lara Kleinesudek, Dr. Anna-Lena Jung, Alessia Pantaleoni, Caroline Reuter, and Dr. Saleh Hassan Sharif Ahmed, for their active support during the work progress. We are grateful to Dr. Katrin Roth from Cellular Imaging

Unit for microscopy support, Dr. Annette Ramaswamy from the Department of Pathology for pancreas tissue evaluation, and Dr. Ina Petra Pfefferle from the Comprehensive Biomaterial Bank for tissue archiving. Further, we thank Viktoria Wischmann, Inge Sprenger, and Silke Caspari for their excellent technical assistance. This work was funded by the DFG (Deutsche Forschungsgemeinschaft) to DKB and UMB as part of the KFO325 (BA 1467/6, BA 2292/5) and to UMB as part of TRR81 A03, SFB1213 A06, BA 2292/1, and BA 2292/4.

### Author contributions

AR: Investigation, Validation, Formal Analysis, Visualization. DH: Investigation, Validation, Formal Analysis, Visualization, Writing—review and editing. CB: Investigation, Validation, Formal Analysis, Visualization, Writing—review and editing. MM: Investigation, Validation, Formal Analysis, Visualization, Writing—review and editing. YV-Y: Investigation. HR: Investigation, Formal Analysis. LH: Investigation. EKra: Investigation, Validation, Writing—review and editing. EKre: Resources. RF: Resources. CUK: Resources, Methodology. ML: Resources, Methodology, Writing—review and editing. EPS: Supervision, Writing—review and editing. DKB: Funding acquisition, Supervision, Writing—review and editing. U-MB: Project Administration, Funding acquisition, Conceptualization, Supervision, Formal Analysis, Visualization, Writing—original draft.

### Conflict of interest

The authors declare that they have no conflict of interest.

## References

- Anaya J (2016) OncoLnc: linking TCGA survival data to mRNAs, miRNAs, and lncRNAs. *PeerJ Comput Sci* 2: e67
- Ayrault O, Olivier A, Karayan L, Lucie K, Riou J-F, Jean-François R, Larsen C-J, Christian-Jacques L, Séité P, Paule S (2003) Delineation of the domains required for physical and functional interaction of p14ARF with human topoisomerase I. *Oncogene* 22: 1945–1954
- Bao X, Siprashvili Z, Zarnegar BJ, Shenoy RM, Rios EJ, Nady N, Qu K, Mah A, Webster DE, Rubin AJ et al (2017) CSNK1a1 regulates PRMT1 to maintain the progenitor state in self-renewing somatic tissue. *Dev Cell* 43: 227–239
- Berberich H, Terwesten F, Rakow S, Sahu P, Bouchard C, Meixner M, Philipsen S, Kolb P, Bauer U-M (2017) Identification and in silico structural analysis of Gallus gallus protein arginine methyltransferase 4 (PRMT4). *FEBS Open Bio* 7: 1909–1923
- Blanc RS, Vogel G, Li X, Yu Z, Li S, Richard S (2017) Arginine methylation by PRMT1 regulates muscle stem cell fate. *Molecular Cell Biol* 37: e00457-16
- Boisvert FM, Dery U, Masson JY, Richard S (2005a) Arginine methylation of MRE11 by PRMT1 is required for DNA damage checkpoint control. *Genes Dev* 19: 671–676
- Boisvert FM, Rhie A, Richard S, Doherty AJ (2005b) The GAR motif of 53BP1 is arginine methylated by PRMT1 and is necessary for 53BP1 DNA binding activity. *Cell Cycle* 4: 1834–1841
- Bouchard C, Sahu P, Meixner M, Nötzold RR, Rust MB, Kremmer E, Feederle R, Hart-Smith G, Finkernagel F, Bartkuhn M et al (2018) Genomic location of PRMT6-Dependent H3R2 methylation is linked to the transcriptional outcome of associated genes. *Cell Rep* 24: 3339–3352
- Chen D, Kon N, Zhong J, Zhang P, Yu L, Gu W (2013) Differential effects on ARF stability by normal versus oncogenic levels of c-Myc expression. *Mol Cell* 51: 46–56
- Chen D, Shan J, Zhu W-G, Qin J, Gu W (2010) Transcription-independent ARF regulation in oncogenic stress-mediated p53 responses. *Nature* 464: 624–627
- Cheung N, Chan LC, Thompson A, Cleary ML, So CW (2007) Protein arginine-methyltransferase-dependent oncogenesis. *Nat Cell Biol* 9: 1208–1215
- Cheung N, Fung TK, Zeisig BB, Holmes K, Rane JK, Mowen KA, Finn MG, Lenhard B, Chan LC, So CW (2016) Targeting aberrant epigenetic networks mediated by PRMT1 and KDM4C in acute myeloid leukemia. *Cancer Cell* 29: 32–48
- Deer EL, González-Hernández J, Coursen JD, Shea JE, Ngatia J, Scaife CL, Firpo MA, Mulvihill SJ (2010) Phenotype and genotype of pancreatic cancer cell lines. *Pancreas* 39: 425–435
- Eram MS, Shen Y, Szweczyk MM, Wu H, Senisterra G, Li F, Butler KV, Kaniskan HÜ, Speed BA, Dela Seña C et al (2016) A Potent, Selective, and cell-active inhibitor of human type I protein arginine methyltransferases. *ACS Chem Biol* 11: 772–781
- Eymin B, Claverie P, Salon C, Leduc C, Col E, Brambilla E, Khochbin S, Gazzeri S (2006) p14ARF activates a Tip60-dependent and p53-independent ATM/ATR/CHK pathway in response to genotoxic stress. *Mol Cell Biol* 26: 4339–4350
- Favia A, Salvatori L, Nanni S, Iwamoto-Stohl LK, Valente S, Mai A, Scagnoli F, Fontanella RA, Totta P, Nasi S et al (2019) The Protein Arginine Methyltransferases 1 and 5 affect Myc properties in glioblastoma stem cells. *Sci Rep* 9: 1–13
- Gallagher SJ, Kefford RF, Rizos H (2006) The ARF tumour suppressor. *Int J Biochem Cell Biol* 38: 1637–1641
- Guccione E, Richard S (2019) The regulation, functions and clinical relevance of arginine methylation Nature reviews | Molecular cell Biology. *Nat Rev Mol Cell Biol* 20: 642–657
- Hezel AF, Kimmelman AC, Stanger BZ, Hezel AF, Kimmelman AC, Stanger BZ, Bardeesy N, Depinho RA (2006) Genetics and biology of pancreatic ductal adenocarcinoma Genetics and biology of pancreatic ductal adenocarcinoma. *Genes Dev* 20: 1218–1249
- Hyllus D, Stein C, Schnabel K, Schiltz E, Imhof A, Dou Y, Hsieh J, Bauer U-M (2007) PRMT6-mediated methylation of R2 in histone H3 antagonizes H3 K4 trimethylation. *Genes Dev* 21: 3369–3380
- Itahana K, Zhang Y (2008) Mitochondrial p32 is a critical mediator of ARF-induced apoptosis. *Cancer Cell* 13: 542–553
- Karayan L, Riou JF, Séité P, Migeon J, Cantereau A, Larsen CJ (2001) Human ARF protein interacts with topoisomerase I and stimulates its activity. *Oncogene* 20: 836–848
- Kim WY, Sharpless NE (2006) The regulation of INK4/ARF in cancer and aging. *Cell* 127: 265–275
- Ko A, Shin JY, Seo J, Lee KD, Lee EW, Lee MS, Lee HW, Choi IJ, Jeong JS, Chun KH et al (2012) Acceleration of gastric tumorigenesis through MKRN1-mediated posttranslational regulation of p14ARF. *J Natl Cancer Inst* 104: 1660–1672
- Korgaonkar C, Hagen J, Tompkins V, Frazier AA, Allamargot C, Quelle FW, Quelle DE (2005) Nucleophosmin (B23) Targets ARF to nucleoli and inhibits its function. *Mol Cell Biol* 25: 1258–1271
- Kuo ML, Den Besten W, Bertwistle D, Roussel MF, Sherr CJ (2004) N-terminal polyubiquitination and degradation of the Arf tumor suppressor. *Genes Dev* 18: 1862–1874
- Lee C, Smith BA, Bandyopadhyay K, Gjerset RA (2005) DNA damage disrupts the p14ARF-B23(nucleophosmin) interaction and triggers a transient subnuclear redistribution of p14ARF. *Cancer Res* 65: 9834–9842
- Liu Q, Dreyfuss G (1995) *In vivo* and *in vitro* arginine methylation of RNA-binding proteins. *Mol Cell Biol* 15: 2800–2808
- Montenegro MF, González-Guerrero R, Sánchez-del-Campo L, Piñero-Madróna A, Cabezas-Herrera J, Rodríguez-López JN (2020)

- PRMT1-dependent methylation of BRCA1 contributes to the epigenetic defense of breast cancer cells against ionizing radiation. *Sci Rep* 10: 13275–13288
- Moulin S, Llanos S, Kim SH, Peters G (2008) Binding to nucleophosmin determines the localization of human and chicken ARF but not its impact on p53. *Oncogene* 27: 2382–2389
- Musiani D, Giambrodo R, Massignani E, Ippolito MR, Maniaci M, Jammula S, Manganaro D, Cuomo A, Nicosia L, Pasini D et al (2020) PRMT1 is recruited via DNA-PK to chromatin where it sustains the senescence-associated secretory phenotype in response to Cisplatin. *Cell Rep* 30: 1208–1222
- Ozenne P, Eymin B, Brambilla E, Gazzeri S (2010) The ARF tumor suppressor: Structure, functions and status in cancer. *Int J Cancer* 127: 2239–2247
- Pawlak MR, Scherer CA, Chen J, Roshon MJ, Ruley HE (2000) Arginine N-methyltransferase 1 is required for early postimplantation mouse development, but cells deficient in the enzyme are viable. *Mol Cell Biol* 20: 4859–4869
- Rizos H, Darmanian AP, Mann CJ, Kefford RF (2000) Two arginine rich domains in the p14ARF tumour suppressor mediate nucleolar localization. *Oncogene* 19: 2978–2985
- Rodway H, Llanos S, Rowe J, Peters G (2004) Stability of nucleolar versus non-nucleolar forms of human p14 ARF. *Oncogene* 23: 6186–6192
- Rust HL, Subramanian V, West GM, Young DD, Schultz PG, Thompson PR (2014) Using unnatural amino acid mutagenesis to probe the regulation of PRMT1. *ACS Chem Biol* 9: 649–655
- Sakamaki JJ, Daitoku H, Ueno K, Hagiwara A, Yamagata K, Fukamizu A (2011) Arginine methylation of BCL-2 antagonist of cell death (BAD) counteracts its phosphorylation and inactivation by Akt. *Proc Natl Acad Sci USA* 108: 6085–6090
- Schindelin J, Arganda-Carrera I, Frise E, Verena K, Mark L, Tobias P, Stephan P, Curtis R, Stephan S, Benjamin S et al (2009) Fiji - an Open platform for biological image analysis. *Nat Methods* 9: 676–682
- Sherr CJ (2006) Divorcing ARF and p53: an unsettled case. *Nat Rev Cancer* 6: 663–673
- Shia WJ, Okumura AJ, Yan M, Sarkeshik A, Lo MC, Matsuura S, Komeno Y, Zhao X, Nimer SD, Yates JR et al (2012) PRMT1 interacts with AML1-ETO to promote its transcriptional activation and progenitor cell proliferative potential. *Blood* 119: 4953–4962
- Song C, Chen T, He L, Ma N, Li J, Rong YF, Fang Y, Liu M, Xie D, Lou W (2020) PRMT1 promotes pancreatic cancer growth and predicts poor prognosis. *Cell Oncol* 43: 51–62
- Stott FJ, Bates S, James MC, McConnell BB, Starborg M, Brookes S, Palmero I, Ryan K, Hara E, Vousden KH et al (1998) The alternative product from the human CDKN2A locus, p14(ARF), participates in a regulatory feedback loop with p53 and MDM2. *EMBO J* 17: 5001–5014
- Streubel G, Bouchard C, Berberich H, Zeller MS, Teichmann S, Adamkiewicz J, Muller R, Klempnauer KH, Bauer UM (2013) PRMT4 is a novel coactivator of c-Myb-dependent transcription in haematopoietic cell lines. *PLoS Genet* 9: e1003343
- Tang J, Frankel A, Cook RJ, Kim S, Paik WK, Williams KR, Clarke S, Herschman HR (2000) PRMT1 is the predominant type I protein arginine methyltransferase in mammalian cells. *J Biol Chem* 275: 7723–7730
- Vadnais C, Chen R, Fraszczak J, Yu Z, Boulais J, Pinder J, Frank D, Khandanpour C, Hébert J, Delleire G et al (2018) GFI1 facilitates efficient DNA repair by regulating PRMT1 dependent methylation of MRE11 and 53BP1. *Nat Commun* 9: 1–14
- Wang X, Zha M, Zhao X, Jiang P, Du W, Tam AYH, Mei Y, Wu M (2013) Siva1 inhibits p53 function by acting as an ARF E3 ubiquitin ligase. *Nat Commun* 4: 1551
- Wang Y, Hsu J-M, Kang Y, Wei Y, Lee P-C, Chang S-J, Hsu Y-H, Hsu JL, Wang H-L, Chang W-C et al (2016) Oncogenic functions of Gli in pancreatic adenocarcinoma are supported by its PRMT1-mediated methylation. *Cancer Res* 76: 7049–7058
- Yamagata K, Daitoku H, Takahashi Y, Namiki K, Hisatake K, Kako K, Mukai H, Kasuya Y, Fukamizu A (2008) Arginine methylation of FOXO transcription factors inhibits their phosphorylation by Akt. *Mol Cell* 32: 221–231
- Yang Y, Bedford MT (2013) Protein arginine methyltransferases and cancer. *Nat Rev Cancer* 13: 37–50
- Yoshimatsu M, Toyokawa G, Hayami S, Unoki M, Tsunoda T, Field HI, Kelly JD, Neal DE, Maehara Y, Ponder BA et al (2011) Dysregulation of PRMT1 and PRMT6, Type I arginine methyltransferases, is involved in various types of human cancers. *Int J Cancer* 128: 562–573
- Yu Z, Chen T, Hebert J, Li E, Richard S (2009) A mouse PRMT1 null allele defines an essential role for arginine methylation in genome maintenance and cell proliferation. *Mol Cell Biol* 29: 2982–2996
- Zhang Y, Xiong Y (1999) Mutations in human ARF exon 2 disrupt its nucleolar localization and impair its ability to block nuclear export of MDM2 and p53. *Mol Cell* 3: 579–591
- Zhao X, Jankovic V, Gural A, Huang G, Pardanani A, Menendez S, Zhang J, Dunne R, Xiao A, Erdjument-Bromage H et al (2008) Methylation of RUNX1 by PRMT1 abrogates SIN3A binding and potentiates its transcriptional activity. *Genes Dev* 22: 640–653
- Zheng S, Moehlenbrink J, Lu YC, Zalmas LP, Sagum CA, Carr S, McGouran JF, Alexander L, Fedorov O, Munro S et al (2013) Arginine methylation-dependent reader-writer interplay governs growth control by E2F-1. *Mol Cell* 52: 37–51



**License:** This is an open access article under the terms of the Creative Commons Attribution-NonCommercial-NoDerivs 4.0 License, which permits use and distribution in any medium, provided the original work is properly cited, the use is non-commercial and no modifications or adaptations are made.



# Extracellular Vesicle-Based Detection of Pancreatic Cancer

Yesim Verel-Yilmaz<sup>1†</sup>, Juan Pablo Fernández<sup>1†</sup>, Agnes Schäfer<sup>2</sup>, Sheila Nevermann<sup>1</sup>, Lena Cook<sup>2</sup>, Norman Gercke<sup>1</sup>, Frederik Helmprobst<sup>3,4</sup>, Christian Jaworek<sup>2</sup>, Elke Pogge von Strandmann<sup>5</sup>, Axel Pagenstecher<sup>3</sup>, Detlef K. Bartsch<sup>1</sup>, Jörg W. Bartsch<sup>2†</sup> and Emily P. Slater<sup>1\*†</sup>

<sup>1</sup> Department of Visceral, Thoracic and Vascular Surgery, Philipps University Marburg, Marburg, Germany, <sup>2</sup> Department of Neurosurgery, Philipps University Marburg, Marburg, Germany, <sup>3</sup> Department of Neuropathology, Philipps University Marburg, Marburg, Germany, <sup>4</sup> Core Facility-Mouse Pathology and Electron Microscopy (MPEM), Philipps University Marburg, Marburg, Germany, <sup>5</sup> Institute for Tumorimmunology, Philipps University Marburg, Marburg, Germany

## OPEN ACCESS

### Edited by:

Jeffrey David Galley,  
The Ohio State University,  
United States

### Reviewed by:

Cheng Wang,  
Nanjing University, China  
Xinlei Li,  
Nationwide Children's Hospital,  
United States

### \*Correspondence:

Emily P. Slater  
slater@med.uni-marburg.de

<sup>†</sup>These authors have contributed  
equally to this work

### Specialty section:

This article was submitted to  
Molecular and Cellular Pathology,  
a section of the journal  
Frontiers in Cell and Developmental  
Biology

Received: 20 April 2021

Accepted: 29 June 2021

Published: 23 July 2021

### Citation:

Verel-Yilmaz Y, Fernández JP,  
Schäfer A, Nevermann S, Cook L,  
Gercke N, Helmprobst F, Jaworek C,  
Pogge von Strandmann E,  
Pagenstecher A, Bartsch DK,  
Bartsch JW and Slater EP (2021)  
Extracellular Vesicle-Based Detection  
of Pancreatic Cancer.  
Front. Cell Dev. Biol. 9:697939.  
doi: 10.3389/fcell.2021.697939

Due to a grim prognosis, there is an urgent need to detect pancreatic ductal adenocarcinoma (PDAC) prior to metastasis. However, reliable diagnostic imaging methods or biomarkers for PDAC or its precursor lesions are still scarce. ADAM8, a metalloprotease-disintegrin, is highly expressed in PDAC tissue and negatively correlates with patient survival. The aim of our study was to determine the ability of ADAM8-positive extracellular vesicles (EVs) and cargo microRNAs (miRNAs) to discriminate precursor lesions or PDAC from healthy controls. In order to investigate enrichment of ADAM8 on EVs, these were isolated from serum of patients with PDAC ( $n = 52$ ), precursor lesions ( $n = 7$ ) and healthy individuals ( $n = 20$ ). Nanoparticle Tracking Analysis and electron microscopy indicated successful preparation of EVs that were analyzed for ADAM8 by FACS. Additionally, EV cargo analyses of miRNAs from the same serum samples revealed the presence of miR-720 and miR-451 by qPCR and was validated in 20 additional PDAC samples. Statistical analyses included Wilcoxon rank test and ROC curves. FACS analysis detected significant enrichment of ADAM8 in EVs from patients with PDAC or precursor lesions compared to healthy individuals ( $p = 0.0005$ ). ADAM8-dependent co-variables, miR-451 and miR-720 were also diagnostic, as patients with PDAC had significantly higher serum levels of miR-451 and lower serum levels of miR-720 than healthy controls and reached high sensitivity and specificity (AUC = 0.93 and 1.00, respectively) to discriminate PDAC from healthy control. Thus, detection of ADAM8-positive EVs and related cargo miR-720 and miR-451 may constitute a specific biomarker set for screening individuals at risk for PDAC.

**Keywords:** pancreatic cancer, extracellular vesicles, ADAM8, serum biomarkers, miRNA

## INTRODUCTION

Pancreatic cancer is the fourth leading cause of cancer-related deaths in the world with an incidence of 45 in 100,000 and a 5-year survival rate of around 9% (Siegel et al., 2020). Among pancreatic cancer, pancreatic ductal adenocarcinoma (PDAC) is the most common type with more than 90% of all cases. A number of factors are responsible for the poor prognosis of PDAC that combines the difficulties in detecting the tumor in early stages, an aggressive biological behavior to account



for metastasis and the resistance to existing adjuvant therapies. To detect PDAC in early stages, only a few biomarkers are used routinely that are able to detect its presence and the lesions prior to its derivation (Bartsch et al., 2018). Exosomes are a defined type of extracellular vesicle (EV) ranging in size from 30 to 100 nm and secreted by all cell types including cancer cells. In the context of cancer, exosomes produced in tumor cells contain an abundance of cell-specific molecules that may facilitate the discrimination between cancer afflicted patients and healthy individuals (Sumrin et al., 2018).

Exosome cargo consists of proteins, nucleic acids and lipids (Colombo et al., 2014). Their composition is not only a reflection of the cell they originated from, but also appears to be a regulated process that remains not completely understood (Minciacchi et al., 2015). Content sorting and exosome release seem to not only depend on the type of donor cell, but also on its physiological or pathological state, different stimuli and the pathway of exosome biogenesis (Minciacchi et al., 2015). There are, however, marker proteins that have been found to be specific to EVs because they are related to their pathway of biogenesis. These proteins are, for example, members of the tetraspanin family (CD9, CD81) that are characteristic to exosomes, or flotillins (flotillin-1–2), which are frequently observed in exosomes and microvesicles alike (Kowal et al., 2016). Because exosome content is specific to their donor cell and exosomes can be isolated from bodily fluids such as blood, saliva, ascites or urine, they make promising candidates for early tumor diagnostics.

One rationale to use EVs as early diagnostic markers is their potential to transport tumor-associated micro RNAs (miRNAs) encapsulated in serum exosomes. MiRNAs are small non-coding RNAs of about 18–22 nt long that can be transferred to adjacent cells in the tumor microenvironment to modulate gene expression (Zonari et al., 2013; Su et al., 2016).

As protein cargo, membrane proteins involved in extracellular communication and remodeling are excellent candidates for exosome loading. Among these proteins metalloprotease-disintegrins (ADAM) are potential cargo proteins (reviewed in Shimoda and Khokha, 2017). Due to the interaction with the exosomal marker protein CD9, ADAM10 was one of the first members of the ADAM protease family found to be associated with exosomes (Keller et al., 2009). In previous studies, ADAM8 was defined as an ADAM protease associated with tumor progression and metastasis formation in PDAC (Valkovskaya et al., 2007; Schlomann et al., 2015). In addition, ADAM8 is expressed in tumor associated immune cells such as macrophages, NK cells and neutrophils (Jaworek et al., 2021). These data suggest that ADAM8 itself could be a diffusible molecule that is, similarly to the ADAM protease ADAM10, released in exosomes. Recently, much attention has been addressed to EVs, which may serve as a strategy of monitoring and managing disease status (Cufaro et al., 2019). Since ADAM8 expression is high in PDAC, it is likely that EVs isolated from its precursor lesions, Pancreatic intraepithelial Neoplasia (PanINs) types 2 and 3, could be packed with ADAM8 and ADAM8-associated molecular markers such as miRNAs as shown for breast cancer with correlated expression levels of ADAM8 and miRNA-720 (Das et al., 2016). MiRNAs are integral components

of almost every cancer-related biological process, including cellular differentiation, proliferation, migration, apoptosis, EMT and angiogenesis. Here we hypothesized that high ADAM8 expression levels in pancreatic cancer is reflected by release of EVs expressing ADAM8 on their surface and that ADAM8 expression might cause miRNAs associated with ADAM8 expression to be cargo for ADAM8-positive EVs, so that these EVs can be used to detect pancreatic cancer in patient serum at early stages.

## MATERIALS AND METHODS

### Patient Cohort

Patients with familial pancreatic cancer (FPC) or PDAC treated at the Department of Visceral Surgery at University Hospital Marburg were enrolled in our study. All patients provided written informed consent prior to participating in this study. Ethical approval was granted from the local ethics committee at Marburg University, Faculty of Medicine (File No. 5/03). All tumors were histologically staged by an experienced pathologist according to the UICC-TNM (Union for International Cancer Control; tumor, node, metastasis) classification 2017 (Gospodarowicz and Brierley, 2017).

### Extracellular Vesicle Preparation

250  $\mu$ l of serum were diluted with 4.5 ml Hank's Salt Saline Buffer in a 15 ml falcon tube in order to lower sample viscosity and centrifuged at  $800 \times g$  for 5 min in order to eliminate any remaining cells. The supernatant was transferred to a new 15 ml falcon tube and centrifuged at  $2,000 \times g$  for 10 min to remove dead cells or cell debris (Théry et al., 2006; Melo et al., 2015). The supernatant was then transferred to a 5 ml syringe and filtered through a 0.2  $\mu$ m pore filter and transferred to a 6.0 ml polypropylene bell-top quick-seal centrifuge tube and filled with Hank's Balanced Salt Solution (HBSS). The tubes were centrifuged at  $100,000 \times g$  and  $4^\circ\text{C}$  for 70 min. The pellet was resuspended in HBSS and transferred to a polypropylene 1.5 ml microcentrifuge tube and was centrifuged with an Optima MAX-XP Ultracentrifuge in a TLA-55 fixed angle rotor at  $100,000 \times g$  and  $4^\circ\text{C}$  for 100 min. The supernatant was discarded, and the pellet resuspended with 50  $\mu$ l HBSS. Samples were stored at  $-80^\circ\text{C}$ . In order to determine the particle size and concentration of isolated EVs, NTA was performed with the ZetaView® BASIC PMX-120 and the corresponding software ZetaView®.

### Western Blot Analysis

To further phenotype isolated EVs, enriched proteins were detected in Western blots. Twenty  $\mu$ g protein determined by standard BCA were boiled in Laemmli buffer without  $\beta$ -Mercaptoethanol (60 mM Tris-HCl, pH = 6.8; 2% SDS; 10% Glycerol; 0.01% Bromphenol-Blue) for 5 min. Protein separation was performed by SDS-PAGE followed by a transfer onto PVDF membranes. Successful transfer was confirmed by Ponceau S staining. To block unspecific binding, membranes were immersed in 4% BSA in TBST (50 mM

Tris, pH = 7.5; 150 mM NaCl; 0.1% Tween-20) for 1 h, followed by incubation with primary antibody against CD9 (CBL162; Chemicon International, Temecula, CA, United States, 1:1,000 in 4% BSA in TBST) at 4°C overnight. After washing three times, blots were incubated with the respective secondary antibody for 1 h. After an additional washing step, signals were detected with SuperSignal™ West Pico PLUS Chemiluminescent Substrate (Thermo Fisher Scientific, Rockford, IL, United States). Additional antibodies were used to characterize the EVs isolated. These included CD81 (sc-166029; Santa Cruz Biotechnology), Flotillin-1 (PA5-18053; Thermo Fisher Scientific), hADAM8 (MAB10311; R&D Systems) and Calnexin (2679; Cell Signaling Technology).

### FACS Analyses

FACS analyses were performed as previously described (Bartsch et al., 2018). Briefly,  $1.5 \times 10^9$  EVs were coupled to 10  $\mu$ l of 4  $\mu$ m aldehyde/sulfate latex beads, 4% w/v in 100  $\mu$ l PBS and incubated for 15 min at room temperature. Then 900  $\mu$ l of PBS were added to reach a final volume of 1,000  $\mu$ l and EVs and beads were incubated for another 30 min at room temperature. Beads were then blocked by adding 50  $\mu$ l 10% BSA. Samples were centrifuged at 9,900 rpm for 1 min. Supernatant was discarded leaving a volume of 100  $\mu$ l in the tubes. Samples were further blocked by incubation with 5  $\mu$ l Human True Stain FcX Blocking Solution for 10 min at room temperature. Samples were then centrifuged again at 9,000 rpm for 1 min and the supernatant was discarded. Pellets were resuspended in 20  $\mu$ l 2% BSA. Now, one half of the samples was incubated with 3  $\mu$ l anti-ADAM8 (MAB10311, R&D Systems) at 4°C overnight. The next day, all samples were washed in 1 ml 2% BSA and centrifuged at 9,900 rpm for 1 min. All samples were treated with 20  $\mu$ l of a blocking solution consisting of Human True Stain FcX Blocking Solution (BioLegend, San Diego, CA, United States) and 2% BSA and incubated with 3  $\mu$ l alexa-488-tagged secondary antibody (Abcam, Cambridge, United Kingdom) at 4°C for 1 h. In a final step, samples were washed twice in 1 ml 2% BSA. The final bead pellet was resuspended in 1 ml PBS and transferred to 5 ml Flow Cytometry Tubes. Samples were stored at 4°C in the dark until measurement. The percentage of ADAM8-positive beads out of 100,000 total events was then calculated in a FACS analysis.

### Electron Microscopy

EVs were stained for electron microscopy as previously described (Théry et al., 2006). Briefly, purified extracellular vesicles were fixed with an equal amount of 4% PFA. An amount of 5–7  $\mu$ l was placed on a Formvar/carbon coated 200 mesh copper (Ted Pella Inc., Redding, CA) electron microscopy grid and incubated for 20 min. After the membrane adsorbed the vesicles the grids were washed with sterile filtered PBS and fixed for 5 min with 1% glutaraldehyde. The grids were washed 8 times for 2 min with sterile filtered water and then incubated with 1% uranyl acetate for 5 min. After an additional incubation with 2% methyl cellulose supplemented with 4% uranyl acetate (ratio 9:1) on ice, the excess fluid was removed with filter paper and the grids were air dried for up to 10 min. The exosomes were imaged with a Zeiss EM 900 at 80 kV.

### Protease Activity Assay

Serum EVs isolated from either PDAC patients or healthy individuals were tested for ADAM8 activity by determining cleavage of a FRET-based polypeptide substrate with a high Kcat/Km for ADAM8 (PEPDab13, BioZyme, Inc., North Carolina, United States) as previously described (Schlömman et al., 2019). Briefly, 10  $\mu$ M of PEPDab13 in 50  $\mu$ l assay buffer (1 mM ZnCl<sub>2</sub>, 20 mM Tris-HCl pH 8.0, 10 mM CaCl<sub>2</sub>, 150 mM NaCl, 0.0006% Brij-35) was incubated with  $3.75 \times 10^8$  EVs in a total volume of 100  $\mu$ l. Resulting fluorescence was monitored every 2 min for 6 h at 37°C with a multiwell plate reader (FLUOstar OPTIMA, BMG Labtech, Offenburg, Germany) using  $\lambda_{ex}$  of 485 nm and an  $\lambda_{em}$  of 530 nm.

### Serum Exosome miRNA Analysis

Total RNA carried by exosomes or other EVs in 250  $\mu$ l of serum was extracted using the ExoRNeasy Serum/Plasma Midi Kit from Qiagen (Hilden, Germany) with the addition of a spike of 25 fmol of synthetic cel-miR-54 DNA as recommended by the manufacturer. The RNA was converted to cDNA using the miRNA Reverse Transcription Kit, miScript II RT Kit, also from Qiagen. The cDNA synthesis reaction was diluted and incubated with QuantiTect® SYBR Green PCR Master Mix, miScript Universal Primer and specific miScript Primer Assays. The real-time PCR reactions were run in a StepOnePlus Real time PCR System from Applied Biosystems (Darmstadt, Germany). The  $\Delta$  threshold cycle (Ct) values were then calculated by subtracting the cel-miR-54 Ct value from the specific miRNA Ct value. For the analyses of cell lines SNORD95 was chosen as the endogenous control as previously described (Sperveslage et al., 2014). Ct values of each target miRNA transcript were normalized against the Ct value of SNORD95. Relative change in exosomal miRNA expression comparing wild type and knock-out cells was calculated using the  $\Delta\Delta$ Ct method.

### Statistical Analyses

A Wilcoxon signed-rank test and a *t*-test were performed to assess whether the patient values were significantly different from control samples. A *p*-value of < 0.05 was considered to be statistically significant. The receiver operating characteristic curve analyses were performed using GraphPad Prism version 6 (GraphPad Software, La Jolla, CA, United States).

## RESULTS

### Clinicopathological Characteristics of the Recruited Patients, Including IAR With High-Risk Precursor Lesions

The characteristics of the 72 PDAC patients that were included in the study are presented in Table 1.

### Preparation of Extracellular Vesicles From Patient Serum Samples

Extracellular vesicles including exosomes with an average diameter < 120 nm were isolated from patient serum using

**TABLE 1** | Clinicopathological characteristics of the recruited patients.

		Cohort (n = 72)
<b>Gender</b>	Males (%)	37 (51%)
	Females (%)	35 (49%)
Median age at surgery, years (range)		68 (47–85)
<b>UICC stage</b>	I	11 (15.3%)
	II	10 (13.9%)
	III	46 (63.9%)
	IV	5 (6.9%)
Median survival, months (range)		22 (1–92)
<b>Location</b>	Pancreas	
	Head	65 (90.3%)
	body or tail	7 (9.7%)

In addition, 7 individuals at risk (IAR) who had undergone surgery for removal of precursor lesions were also recruited. These included 2 males and 5 females with a median age of 54 years. Histologically verified precursor lesions included 1 main duct intra ductal papillary mucinous neoplasm (IPMN) with high grade dysplasia, 2 PanIN 3 and 4 PanIN 2. The healthy controls (n = 20) had a median age of 40 years and included 10 males and 10 females.

a range of purification steps including ultracentrifugation and filtration. The exosomes present in these preparations were identified by a number of analytical methods including ZetaView® analyses and electron microscopy to confirm existence of a double membrane and the proper size

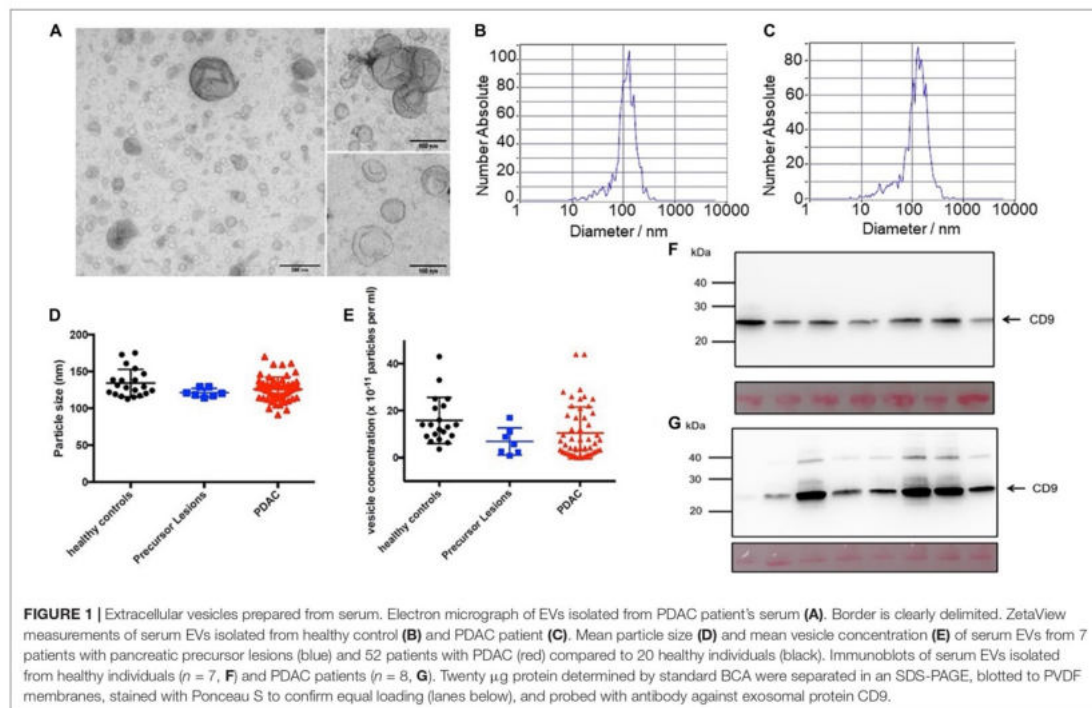
corresponding to exosomes (Figures 1A–C). The particle size and vesicle concentration did not vary among the preparations from the different sources (Figures 1D,E). In addition, CD9 was found in all preparations. However, whereas the control samples had relatively constant amounts of CD9 (Figure 1F), the tumor samples varied in abundance (Figure 1G). Additional markers were also tested to characterize the EVs. The preparations were also positive for CD81, Flotillin-1 and ADAM8, but were negative for calnexin (Supplementary Figure 1).

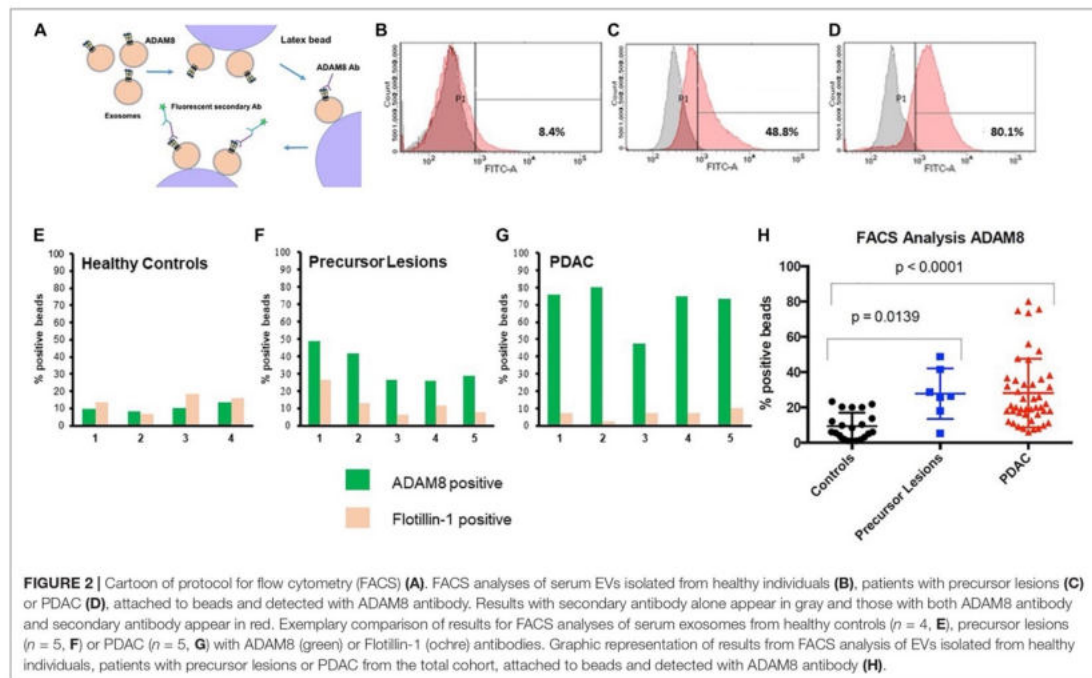
### Diagnostic FACS Analysis of ADAM8 in Exosomes

In order to detect ADAM8 on the surface of exosomes, a bead-coupled FACS analysis was performed (Figure 2). Positive ADAM8 signals were observed both in control individuals and in PDAC patients. However, their proportion was significantly different, so that an enrichment of ADAM8 in serum exosomes from patients with PDAC or its precursor lesions compared to healthy individuals was observed ( $p < 0.0001$  or  $p = 0.0139$ , respectively).

### Cargo Analysis of Serum Derived EVs From Control and PDAC Patients

Since ADAM8 is located on EVs as shown by bead-coupled FACS analysis, we investigated whether ADAM8 confers enzymatic activity to EVs enriched in ADAM8. Activity of ADAM8 can



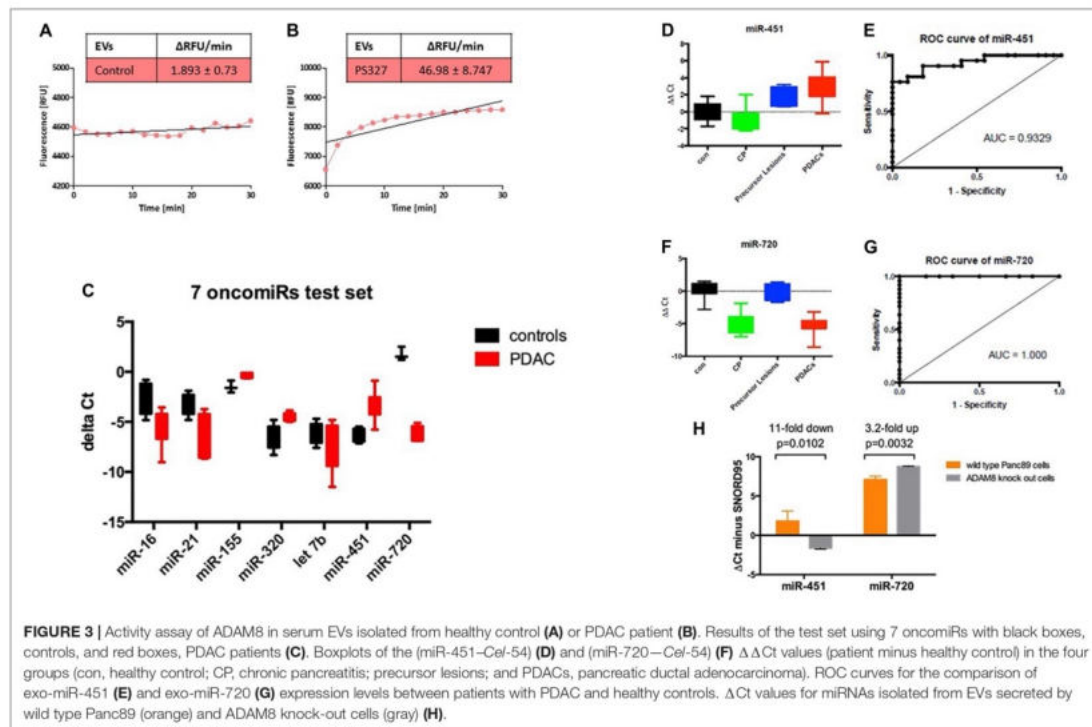


be detected by using a FRET-based peptide representing the cleavage site of CD23 (Schlomann et al., 2019). Cleavage analysis of EVs isolated from either a control individual or a PDAC patient revealed a strongly enhanced proteolytic activity in EVs from the PDAC patient (Figures 3A,B). Although the FRET-based peptide is not specific for ADAM8 activity, it is very likely that the increased activity originates from ADAM8 as the FACS analysis suggests. In addition to the protein cargo analysis, a systematic screening for miRNAs was performed on EVs derived from control individuals and PDAC patients (Figure 3C). Interestingly, a set of 7 oncomiRNAs were found to be differentially regulated with the strongest upregulation for miRNA-451 and the strongest down-regulation for miRNA-720 (Figure 3C). To confirm differential regulation of these miRNAs in the PDAC patient cohort, exosomal miRNAs were isolated from the same serum samples and analyzed for miR-720 and miR-451 by semi-quantitative real time RT-PCR. Serum samples had been spiked with synthetic *C. elegans* miR-54 before miRNA isolation to be used as a normalization control. Statistical analyses were performed using the Wilcoxon rank test and ROC curve analysis. The miR-720 and miR-451 were also diagnostic, as patients with PDAC had significantly higher serum exosome levels of miR-451 and lower serum exosome levels of miR-720 than healthy controls and reached high sensitivity and specificity with an AUC = 0.9329 and 1.000, respectively, to discriminate PDAC (Figures 3D–G). In addition, serum exosomes were also isolated from patients with chronic pancreatitis (CP;  $n = 10$ )

and precursor lesions ( $n = 7$ ). Whereas serum exosomes from patients with precursor lesions had increased levels of miR-451, approaching the levels found in PDACs, CP patient serum exosomes did not. In contrast, the serum exosomes isolated from CP patients had lower levels of miR-720, similar to the PDAC serum exosomes, while the exosomes derived from serum of patients with precursor lesions had levels comparable to the healthy controls. Analysis of these miRNAs in Panc89 wild type and ADAM8 knock-out cells demonstrated that the levels of exosomal miR-451 decrease and the levels of exosomal miR-720 increase upon knock-out of ADAM8, suggesting a regulatory component of ADAM8 on these miRNAs (Figure 3H).

## DISCUSSION

EV based serum diagnostics provides an additional and powerful diagnostic component in the field of liquid biopsies (Yee et al., 2020). With regard to EV diagnostic in PDAC, the concentration and size of EVs in patient serum has been correlated with tumor differentiation and overall survival in PDAC patients (Badovinac et al., 2021), but no specific cargo analysis of "diagnostic" EVs in serum has been reported up to now. In this respect, our results provide some novelties: First of all, we identified ADAM8, a protease with a therapeutic potential in PDAC, to be located in EVs that meet all criteria for exosomes. By establishing a bead-supported FACS analysis method to analyze surface located ADAM8 in EVs, we demonstrated that ADAM8-positive EVs



were significantly enriched in PDAC patients and were gradually increased with increasing tumor staging, at least when comparing precursor lesions with fully developed adenocarcinoma. From the biochemical point of view, we hypothesized that ADAM8 integrated in EV membranes should be enzymatically active. By peptide cleavage assays, we were able to confirm that ADAM8-enriched EVs show remarkable activities compared to those EVs from control individuals. These data support the notion that a FACS based analysis of EVs from PDAC patients can be performed to detect membrane proteins that are topologically oriented to the extracellular compartment.

In addition to the pure presence of ADAM8, we investigated potential exosomal miRNAs as EV cargo that could be regulated by ADAM8. A panel of “oncomiRNAs” including let-7b was screened from exosomal miRNAs extracted from healthy control individuals and PDAC patients, respectively. We found that ADAM8-positive EVs are specifically equipped with miRNAs that show a functional relevance in PDAC as exemplified by the results with miR-451 and miR-720 in serum EVs from these patients. From all miRNAs examined, exosomal (exo)-miRNA-720 and exo-miRNA-451 were the most significantly dysregulated. Exosomal miRNA-720 was significantly down-regulated in serum samples from chronic pancreatitis and PDAC patients and therefore suggested perfect accuracy in the diagnosis of CP and PDAC either in its hereditary or sporadic form (AUC = 1), exosomal miRNA-451 showed

the highest up-regulation in precursor lesions and in PDAC, but not in samples from CP patients and was able to discriminate between precursor lesion or PDAC-afflicted patients and healthy individuals with relatively high accuracy and an AUC of 0.9329.

To further analyze the correlation of ADAM8 expression with miRNA expression levels, we used the PDAC cell line Panc89 with a genetic knockout of the *ADAM8* gene (Cook et al., manuscript in preparation). Using these cell lines, we further demonstrate that the regulation of miRNA-451 and miRNA-720 is dependent on ADAM8 expression levels, respectively. ADAM8 expression is inversely correlated with miRNA-720 levels, as an ADAM8-knockout in Panc89 cells leads to an increase in miRNA-720 levels (average 3.2-fold higher in Panc89\_A8KO cells vs. Panc89\_A8Ctrl cells), in accordance with the finding that we found decreased levels of miRNA-720 and increased ADAM8 levels in PDAC patients compared to control individuals. In contrast, miRNA-451 is positively correlated with ADAM8 expression levels, as this miRNA is decreased in Panc89\_A8KO cells vs. Panc89\_A8Ctrl cells. Similarly, we found increased miRNA-451 levels in PDAC patients with a higher ADAM8 expression. For both these miRNAs, functional roles in PDAC were reported that are in accordance with their described abundance in PDAC patient sera. In particular, it was shown that miRNA-720 inhibits pancreatic cancer cell proliferation and invasion by directly targeting cyclin D1 (Zhang et al., 2017)

so that down-regulation of miRNA-720 as observed in PDAC patients compared to healthy individuals has a potential tumor-promoting effect. ADAM8-dependent regulation of miRNA-720 was reported earlier in the breast cancer cell line MDA-MB-231 (Das et al., 2016) however in the opposite direction, an observation that we could reproduce with a CRISPR/Cas9 generated knockout of *ADAM8* in this cell line. In contrast, miRNA-451 can promote cell proliferation and metastasis in PDAC by down-regulating CAB39 (Calcium binding protein 39), a tumor suppressor upstream of STK11 (serine-threonine kinase 11) (Guo et al., 2017). Thus, as observed here, upregulation of miRNA-451 downregulated a tumor suppressor pathway. With miRNA-451 detecting precursor lesions and PDAC, but not chronic pancreatitis (CP) and miRNA 720 detecting CP but not precursor lesions in conjunction with ADAM8-positive EVs, we can achieve a high degree of specificity and sensitivity in serum EV analysis to predict pancreatic precursor lesion and PDAC while discriminating between chronic pancreatitis patients and healthy individuals.

## CONCLUSION

Enrichment of ADAM8 in serum exosomes as well as the measurement of exosomal miRNAs, miR-720 and miR-451, may contribute to a biomarker profile for the screening of individuals for PDAC. More generally, our data provide evidence for an EV based communication in the PDAC tumor microenvironment that can be triggered in the pro-oncogenic direction by the presence of ADAM8. This biological signature in turn can be exploited for diagnostic purposes to detect PDAC lesions and fully developed PDAC, as demonstrated here.

## DATA AVAILABILITY STATEMENT

The raw data supporting the conclusions of this article will be made available by the authors, without undue reservation.

## REFERENCES

- Badovinac, D., Goričar, K., Zavrtnik, H., Petrič, M., Lavrin, T., Mavec, N., et al. (2021). Plasma extracellular vesicle characteristics correlate with tumor differentiation and predict overall survival in patients with pancreatic ductal adenocarcinoma undergoing surgery with curative intent. *J. Pers. Med.* 11:77. doi: 10.3390/jpm11020077
- Bartsch, D. K., Gercke, N., Strauch, K., Wieboldt, R., Matthäi, E., Wagner, V., et al. (2018). The combination of miRNA-196b, LCN2, and TIMP1 is a potential set of circulating biomarkers for screening individuals at risk for familial pancreatic cancer. *J. Clin. Med.* 7:295. doi: 10.3390/jcm7100295
- Colombo, M., Raposo, G., and Théry, C. (2014). Biogenesis, secretion, and intercellular interactions of exosomes and other extracellular vesicles. *Annu. Rev. Cell Dev. Biol.* 30, 255–289. doi: 10.1146/annurev-cellbio-101512-122326
- Cufaro, M. C., Pieragostino, D., Lanuti, P., Rossi, C., Cicalini, I., Federici, L., et al. (2019). Extracellular vesicles and their potential use in monitoring cancer progression and therapy: the contribution of proteomics. *J. Oncol.* 2019:1639854. doi: 10.1155/2019/1639854
- Das, S. G., Romagnoli, M., Mineva, N. D., Barillé-Nion, S., Jézéquel, P., Campone, M., et al. (2016). miR-720 is a downstream target of an ADAM8-induced ERK

## ETHICS STATEMENT

The studies involving human participants were reviewed and approved by the Ethics Committee of the Marburg University, Faculty of Medicine (File No. 5/03). The patients/participants provided their written informed consent to participate in this study.

## AUTHOR CONTRIBUTIONS

ES, DB, and JB conceived the study. YV-Y, JF, AS, SN, LC, NG, FH, CJ, EP, and AP performed the experiments and provided resources. ES and JB wrote the manuscript. All authors approved the submitted version.

## FUNDING

Work was supported by the Deutsche Forschungsgemeinschaft (DFG) with a Clinical Research Unit grant (CRU 325) and grants to JB (BA-1606/4-1), to ES (SL-17/5-1), to DB (BA-1467/6-1), and to EP (PO-1408/14-1 and GRK 2573/1).

## ACKNOWLEDGMENTS

We wish to thank all patients for participation in the study, Günter Klöppel for histological verification of precursor lesions and all members of the Department of Pathology, Marburg University, in particular Annette Ramaswamy, Corinna Keber and Carsten Denkert.

## SUPPLEMENTARY MATERIAL

The Supplementary Material for this article can be found online at: <https://www.frontiersin.org/articles/10.3389/fcell.2021.697939/full#supplementary-material>

signaling cascade that promotes the migratory and invasive phenotype of triple-negative breast cancer cells. *Breast Cancer Res.* 18:40. doi: 10.1186/s13058-016-0699-z

Gospodarowicz, M. K., and Brierley, J. D. (2017). *TNM Classification of Malignant Tumors*. Oxford: Wiley-Blackwell.

Guo, R., Gu, J., Zhang, Z., Wang, Y., and Gu, C. (2017). miR-451 promotes cell proliferation and metastasis in pancreatic cancer through targeting CAB39. *Biomed. Res. Int.* 2017:2381482. doi: 10.1155/2017/2381482

Jaworek, C., Verel-Yilmaz, Y., Driesch, S., Ostgathe, S., Cook, L., Wagner, S., et al. (2021). Cohort analysis of ADAM8 expression in the PDAC tumor stroma. *J. Pers. Med.* 11:113. doi: 10.3390/jpm11020113

Keller, S., König, A.-K., Marmé, F., Runz, S., Wolterink, S., Koensgen, D., et al. (2009). Systemic presence and tumor-growth promoting effect of ovarian carcinoma released exosomes. *Cancer Lett.* 278, 73–81. doi: 10.1016/j.canlet.2008.12.028

Kowal, J., Arras, G., Colombo, M., Jouve, M., Morath, J. P., Prindl-Bengtson, B., et al. (2016). Proteomic comparison defines novel markers to characterize heterogeneous populations of extracellular vesicle subtypes. *Proc. Natl. Acad. Sci. U.S.A.* 113, E968–E977. doi: 10.1073/pnas.1521230113

- Melo, S. A., Luecke, L. B., Kahlert, C., Fernandez, A. F., Gammon, S. T., Kaye, J., et al. (2015). Glypican-1 identifies cancer exosomes and detects early pancreatic cancer. *Nature* 523, 177–182. doi: 10.1038/nature14581
- Minciacchi, V. R., You, S., Spinelli, C., Morley, S., Zandian, M., Aspuria, P. J., et al. (2015). Large oncosomes contain distinct protein cargo and represent a separate functional class of tumor-derived extracellular vesicles. *Oncotarget* 6, 11327–11341. doi: 10.18632/oncotarget.3598
- Schlomann, U., Dorzweiler, K., Nuti, E., Tuccinardi, T., Rossello, A., and Bartsch, J. W. (2019). Metalloprotease inhibitor profiles of human ADAM8 in vitro and in cell-based assays. *Biol. Chem.* 400, 801–810. doi: 10.1515/hsz-2018-0396
- Schlomann, U., Koller, G., Conrad, C., Ferdous, T., Golfi, P., Garcia, A. M., et al. (2015). ADAM8 as a drug target in pancreatic cancer. *Nat. Commun.* 6:6175. doi: 10.1038/ncomms7175
- Shimoda, M., and Khokha, R. (2017). Metalloproteinases in extracellular vesicles. *Biochim. Biophys. Acta Mol. Cell Res.* 1864(11 Pt A), 1989–2000. doi: 10.1016/j.bbamcr.2017.05.027
- Siegel, R. L., Miller, K. D., and Jemal, A. (2020). Cancer statistics, 2020. *CA Cancer J. Clin.* 70, 7–30. doi: 10.3322/caac.21590
- Sperveslage, J., Hoffmeister, M., Henopp, T., Klöppel, G., and Sipos, B. (2014). Establishment of robust controls for the normalization of miRNA expression in neuroendocrine tumors of the ileum and pancreas. *Endocrine* 46, 226–230. doi: 10.1007/s12020-014-0202-
- Su, M.-J., Aldawsari, H., and Amiji, M. (2016). Pancreatic cancer cell exosome-mediated macrophage reprogramming and the role of microRNAs 155 and 125b2 transfection using nanoparticle delivery systems. *Sci. Rep.* 6:30110. doi: 10.1038/srep30110
- Sumrin, A., Moazzam, S., Khan, A. A., Ramzan, I., Batool, Z., Kaleem, S., et al. (2018). Exosomes as biomarker of cancer. *Braz. Arch. Biol. Technol.* 61. doi: 10.1590/1678-4324-2018160730
- Théry, C., Amigorena, S., Raposo, G., and Clayton, A. (2006). Isolation and characterization of exosomes from cell culture supernatants and biological fluids. *Curr. Protoc. Cell Biol.* 30, 3.22.21–23.22.29.
- Valkovskaya, N., Kaye, H., Felix, K., Hartmann, D., Giese, N. A., Osinsky, S. P., et al. (2007). ADAM8 expression is associated with increased invasiveness and reduced patient survival in pancreatic cancer. *J. Cell Mol. Med.* 11, 1162–1174. doi: 10.1111/j.1582-4934.2007.00082.x
- Yee, N. S., Zhang, S., He, H.-Z., and Zheng, S.-Y. (2020). Extracellular vesicles as potential biomarkers for early detection and diagnosis of pancreatic cancer. *Biomedicines* 8:581. doi: 10.3390/biomedicines8120581
- Zhang, Y., Su, Y., Zhao, Y., Lv, G., and Luo, Y. (2017). MicroRNA-720 inhibits pancreatic cancer cell proliferation and invasion by directly targeting cyclin D1. *Mol. Med. Rep.* 16, 9256–9262. doi: 10.3892/mmr.2017.7732
- Zonari, E., Pucci, F., Saini, M., Mazzieri, R., Politi, L. S., Gentner, B., et al. (2013). A role for miR-155 in enabling tumor-infiltrating innate immune cells to mount effective antitumor responses in mice. *Blood* 122, 243–252. doi: 10.1182/blood-2012-08-449306

**Conflict of Interest:** The authors declare that the research was conducted in the absence of any commercial or financial relationships that could be construed as a potential conflict of interest.

**Publisher's Note:** All claims expressed in this article are solely those of the authors and do not necessarily represent those of their affiliated organizations, or those of the publisher, the editors and the reviewers. Any product that may be evaluated in this article, or claim that may be made by its manufacturer, is not guaranteed or endorsed by the publisher.

Copyright © 2021 Verel-Yilmaz, Fernández, Schäfer, Nevermann, Cook, Gercke, Helmprobst, Jaworek, Pogge von Strandmann, Pagenstecher, Bartsch, Bartsch and Slater. This is an open-access article distributed under the terms of the Creative Commons Attribution License (CC BY). The use, distribution or reproduction in other forums is permitted, provided the original author(s) and the copyright owner(s) are credited and that the original publication in this journal is cited, in accordance with accepted academic practice. No use, distribution or reproduction is permitted which does not comply with these terms.

## 8 Appendix

### 8.1 Curriculum Vitae

#### Personal information

Name: Yeşim Yılmaz  
Adress: Brahmsstraße 6, 63069 Offenbach am Main  
E-mail: yesimverel@hotmail.de  
Mobile: +49 162 638 47 68  
Born: 4<sup>th</sup> August 1991 in Günzburg, Germany  
Nationality: German

#### Education

since 05/18	<b>Promotion</b> Institute of VTG Surgery/ Lab, Faculty of Medicine, Philipps University of Marburg, Prof. Dr. Detlef K. Bartsch, “Roles of ADAM8 & PRMTs in tumor- stroma- interactions in PDAC”
12/17- 02/18	<b>Voluntary unpaid internship</b> Institut of Cardiovascular Regeneration, University of Frankfurt a. M., Prof. Dr. Stefanie Dimmeler, “Hypoxia-induced long non-coding RNA NTRAS regulates alternative splicing and endothelial barrier function”
10/15- 08/17	<b>Master’s program in Molecular Biosciences</b> Goethe University, Frankfurt a. M., Institute Molecular Cell Biology of Plants, Prof. Dr. Enrico Schleiff, “Alternative splicing of plant heat stress transcription factors”
05/15- 05/16	Membership in Gesellschaft für Biochemie und Molekularbiologie e.V.
03/15- 04/15	<b>Field study</b> Tabasco/ South of Mexico
09/13- 07/14	<b>Semesters abroad</b> Middle East Technical University, Ankara/ Turkey
10/11- 08/15	<b>Bachelor’s program in Biosciences</b> Goethe University, Frankfurt a. M. Institute Ecology, Evolution & Diversity, Prof. Dr. Martin Plath, “The influence of inter- individual differences on strategic male mate choice”
03/04- 08/11	<b>Grammar school</b> Simpert- Krämer- Gymnasium, Krumbach



## Skills

- Laboratory technics: EMSA, Cloning Primer design, Mini-gene construction, Immunohistochemistry, Immunoprecipitation for iCLIP, FACS, SDS PAGE, Western Blotting, Cell Transformation, Cell Transformation, Cell Tranfection, Protein Purification, Sequencing, RNA extraction, cDNA preparation, PCR, qRT-PCR, Tube formation assay, Ultrazentrifugation, Exosome extraction, Immunogold labelling
- Languages: Turkish, German & English (excellent)  
Italian (three years, B2) (medium level)  
Spanish (two years, B2) (medium level)  
Latin (four years) (excellent)
- Musical instrument: Violinist in Orchestra

## Publications

- 07/21 **Extracellular Vesicle-Based Detection of Pancreatic Cancer**  
Verel-Yilmaz, Y., Fernández, J. P., Schäfer, A., Nevermann, S., Cook, L., Gercke, N., ... & Slater, E. P. (2021). Extracellular Vesicle-Based Detection of Pancreatic Cancer. *Frontiers in Cell and Developmental Biology*, 9.
- 05/21 **PRMT1 promotes the tumor suppressor function of p14<sup>ARF</sup> and indicative for pancreatic cancer prognosis**  
Repenning, A., Happel, D., Bouchard, C., Meixner, M., Verel-Yilmaz, Y., Raifer, H., ... & Bauer, U. M. (2021). PRMT1 promotes the tumor suppressor function of p14ARF and is indicative for pancreatic cancer prognosis. *The EMBO Journal*, 40(13), e106777.
- 01/21 **Cohort Analysis of ADAM8 Expression in the PDAC Tumor Stroma**  
Jaworek, C., Verel-Yilmaz, Y., Driesch, S., Ostgathe, S., Cook, L., Wagner, S., ... & Bartsch, J. W. (2021). Cohort analysis of ADAM8 expression in the PDAC tumor stroma. *Journal of Personalized Medicine*, 11(2), 113.
- 06/16 **Does personality affect premating isolation between locally- adapted populations**  
Sommer-Trembo, C., Bierbach, D., Arias-Rodriguez, L., Verel, Y., Jourdan, J., Zimmer, C., ... & Plath, M. (2016). Does personality affect premating isolation between locally-adapted populations?. *BMC evolutionary biology*, 16(1), 1-13.

## **8.2 Verzeichnis akademischer Lehrer**

Meine akademischen Lehrer waren die Damen und Herren in Marburg  
Bauer, D. K. Bartsch, J. W. Bartsch, Dörsam, Gercke, Helmprobst,  
Meixner, Pagenstecher, Pogge von Strandmann, Ramaswamy, Roth, Slater,  
Wischmann.

### 8.3 Danksagung

Diese Dissertation ist mir mit der Unterstützung vieler Menschen gelungen. Daher möchte ich an dieser Stelle den folgenden Personen meinen aufrichtigen Dank aussprechen: Hiermit möchte ich mich zuerst bei Prof. Dr. D. K. Bartsch und Prof. Dr. U.-M. Bauer für ihr gemeinsames Interesse an meiner Arbeit und dafür, dass ich in deren Forschungsgruppe mitarbeiten durfte, bedanken. Sie haben mir immer mit kompetenten Ratschlägen und Anregungen geholfen. Diese haben es mir ermöglicht, meine Arbeit sinnvoll zu strukturieren.

Besonders danke ich Dr. Slater und Prof. Dr. J.-W. Bartsch von Herzen dafür, dass sie mich die ganze Zeit während meines Projektes unterstützt haben. Ich danke ihnen für ihre freundliche Hilfsbereitschaft zu jeder Zeit und insbesondere dafür, dass ich unzählige Male während der Arbeit wissenschaftliche Fragen stellen durfte, deren Antworten mir weitergeholfen haben, meine wissenschaftliche Laufbahn erfolgreich weiterzuführen. Während meiner Zeit als Doktorandin habe ich von ihnen sehr Vieles, auch für das Leben, gelernt. Sie haben mich zu der Person gemacht, die ich jetzt geworden bin.

Insbesondere bedanke ich mich bei meinen Arbeitskollegen im VTG-Labor, vor allem bei Elvira Matthäi und Norman Gercke, für ihre freundlichen Ratschläge und uneingeschränkte Hilfsbereitschaft zu jeder Zeit, die mir ein großartiges Arbeitsumfeld geschaffen haben. Es war eine sehr schöne Zeit, die ich mit ihnen im Labor genossen habe und auch nie vergessen werde. Sie haben dazu beigetragen, dass diese Studie zu einer angenehmen Erfahrung geworden ist.

Als nächstes möchte ich mich bei meiner lieben Viktoria Wischmann aus der Pathologie danken. Sie hat mir immer geholfen, wenn ich keinen Ausweg gefunden habe und hat mich tatkräftig in meinen Laborarbeiten unterstützt und mir wertvolle Ratschläge mitgegeben. Ich danke ihr vom ganzen Herzen für die schöne Zeit. Meiner Familie möchte ich herzlich für die Unterstützung danken. Ohne sie wäre ich jetzt nicht da, wo ich heute bin. Insbesondere möchte ich auch meinen wahren Freunden, die ich als Familienmitglieder betrachte, Esra und Maryam, dafür danken, dass sie mich auf jede erdenkliche Weise unterstützt haben. Sie haben mir immer den Rücken gestärkt und mich immer wieder aufgebaut und motiviert, durchzuhalten. Schön, dass es sie gibt. Ich bin so dankbar für all die gute Laune und Ratschläge.

## 8.4 Ehrenwörtliche Erklärung

Ich erkläre ehrenwörtlich, dass ich die dem Fachbereich Medizin Marburg zur Promotionsprüfung eingereichte Arbeit mit dem Titel „Roles of ADAM8 and PRMTs in tumor-stroma-interactions in Pancreatic Ductal Adenocarcinoma” in der Klinik für Visceral-, Thorax- und Gefäßchirurgie unter der gemeinsamen Leitung von Prof. Dr. med. Detlef K. Bartsch und Prof. Dr. rer. nat. Jörg-Walter Bartsch ohne sonstige Hilfe selbst durchgeführt und bei der Abfassung der Arbeit keine anderen als die in der Dissertation aufgeführten Hilfsmittel benutzt habe. Ich habe bisher an keinem in- oder ausländischen Medizinischen Fachbereich ein Gesuch um Zulassung zur Promotion eingereicht, noch die vorliegende oder eine andere Arbeit als Dissertation vorgelegt.

Ich versichere, dass ich sämtliche wörtlichen oder sinngemäßen Übernahmen und Zitate kenntlich gemacht habe.

Mit dem Einsatz von Software zur Erkennung von Plagiaten bin ich einverstanden.

Vorliegende Arbeit wurde in folgenden Publikationsorganen veröffentlicht:

Jaworek, C., et al. (2021). “Cohort analysis of ADAM8 expression in the PDAC tumor stroma”. Journal of personalized medicine, Vol. 11 No.2

Repenning, A., et al. (2021). “PRMT1 promotes the tumor suppressor function of p14ARF and is indicative for pancreatic cancer prognosis”. The EMBO Journal, Vol. 40 No. 13, p. 106777.

Verel-Yilmaz, Y., et al. (2021). “Extracellular vesicle-based detection of pancreatic cancer”. Frontiers in cell and developmental biology, Vol. 9, p. 697939.

**Ort, Datum, Unterschrift Doktorandin**

---

Die Hinweise zur Erkennung von Plagiaten habe ich zur Kenntnis genommen.

**Ort, Datum, Unterschrift Referent**

---